BIPEDAL HUMANOID ROBOT WALKING REFERENCE TUNING BY THE USE OF EVOLUTIONARY ALGORITHMS

by
TUNÇ AKBAŞ

Submitted to the Graduate School of Engineering and Natural Sciences in partial fulfillment of the requirements for the degree of Master of Science

Sabanci University
August 2012

BIPEDAL HUMANOID ROBOT WALKING REFERENCE TUNING BY THE USE OF EVOLUTIONARY ALGORITHMS

APPROVED BY:

Assoc. Prof. Dr. Kemalettin ERBATUR
(Thesis Advisor)

Prof. Dr. Asif Şabanoviç

Assoc. Prof. Dr. Özgür ERÇETİN
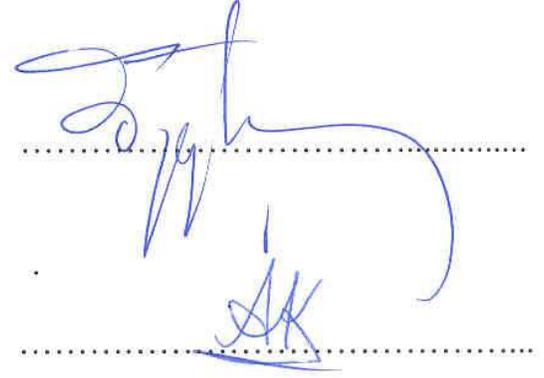
Assoc. Prof. Dr. Ali KOŞAR
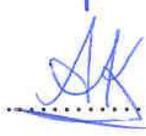
Assist. Prof. Dr. Hakan ERDOĞAN

DATE OF APPROVAL: 06.08.2012

BIPEDAL HUMANOID ROBOT WALKING REFERENCE TUNING BY THE USE OF
EVOLUTIONARY ALGORITHMS

Tunç AKBAŞ

Mechatronics Engineering, Ms. Thesis, 2012

Thesis Supervisor: Assoc. Prof. Dr. Kemalettin ERBATUR

Keywords: Humanoid robots, bipedal walking reference generation, bipedal gait tuning,
genetic algorithms

ABSTRACT

Various aspects of humanoid robotics attracted the attention of researchers in the past four decades. One of the most challenging tasks in this area is the control of bipedal locomotion. The dynamics involved are highly nonlinear and hard to stabilize. A typical full-body humanoid robot has more than twenty joints and the coupling effects between the links are significant. Reference generation plays a vital role for the success of the walking controller. Stability criteria including the Zero Moment Point (ZMP) criterion are extensively applied for this purpose. However, the stability criteria are usually applied on simplified models like the Linear Inverted Pendulum Model (LIPM) which only partially describes the equations of the motion of the robot. There are also trial and error based techniques and other ad-hoc reference generation techniques as well.

This background of complicated dynamics and difficulties in reference generation makes automatic gait (step patterns of legged robots) tuning an interesting area of research. A natural command for a legged robot is the velocity of its locomotion. A number of walk parameters including temporal and spatial variables like stepping period and step size need to be set properly in order to obtain the desired speed. These problems, when considered from

kinematics point of view, do not have a unique set of walking parameters as a solution. However, some of the solutions can be more suitable for a stable walk, whereas others may lead to instability and cause robot to fall.

This thesis proposes a gait tuning method based on evolutionary methods. A velocity command is given as the input to the system. A ZMP based reference generation method is employed. Walking simulations are performed to assess the fitness of artificial populations. The fitness is measured by the amount of support the simulated bipedal robot received from torsional virtual springs and dampers opposing the changes in body orientation. Cross-over and mutation mechanisms generate new populations. A number of different walking parameters and fitness functions are tested to improve this tuning process.

The walking parameters obtained in simulations are applied to the experimental humanoid platform SURALP (**S**abanci **U**niversity **R**ese**A**rch **L**abaratory **P**latform). Experiments verify the merits of the proposed reference tuning method.

İKİ BACAKLI İNSANSI ROBOTLAR İÇİN EVRİMSEL ALGORİTMALAR

KULLANILARAK YÜRÜME REFERANSI AYARLANMASI

Tunç AKBAŞ

Mekatronik Mühendisliği Programı, Master Tezi, 2012

Tez Danışmanı: Doç. Dr. Kemalettin ERBATUR

Anahtar Kelimeler: İnsansı robotlar, iki bacaklı yürüme referansı oluşturulması, iki bacaklı yürüme biçimi ayarlanması, genetik algoritma

ÖZET

Geçtiğimiz kırk yıl boyunca insansı robotlar alanı birçok açıdan bilim adamlarının ilgisini çekmiş ve ilgi uyandırmıştır. Bu alandaki en zorlu problemlerden biri iki bacaklı hareket kontrolüdür. Bu problemin içinde bulunan dinamikler lineer değildir ve zor dengelenmektedir. Tipik bir tam vücutlu insansı robotta yirmiden fazla sayıda eklem bulunur ve bu eklemler arasında bağlanma etkileşimleri oldukça önem taşır. Bir yürüme kontrollörünün başarılı bir şekilde çalışmasında referans oluşturulması anahtar bir rol oynar. Bu açıdan dengeli bir referans sentezi yüksek bir değer taşır. Bu konuda Sıfır Moment Noktasını'da kapsayan denge kriterleri yaygın bir şekilde kullanılmaktadır. Ancak bu denge kriterleri genellikle Ters Lineer Sarkaç Modeli gibi robotun hareket denklemlerini kısmen sağlayan basitleştirilmiş modeller üzerinden uygulanır. Bu yöntemin yanı sıra çeşitli deneme yanılma tabanlı ve geçici olarak belirlenmiş yöntemlerde mevcuttur.

Karışık dinamik denklemler ve referans oluşturma zorlukları otomatik yürüme referansı oluşturulmasının ilginç bir araştırma alanı olmasına sebep olur. Yürüme hızı bacaklı bir robot için doğal bir komuttur. Adım uzunluğu ve periyodu gibi çeşitli değişkenler yürüme hızının

belirlenmesi için ayarlanmalıdır. Kinematik açıdan bakıldığında bu problemin sonsuz miktarda çözümü mevcuttur. Bu doğrultuda bazı çözümler daha dengeli bir yürümeyi sağlarken diğer çözümler dengesiz yürümeye ve robotun düşmesine neden olabilir.

Bu tez evrimsel metodlar yardımıyla yürüme referansı ayarlanmasını önermektedir. Yürüme hızı sistem girdisi olarak belirlenmiştir. Sıfır Moment Noktası tabanlı bir referans oluşum metodu kullanılmıştır. Yürüme simülasyonları yapay bir populasyona uygunluk değerleri biçilerek gerçekleştirilmiştir. Robotun vücut oryantasyon değişikliklerine karşı etki eden sanal torsiyonal süspansiyon sistemleri uygunluk değerlerini belirlemek için kullanılmıştır. Atlama ve mutasyon operatörleri yeni yapay popülasyon oluşumunu sağlamıştır. Bu doğrultuda değişik yürüme referansı parametreleri uygunluk fonksiyonları test edilmiştir.

Yürüme simülasyonlarından elde edilen sonuçlar deneysel bir insansı robot platformu olan SURALP (**S**abancı **Ü**niversitesi **R**obot **A**raştırmaları **L**aboratuvar **P**latformu) üzerinde test edilmiştir. Deneysel sonuçlar uygulanan metodun değerini onaylamıştır.

To my beloved family

ACKNOWLEDGEMENTS

BIPEDAL HUMANOID ROBOT WALKING REFERENCE TUNING BY THE USE OF
EVOLUTIONARY ALGORITHMS

TABLE OF CONTENTS

LIST OF FIGURES

xiii

LIST OF TABLES

LIST OF SYMBOLS

p_x :   x-directional component of Zero Moment Point reference vector

p_y :   y-directional component of Zero Moment Point reference vector

p_z :   z-directional component of Zero Moment Point reference vector

x :   x-directional component of center of mass reference vector

y :   y-directional component of center of mass reference vector

z :   z-directional component of center of mass reference vector

z_c :   Constant height of the Linear Inverted Pendulum

$\ddot{c}_x$:   x-directional acceleration of the robot body

c_x :   x-directional position of the robot body

c_z :   z-directional position of the robot body

$\ddot{c}_y$:   y-directional acceleration of the robot body

c_y :   y-directional position of the robot body

P_x^{ref} :   Reference ZMP for x-direction

P_y^{ref} :   Reference ZMP for y-direction

τ :   Double support phase

T :   Half walking period

ω_n :   Square root of g/c_z

$u(\cdot)$:   Unit step function

$c_x^{ref}(t)$:   COM Reference for x-direction

$c_y^{ref}(t)$:   COM Reference for y-direction

δ	:	Magnitude of peak difference between p_x^{ref} and the non-periodic component of p_x^{ref}
$v_{average}$	:	Average walking velocity
$x_{assymetry}$	:	x-reference offset
T_{ds}	:	Double support period
T_{ss}	:	Single support period
h_s	:	Step height
K_{spring}		Virtual torsional spring coefficent
K_{damper}	:	Virtual torsional damper coefficent
h_{leg}	:	The height of the leg
h_{offset}	:	Distance between foot sole center and the hip frame
$F_{fitness}$	:	Fitness function
$u_{ds_{average}}$	:	Average supporting torque during double support period
$u_{ss_{average}}$	:	Average supporting torque during single support period
ω_{peak}	:	Joint velocity peak
ω_{max}	:	Maximum joint velocity
$K_{penalty}$	:	Penalty coefficient
l_{swing_offset}	:	Swing offset
A	:	The amplitude of the ZMP lateral motion
γ	:	Body yaw angle
β	:	Body pitch angle
α	:	Body roll angle
$u_{sd\,roll}$	:	Supporting torque around roll axis
$u_{sd\,pitch}$	:	Supporting torque around pitch axis
$u_{sd\,yaw}$	:	Supporting torque around yaw axis

LIST OF ABBREVIATIONS

CoM   :   Center of Mass

ZMP   :   Zero Moment Point

LIPM   :   Linear Inverted Pendulum Model

DoF   :   Degrees of Freedom

2D   :   Two Dimensional

3D   :   Three Dimensional

GA   :   Genetic Algorithm

RBFNN   :   Radial Basis Function Neural Network

3D-LIPM   :   Three Dimensional Linear Inverted Pendulum Model

CPG   :   Central Pattern Generator

FFT   :   Fast Fourier Transform

CoG   :   Center of Gravity

Chapter 1

1. INTRODUCTION

Humanoid robotics is a field which improved dramatically in the last 25 years. The bipedal structure is favored in the human environment because of its advantages in obstacle avoidance. A humanoid robot can have virtues in being accepted as a co-worker or care giver by humans too. The field appears to have a promising future.

In order to reach the goal of using humanoid robots in daily life there are a lot of problems to be solved. The bipedal free-fall manipulator is intrinsically hard to stabilize. The commonly large numbers of degrees of freedom (DoF) involved pronounce interlink coupling effects. The dynamics are nonlinear and complex. As a result, walking control is a challenging task. The control of the walking is in conjunction with the gait planning. In order to maintain the stability of walking, stable walking reference generation is necessary.

Another challenge in the field of bipedal walking control is the definition of a stable walk. A robot, conceptually, exhibits a stable walk if it does not fall. In other words, it is hard to call a walk unstable before the robot falls.

Ad-hoc methods do not consider stability of the walk directly. Reference trajectories are devised manually for the Cartesian postures of the feet or for joint positions. Trial and error iterations are then used to adjust trajectory parameters for a balanced walk. The feet or joint trajectories in these approaches usually consist of combinations of lines, higher order polynomials and trigonometric functions. Typically, smooth position and velocity reference curves are employed in order not to invoke vibrations in the robot motion. There are other ad-hoc methods which contrast with the above mentioned ones, in those methods trial and error iterations are performed automatically rather than manually. The generated gait is considered successful if the robot does not fall during the execution of the walking task.

Central Pattern Generators (CPG) are biologically inspired algorithms for the generation of references. Joint or Cartesian space periodic trajectories are generated and gait transitions are addressed in the CPG context. A gait transition refers to a change of walking speed or timing properties on the fly.

It is desirable to base walking references on well-defined stability criteria in the trajectory generation phase. The Zero Moment Point (ZMP) criterion, the Foot Rotation

Indicator (FRI) and the Poincăre maps techniques are quite commonly employed as stability metrics.

The ZMP criterion stands out as the most widely employed stability norm, applicable to multi-body systems. The criterion states that during the walk, the ZMP must lie within the supporting area - often called the support polygon - of the feet in contact with the ground.

The ZMP coordinates are obtained as functions of the positions and accelerations of each of the links and the body of the humanoid robot. It is quite difficult to compute these functions online in the design of reference generation, due to the number of variables involved and the dynamic complexity of the bipedal structure. The aforementioned complexities of the bipedal plant, urges the use of simplified models in the process of gait synthesis. The Linear Inverted Pendulum Model (LIPM) presents a quite basic set of motion equations and found extensive use in this context. It consist of a point mass of constant height and a massless rod which connects the point mass to the ground. With this model a relationship between ZMP and the Center of Mass (CoM) coordinates is obtained. For such methods, robot CoM trajectory is derived from ZMP trajectories which are predefined in such a way that the ZMP is always in the support polygon. Afterwards the reference trajectories for the leg joints are obtained via inverse kinematics using the robot CoM coordinates.

The FRI concept is quite similar to the ZMP. The Poincare Maps are applied for restricted bipedal model with only a few DoF, with limited practical value.

No matter how the reference gait is planned and created, there is a room for final tuning. Usually, there are many parameters to be tuned. The walking performance is related to these parameters nonlinearly. The search space is large. The ad-hoc methods, by their working mechanism, require tuning with simulations and experiments. The methods which are based on planning with a stability criterion use simplified models which do not reflect the plant dynamics fully. Theoretically, an optimal gait design for a humanoid robot can be achieved using dynamic analysis. However, as mentioned before the dynamic equations of biped robots during the walking process are too complex and hard to determine, especially if the whole robot is taken into consideration. A better performance (for example in terms of speed of the walk) or more stable walk (in terms of the position of the ZMP in the support polygon, or in terms of a less oscillatory behavior) can be obtained with tuning. The effectiveness and dexterity of the humanoid robot walking reference generation can be improved further by tuning the parameters involved in walking pattern generation while obeying a stability criterion. Consequently, most studies in the field of humanoid robots employ a heuristic method in order to further improve the walking of a humanoid robot. Also,

even though the works on stable reference generation for walking are very important and encouraging, there are additional requirements to reach the human walking dexterity, efficiency and effectiveness. Generating a walking reference generation by itself is not sufficient for a humanoid robot to adapt to daily-life environment. The improvement of the walking in terms of power consumption and naturalness can be implemented by automatic tuning as well.

Genetic Algorithm (GA) is an heuristic method used often to improve the walking pattern of biped robots [1-4]. It is also known to be a robust method for search and optimization problems [5].

In this work a genetic algorithm is applied for tuning the parameters of walking pattern generation for a given walking velocity. Tuning is performed for a range of velocity commands. A ZMP based approach is used in reference generation. Virtual torsional springs and dampers are attached to the trunk center of biped in order to maintain its balance during the simulations. The exerted forces and torques by these springs and dampers are employed to design a fitness function to assess the stability of the generated walking gait. A Newton-Euler method based full dynamics 3D simulation is employed for a 12-DoF biped robot model to implement the GA. The reference trajectories obtained via simulations in the GA framework are used in walking experiments with the robot SURALP.

The thesis is organized as follows. The next chapter briefly explains the humanoid locomotion terminology and describes the history of successful humanoid robot projects. Chapter 3 presents two different surveys. First survey investigates the developed methods for bipedal robot walking reference generation whereas second one examines the methods used for gait reference tuning and improvement via heuristic methods. The full-body humanoid robot SURALP is briefly represented in terms of hardware, implemented gait reference trajectory generation and control architecture in Chapter 4. The problem definition and implementation of GA on gait reference tuning with unconstrained joint velocities and corresponding simulation results are examined in Chapter 5. Chapter 6 adds joint velocity constraints and introduces a modified fitness function for GA algorithm. Simulation and experimental results are presented. The chapter ends with the discussion on experimental results which point out the importance of lateral motion in walking reference generation. In Chapter 7, a revised chromosome for GA is employed and tested experimentally. Conclusion and future works are presented in Chapter 8.

Chapter 2

2. BIPEDAL LOCOMOTION TERMINOLOGY AND EXAMPLE HUMANOID ROBOT PROJECTS

This chapter presents the fundamental concepts in humanoid locomotion terminology and the successful humanoid robot projects in the history of the field.

2.1. Terminologies in Humanoid Robotics

The motion (including locomotion) of a humanoid is described with respect to planes perpendicular to each other. Figure 2.1 points out the three primary planes which describe the basic human movements. The basic motion of humanoid robots is defined over these three reference planes.
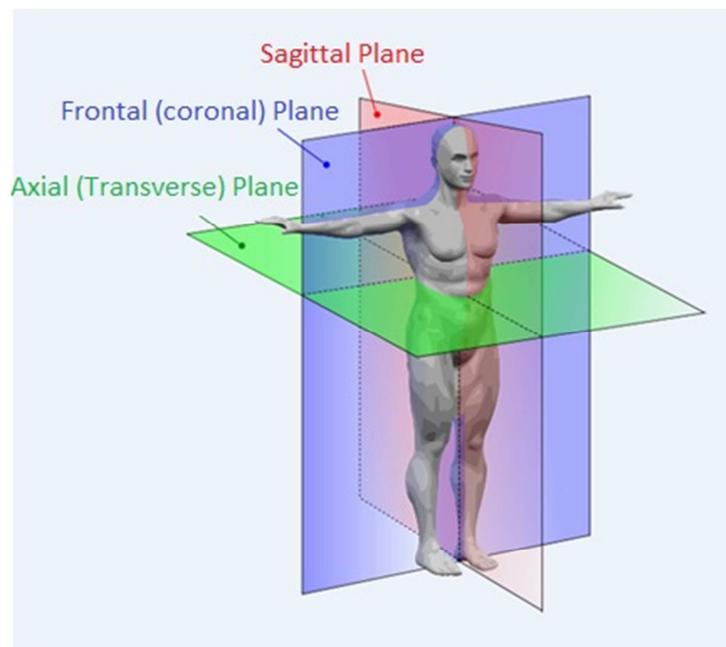
Figure 2.1: Reference body planes [6]

The direction of the straight walk is defined on the sagittal plane. This plane divides the body into left and right sides vertically. In some of the works the walking reference trajectory is obtained by considering the motion in the sagittal plane alone [7-10].

The step patterns of legged robots are defined by the term "gait". If the motion is set to be periodic then the generated pattern is called "gait cycle". [11] The gait cycle of bipedal robots consists of two phases; "swing phase" and "support (stance) phase". [11] In swing phase only one leg of the biped robot is in contact with the ground whereas the other one moves freely to take a step. At the same time the leg which remains in contact with the ground is on its support phase. Support phase by itself can be evaluated in two different subcategories; "single support phase" and "double support phase". In the single support phase only one leg supports the whole weight of the body. On the other hand, in the double support phase the body weight is supported by each foot at the same time.

These phases have to be identified clearly in order to generate a stable walking reference trajectory. In Figure 2.2 a complete walking cycle is represented in order to emphasize the relation between gait cycle, single support phase and double support. The feet of the humanoid robot also defined according to phases of gait cycle. In that sense the foot in support phase is defined as support foot and similarly the foot in swing phase is defined as swing foot.
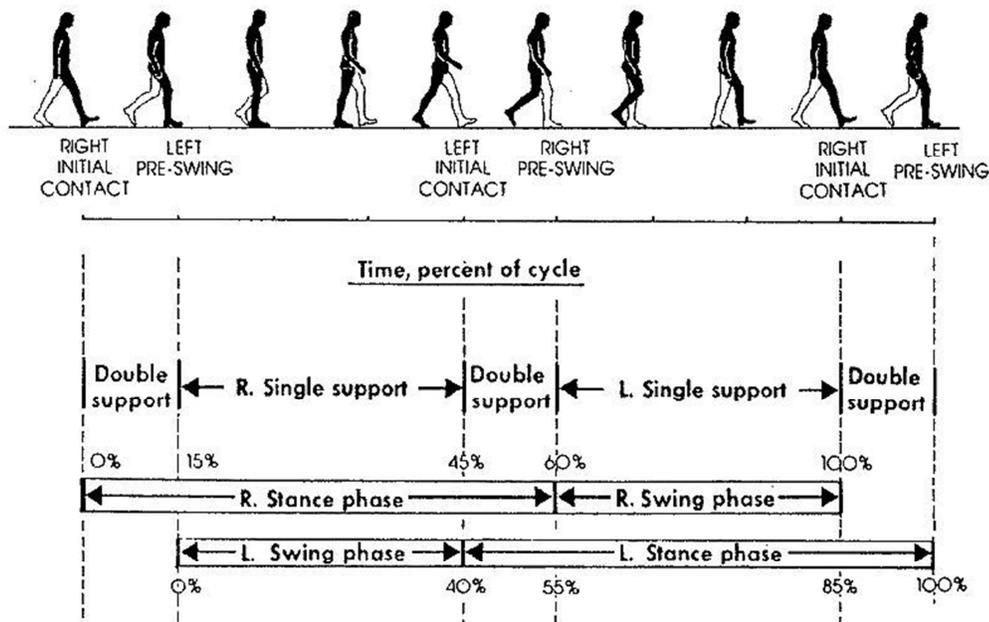
Figure 2.2: A complete walking gait [12]

During the gait cycle at the end of each single support phase there is a distance covered by swing foot. The distance between the toe sections of the feet after the step is defined as the "step size". The total distance travelled by the swing foot is called the "stride

5

length". "Swing offset" is half of the distance between ankle centers of the feet in the lateral direction. Figure 2.3 represents these terms in detail.
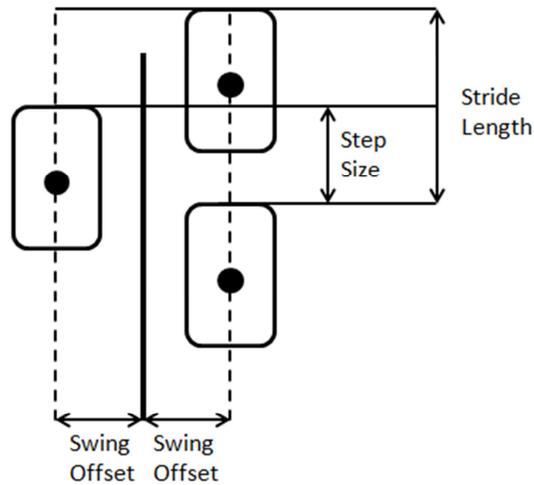
Figure 2.3: Step size and swing offset

Support polygon is another term which has a direct relation with the stability of the robot. Figure 2.4 presents the support polygon. It is defined as the area that is enveloped by the supporting feet/foot.
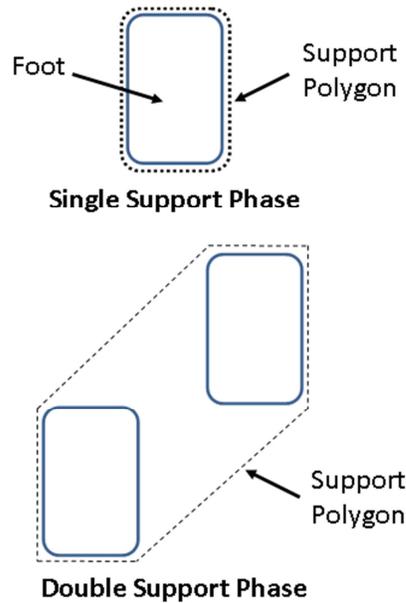
Figure 2.4: Support Polygon

The position of humanoid robot's CoM ground projection, shown in Figure 2.5, is related with stable walking reference generation. If the CoM projection stays in the supporting polygon during the whole walking cycle, the gait will be called static. Although this is a genuine way to generate a stable walking reference, it is slow due to length of single and double support phases.
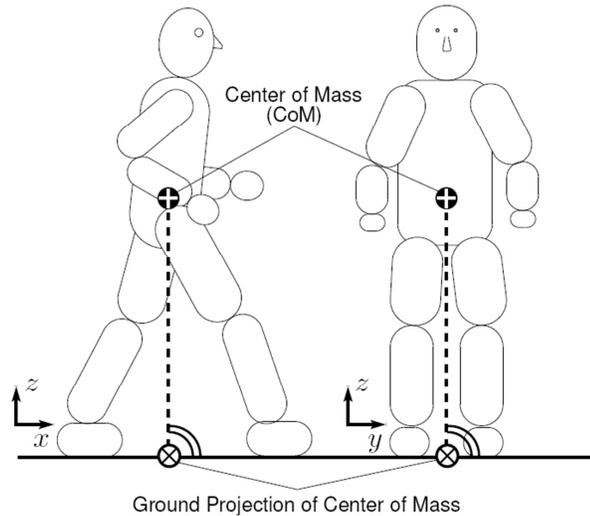
Figure 2.5: CoM and its ground projection [13]

In dynamic gait generation, the CoM of the robot is not restricted by the support polygon unlike static gait. The stability of the dynamic gait is maintained by inertial effects. As a result dynamic gait generation is more challenging compared to static gaits. However, faster locomotion can be accomplished by dynamic gaits. Figure 2.6 shows an example of static walking and pertinent CoM trajectory projection, whereas Figure 2.7 shows a dynamic walking example and the corresponding CoM trajectory projection.
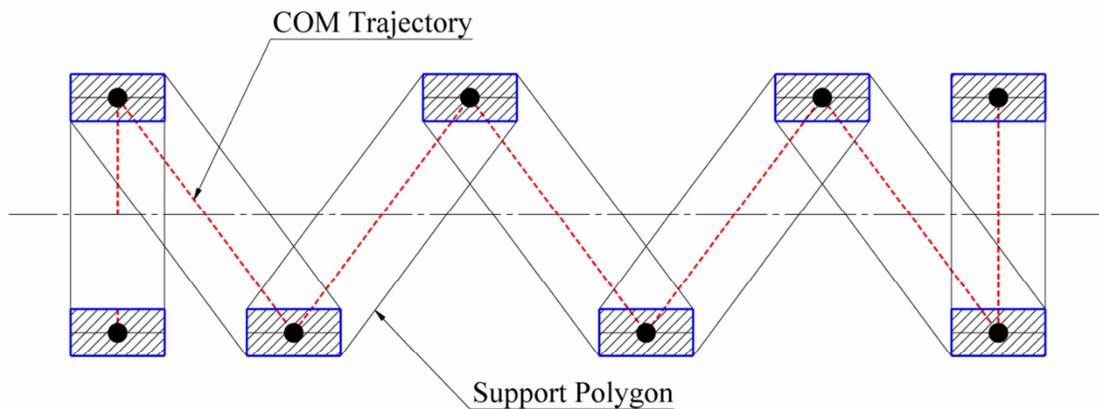
Figure 2.6: Static walking and CoM projection on ground
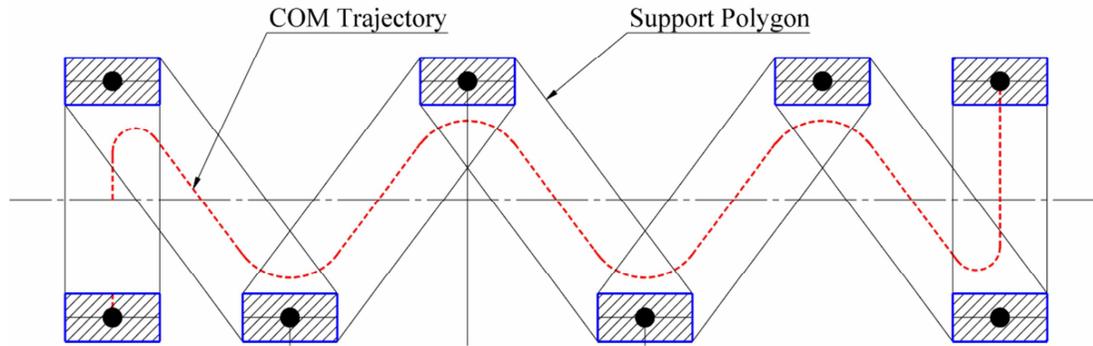
Figure 2.7: Dynamic walking gait cycle and CoM projection on ground

The ZMP criterion is frequently used in order to assess inertial effects in a dynamic walking gait. The term is firstly introduced by Vukobratovic [11]. According to the definition, it is the point on the ground where sum of all torques will be zero. This terminology is often used in the stability analysis of biped robots. If the ZMP lies within the support polygons during the gait, the generated walking is said to be stable.

2.2. Examples of Humanoid Robots

The field of bipedal locomotion and bipedal walking robots is considered as a promising area. The realization and development of the first walking biped robot by Waseda University, by professor Ichiro Kato's robotic team was in late 1960's [14]. The fundamental function of bipedal locomotion (walking) was applied on the artificial lower-limb leg module WL-1 in 1967 [15]. Afterwards WL-3 was developed, having electro-hydraulic servo actuators. It managed human-like movement using swing and stance phases [15]. The first robot with the ability to change direction was WL- 5 in 1972 [15]. The family of these leg modules continues until WL-10RD which was the first biped robot to achieve dynamic walking in 1984 [16]. At the same time period Waseda University also created a biped family which is actuated by artificial muscles attached to an outside pneumatic source [15]. The first of these robots was WAP-1 (1969) which used rubber as artificial muscle, then WAP-2 was introduced with powerful pouch-type artificial muscles [15]. The final member of this family was WAP-3 which achieved three-dimensional automatic biped walking in 1971 [15]. Figure 2.8 shows the WAP and WL family in chronological order. After the improvements and developments made by Waseda University the bipedal locomotion studies gained pace and the works on walking trajectory generation methods carried on with a number of different biped robot designs.
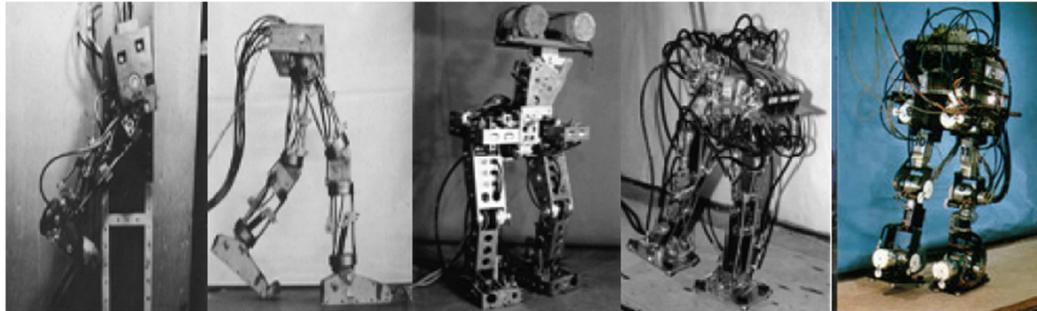
Figure 2.8a: Bipedal Robots developed by Waseda University: WL-1, WL-3, WL-5, WL-9DR and WL-10RD (from left to right)
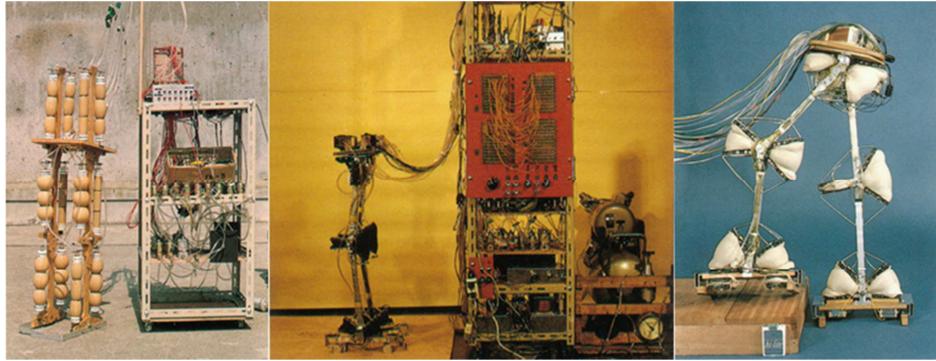
Figure 2.8b: WAP family by University of Waseda: WAP-1, WAP-2 and WAP-3 (left to right)

In 1973 WABOT-1 (WAseda roBOT) was introduced as the first full-scale anthromorphic robot. WABOT-1 was capable of using a static walking gait and it can change the direction of the walk in a way similar to WL-5. Concurrently, Marc Reibert from MIT (Massachusetts Institute of Technology) established the MIT leg lab, which was specially dedicated for biped locomotion and dynamic stability research.[17]

The next goal in the humanoid robotics field is to create an adult-size robot which has human proportions and the size. WABIAN-1 (1996) was the first example of such robot, it had 35 DoF in total which consists of two 3 DoF legs, two 10 DoF arms, a 2 DoF neck, two 2 DoF eyes and a torso with a 3 DoF waist [18]. It has a limb control system, a vision system and a conversation system to mimic human-like actions. In 1999 WABIAN-RII was introduced. It had a more human-like body posture and it was able to mimic the human motions by the realization of body motions by its two 7 DoF legs [19]. Since interaction with the human environment and communication with humans was also the purpose of this project a new prototype, WABIAN-RIV, equipped with vision and voice recognition systems was presented in 2004. Figure 2.9 shows the humanoid robots WABOT-1, WABIAN-RII and WABIAN-RIV of Waseda University.

After the achievements of Waseda University, other universities and a number of corporate technology institutions started to get involved in the field of humanoid robots. HONDA is the first commercial firm to conduct research and development in humanoid robotics in 1986. HONDA's humanoid robot family gained significant interest and popularity all around the world. The members of this humanoid family are considered to be most advanced humanoid robots of their time. The first seven members of HONDA's humanoid
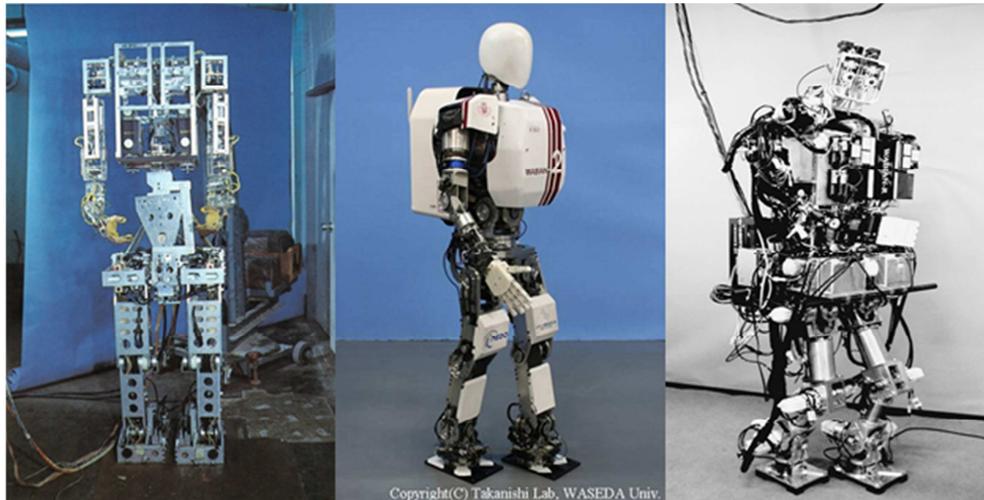
Figure 2.9: Humanoid robot prototypes by Waseda University: WABOT-1, WABIAN-RII and WABIAN-RIV (left to right)

family were leg modules E0 to E6, then the humanoid robots were introduced with P series from P1 to P3. P2 was the first humanoid walking robot which uses wireless communication tools for self-regulation. As a result it was able to walk independent of wires and accomplished more complex motion tasks such as climbing the stairs and object manipulation. From these robots P3 can be considered as a milestone in terms of human-like appearance and posture. This was partially due to the reduced height and weight of this prototype. Compared to P2, P3 was 0.22 meters shorter and 80 kilograms lighter. This prototype allowed the development of a much more sophisticated and advanced humanoid robot generation. Figure 2.10 shows the humanoid family of Honda from E0 to P3.

ASIMO (Advance Step in Innovative Mobility) was the latest generation of HONDA's humanoid robot family. It was introduced to public in year 2000 and gained popularity very quickly in all around the world. Unlike the previous generations, ASIMO had a more teenage-size look. First version of ASIMO was 1.2 m tall and weighed 52 kg with 26 DoF. It has become the most popular humanoid robot with smoother and more versatile human-like motion capabilities. In addition it is equipped with the superior image and voice recognition instruments when compared with previous generation humanoid robots. The second version of ASIMO was announced in 2005. The walking speed of this version can be speed up to 6 km/h and has 8 additional DoF on top the last version. The final version of ASIMO was introduced in 2011. It is capable of running as well as walking and walks in
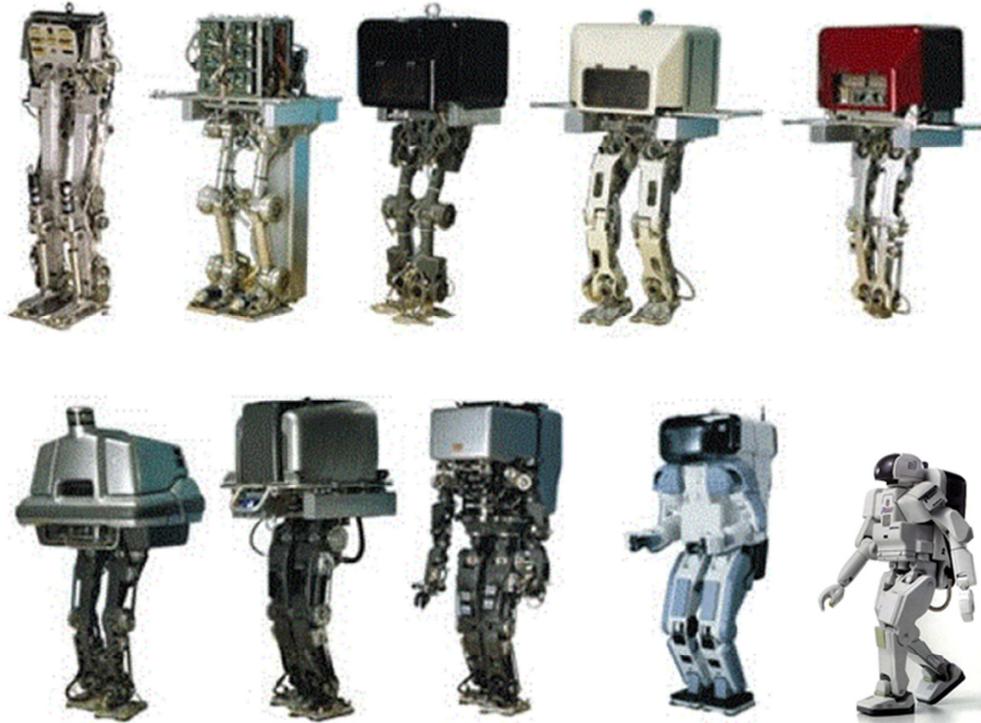
Figure 2.10: HONDA humanoid robots; E0-6 to P1-3

omni-directional patterns. The maximum speed achieved by the latest version was 9 km/h. In addition it has larger upper-body workspace and overall size. The technology called i-WALK helps ASIMO to walk while interacting with the environment [20]. Also, it is one of the first commercially available humanoid robots which can be rented or bought for research and development studies. Currently there are 46 ASIMO robots located in different research facilities around the world. Figure 2.11 shows the latest version of ASIMO.

University of Tokyo contributed to humanoid research field with their humanoid prototype; H5, H6 and H7. Figure 2.12 shows these prototypes. H5 was a child-size humanoid robot with 30 DoF. However it was incapable to achieve full-body motions such as lying-down, supporting body by hand and manipulation.[21] In order to obtain such full-body motions H6 was developed. The motivation behind this generation was to make a humanoid robot capable of proper environmental interaction. This is achieved by improving the arrangement of DoFs, rotation range of joints and maximum torque of joints in H6 [22]. H6 consisted of 35 DoF and it was 1.36 meters tall and weighed 51 kilograms. It was equipped with 3D vision and voice recognition sensors. The current prototype is H7. It was built in human proportions with 1.47 meters of height and 57 kg weight.
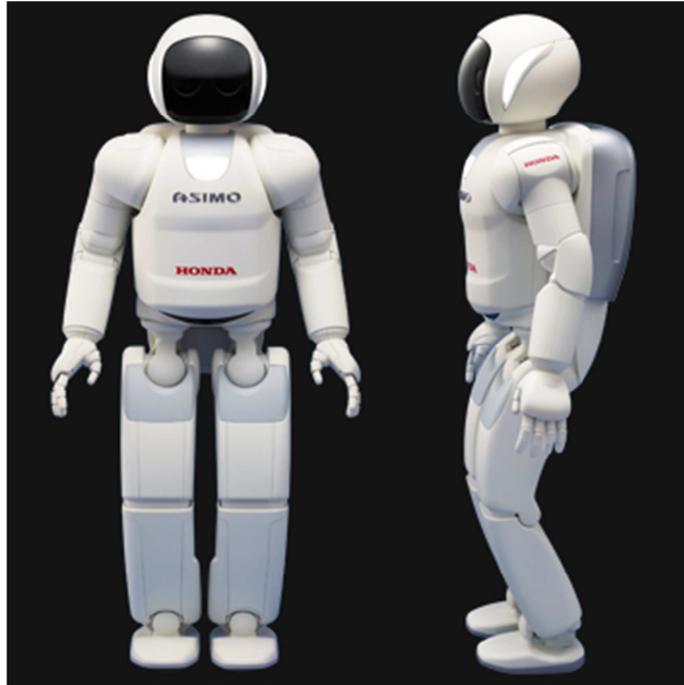
Figure 2.11: ASIMO of HONDA
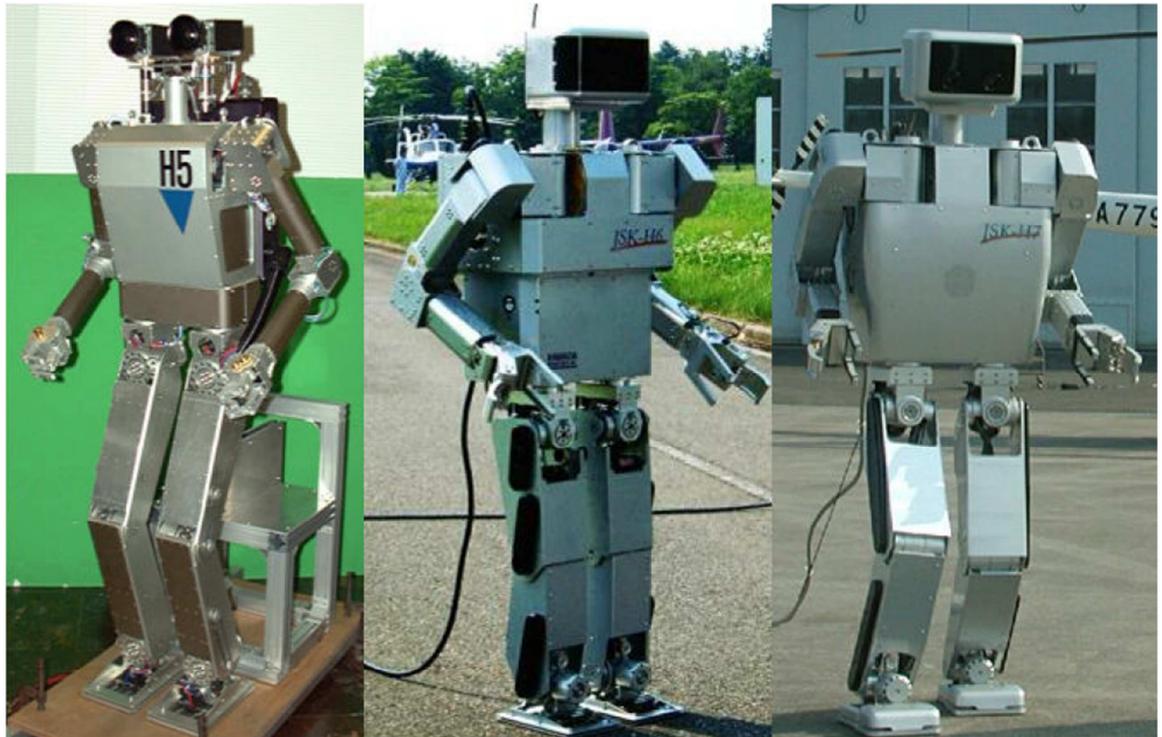
Figure 2.12: Humanoid robot prototypes by University of Tokyo: H5-7 (from left ro right)

After the improvements in the field of humanoid robots by HONDA and other Japanese universities, The Ministry of Economy and Industry (METI) of Japan announced the Humanoid Robot Project (HRP) in 1998. The main motivation behind this project was to use humanoid robots as part of the labor power within society. HRP-1 was the first humanoid robot developed under this project by HONDA Research and Development. It was designed as the next generation after the HONDA P3 robot in terms of shape and controller strategies [23]. Later on National Institute of Advanced Industrial Science and Technology (AIST) commenced their own prototype HRP-2 as the second humanoid robot within the project in 2001. Compared with HRP-1 it was a lighter robot with 58 kg weight and 1.54 meters height. The mechanical design and the controller system of HRP-2 was developed by AIST. The main success of HRP-2 was its compact design. Unlike the previous humanoid robots, it does not use any backpack and has a thinner more human-like body structure. Afterwards HRP-3P was developed. It was designed to perform in rough working environments [24]. The current prototypes of this project are HRP-4 and HRP-4C. The main contribution of HRP-4 was its lighter and cheaper design. HRP-4 weighed only 38 kg with 1.51 meter height and it has 34 DoF [25]. Unlike the pervious prototypes of AIST and HRP-4, HRP-4C is developed straightly by the motivation of humanoid robot usage in entertainment industry such as exhibitions and fashion shows [26]. It is a female humanoid robot designed with a realistic head and a realistic figure of human being [26]. Figure 2.13 shows the prototypes of Humanoid Robot Project by AIST.

Figure 2.13: HRP-2, HRP-3, HRP-4 and HRP-4C (left to right)

Figure 2.14: KHR-1, KHR-2 and KHR-3 (HUBO) of KAIST

Korea Advanced Institute of Science and Technology (KAIST) presented the humanoid robot platform KHR-1 (KAIST Humanoid Robot) in 2002. It was 48 kg of weight and 1.2 meters of height with 25 DoF. Successful stable walking performance was realized by using force/torque and inertial sensors [27]. KHR-2 was the second generation of these robots which was able to walk on uneven surfaces and inclined floor [28]. Current prototype of the KHR series is KHR-3, it has more human-like features, movements and human-friendly character [29]. It is also able to generate a walking trajectory online by varying walking period and stride [30]. Figure 2.14 shows the KHR robots of KAIST.

PAL Robotics and Boston Dynamics can be considered as the most successful commercial robotic firms manage to create their own prototypes. The Reem series was developed by PAL Robotics which is located in Spain. It can be considered as the most advanced adult-size humanoid robot built in Europe. Reem-B , the second prototype of the series, is equipped with sensors that allow it to autonomously learn its environment and to walk within it, avoiding obstacles, with no human intervention [31]. Another commercial humanoid robot, Petman, was introduced by Boston Dynamics (USA) in 2011. It is the first humanoid prototype which able to walk using actual human shoes. In addition, it successfully achieved human-like heel-toe walking [32]. Figure 2.15 shows Reem-B of PAL Robotics and Petman of Boston Dynamics.
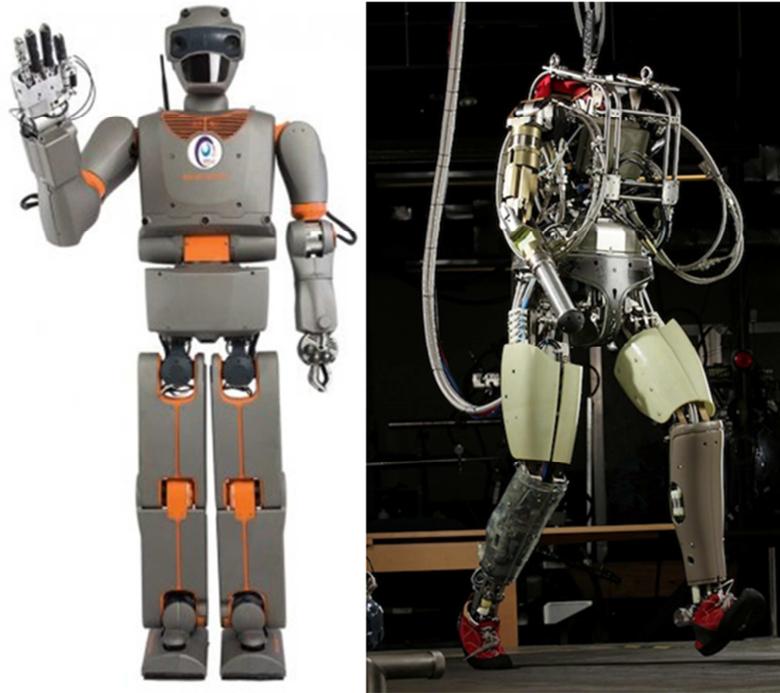
Figure 2.15: Reem-B of PAL Robotics (left) and PETMAN of Boston Dynamics (right)

In addition to the adult-size humanoid robots, the research field of humanoids accommodates kid-size robots as well. There are two advanced kid-size robots introduced in recent years. The first one is the NAO robot of Aldebaran Robotics in France [33]. It has 21 DoF, 0.6 meters height and 4.3 kg weight. The motivation of introducing the NAO robot is to reduce the cost by size, without losing quality and performance. As a result of lower cost NAO robots are available for the use of education, cognitive robotics and in the fields which require robot to robot interaction such as Robot Soccer World Cup (Robocup), an international competition with autonomous robotic soccer matches. In 2007 NAO robot was selected as the platform for the Robocup Standard Platform League (SPL) [34]. DARwIn (Dynamic Anthropomorphic Robot with Intelligence) is another successful kid-size humanoid robot. It was introduced by RoMeLa (Robotics and Mechanisms Laboratory) in USA. It won the 2011 and 2012 kid-size league in Robocup [35]. Similar to NAO, DARwIn is also available commercially. Figure 2.16 shows NAO of Aldebaran and DARwIn of RoMeLa.
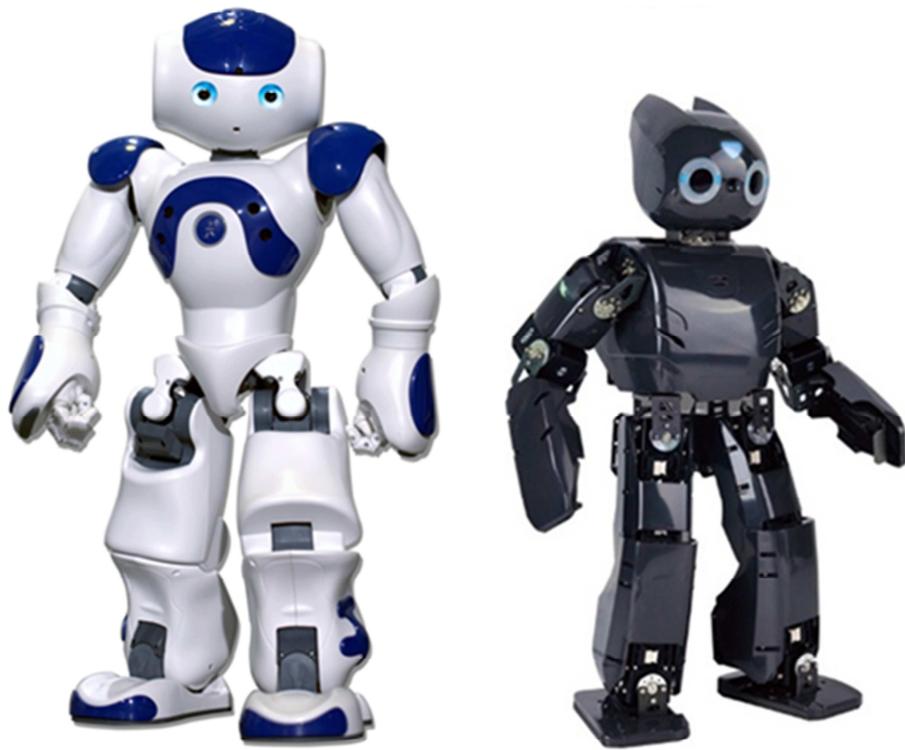
Figure 2.16: NAO of Aldeberan (left) and DARwIn of RoMeLa (right)

Chapter 3

3. A SURVEY ON BIPEDAL ROBOT WALKING REFERENCE GENERATION AND TUNING

One of the vital issues in humanoid robotics field is to generate a stable walking reference for the bipedal structure to serve in daily-life environment of humans. This chapter examines walking reference generation methods used on bipedal robots and the tuning of the generated walking reference trajectories. It is organized as follows. First section describes the walking reference generation techniques under two categories, namely, ZMP based gait reference generation methods and alternative walking reference generation methods. The second section presents the heuristic tuning methods applied on walking reference generation.

3.1. Reference Generation Methods for Bipedal Walking

In this section walking reference generation methods used for biped robots are presented.

3.1.1. Walking Reference Generation Methods Using ZMP Criterion

ZMP criterion is a frequently used method for achieving stable walking reference generation. In order to maintain the stability during the walk period of a robot, the ZMP must lie within the supporting polygon.

The ZMP coordinates are functions of the positions and accelerations of each of the links and body of the humanoid robot. It is quite difficult to make use of these functions in the design of reference generation, due to the number of variables involved and the dynamic complexity of the bipedal structure. As a result, two different approaches are applied to maintain the ZMP based stability during walking. The simplified model based approaches and the approaches using heuristic techniques.

3.1.1.1 Heuristic Method Based Approaches

Heuristic methods, often called experience-based techniques, are often used to solve problems with high-complexity. For the stated problem above, these techniques are suitable to determine sub-optimal or satisfactory results. Fuzzy systems and genetic algorithms are commonly employed within the studies of walking reference generation of the biped robots.

In 2000, Zhang, Wang, Quing and Fu proposed a gait synthesis method which uses the reaction force between the feet and ground [36]. According to proposed method, by treating the entire biped robot as a general *n* segment extended rigid body kinematics chain and determining its response to external forces and moments using D'Alembert's principle, the relation between the joint trajectories and floor reactive force is deduced [36]. Also the requirement of the double support phase is underlined since it allows the move ZMP smoothly between single support phases. In addition, the authors state that the ZMP is highly affected by the CoM displacement caused by swing leg. With these observations a fuzzy logic based ZMP trajectory generation method is introduced in order to achieve heel to toe foot motion during the walking gait. (Heel to toe motion is based on the observations made on human locomotion. It suggests that, in the swing foots landing phase the contact to the ground start with the heel and in take-off phase the contact to the ground is left with the toe.) The authors conjecture that this foot motion reduces the motion range of the trunk [36].

In 2001, Takeda et al. proposed a genetic algorithm based gait synthesis method for biped robots. Minimum energy consumption and minimum torque change is sought [2]. The verification of the stability is obtained by the ZMP criterion. Fitness function of the genetic algorithm consists of two parts. In the first part, the minimum energy function is determined by taking the integrals of the generated torque during walking. The results generated in the first part, for minimum energy consumption, are combined with the second part which determines the rate of change of the torque. The value of these cost functions are attached to every individual in the population. The joint angle reference trajectories are employed as GA variables and written as time polynomials with respect to the given constraints. In order to increase the learning process of GA a Radial Basis Function Neural Network (RBFNN) is adopted. The resulting reference trajectories are tested by a simulation using a 12 DoF biped model of Bonten-Maru I.

3.1.1.2 Approaches Using Simplified models

A simple approximate model could be used for the systems with large number DoF and complex dynamic equations. Considering the dynamic complexity of the bipedal structure such approximation will be suitable. This section examines the ZMP based walking reference generation methods which adopt simple approximate models.

In these works, predefined ZMP trajectories are used to generate a stable walking reference for robot's CoM. This subsection gives a survey on these methods.

Kajita et al focused on real-time walking control of a humanoid robot using a simplified three-dimensional linear inverted pendulum model (3D-LIPM) in 2002 [37]. It allows a separate controller design for the sagittal and frontal motions and simplifies the walking gait generation significantly. Figure 3.1 shows the 3D-LIPM which is used with motion constrained derivation for walking gait trajectory generation. In the experiments an input device, gamepad, is used for straight walking as well as omnidirectional walking. The projection of the robot CoM on walking surface enabled the change of direction in walking and step size together with the online modification of foot placements.
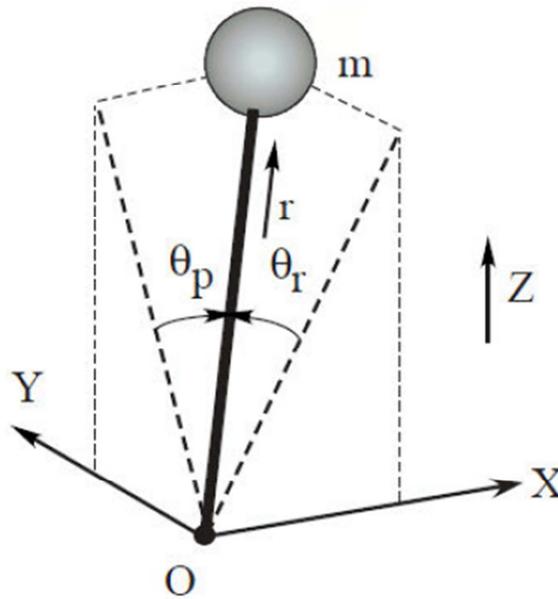
Figure 3.1: 3D inverted pendulum model

Lim, Kaneshima and Takanishi proposed an online walking pattern generation method for biped humanoid robots with trunk in 2002 [38]. They divided the walking gait cycle in five phases namely; stationary, transient, steady, transient and stationary as shown in Figure 3.2. The walking pattern generation works as follows. First, lower-limb motions of the new walking cycle are calculated, updated and connected to the previously generated five-step pattern for online modification. Using the updated walking command the trunk and waist motions are determined according to the trajectories of lower-limb motion and ZMP to compensate the moments created by the lower-limb motions in previous part. Transient and steady phases are necessary for such compensation.
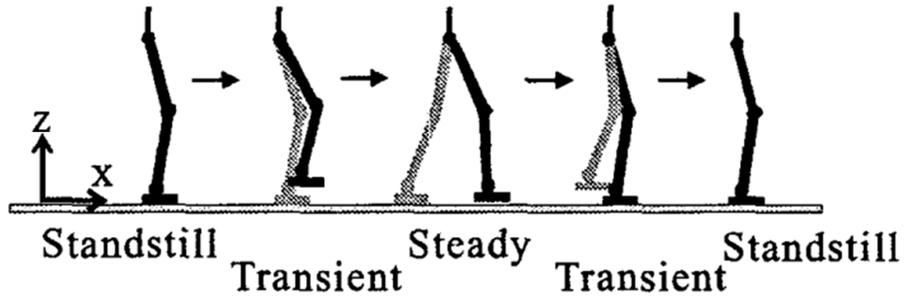
Figure 3.2: A complete walking gait cycle [38]

The scheme in Figure 3.3 points out the stages of this online walking pattern generation method. After the change of walking parameters according to a task or visual information the new five-step lower-limb pattern is created in first stage. According to the pattern of lower-limb, trunk and waist motions and the corresponding ZMP pattern is generated for compensating the moments caused by the lower-limb motions. All together this final pattern is inserted as the following gait cycle.
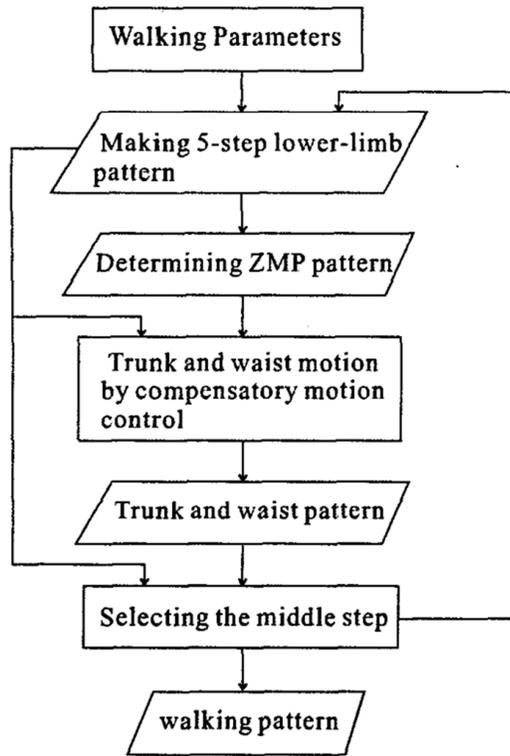
Figure 3.3: Online walking pattern generation architecture [38]

Another real-time walking pattern generator was developed by Sugihara, Nakamura and Inoue in 2002 [39]. In this method the control of center of gravity (CoG) is achieved by the indirect manipulation of ZMP. It consists of four parts; the first and second parts determine the planning and manipulation of the ZMP whereas in the last two parts CoG velocity decomposition to joint angles and local control of joint angles are adjusted. The main advantage of this method is its straightforward applicability. Since it uses a LIPM, the method can be applied to the robots with high DoF easily.

In 2004, Harada, Kajita, Kaneko and Hirukawa presented a real-time walking gait generation method similar to [39] [40]. In this method the reference generations of the CoG and ZMP trajectories are derived simultaneously. Compared with [39] the method proposed in [40] provides a faster and smoother gait transition from the previously calculated gait cycle. In addition [40] uses quasi-real-time connection in addition to the real-time connection between gait transitions. This allows a transition between highly varying step sizes. Due to its virtue, this method allows the regeneration, if the updated gait cycle fails to execute in within the time of current step sequence, of new walking gait cycle.

Kajita et al. presented a gait generation method which uses preview control of ZMP in 2003 [41]. This control method used in offline or online simulations which consists of three terms, the integral action on tracking error of ZMP, the state feedback and the preview action using the future reference. The dynamic model of the biped robot is simplified using a table cart model shown in Figure 3.4. This model is suggestive and intuitive for obtaining of ZMP references.
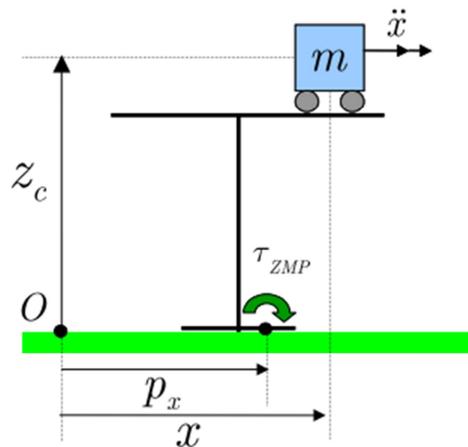
Figure 3.4: A table-cart model [16]

22

Tanaka et al. presented a real-time walking gait change for a humanoid robot HRP-2 in case of an emergency stop, in 2006 [42]. A similar approach to [39] is applied for the gait transition. The proposed method was able to cut the ZMP trajectory in case of an emergency while maintaining the balance of the robot [42]. The gait cycle transition is achieved by making a map of relation between the ZMP modification and the timing of command. The amount of modification was derived using the preview controller as in [41]. A sudden stop scenario was implemented on HRP-2 for the validation of this approach.

In 2006, Verrelst et al. proposed a method which changes the stepping of a gait with a fluent dynamic motion using the ZMP criterion [43]. Stability of this method is tested on HRP-2 by stepping over a large obstacle. Again preview control method is used to derive the modification of the ZMP reference in a way similar to [41]. In the experiments on HRP-2 this method is proven to be useful for reducing the reaction forces for dynamic motions such as overstretching the knees.

Nishiwaki and Kagami applied a stable walking pattern generation system which can update the pattern at a period of 40 milliseconds [44]. Similar to [41], [42] and [43], preview control is adopted for this method.

In 2008, Huang et al. proposed a walking pattern generator for walking on slopes and stairs [45]. This method embraces the preview control method and table-cart model in order to determine the future ZMP locations according to a known slope gradient. This method is applied on a simulation environment for different slope gradients varied between 5 to 20 percentages.

Erbatur and Kurt proposed a forward moving ZMP reference trajectory for a stable and human-like walk. The method employs Fourier series approximation to obtain CoM reference trajectory [46]. This method makes use of the periodicity of walking reference trajectories as is done with Fast Fourier Transforms (FFT) in [47]. The double support phase of the ZMP reference trajectory is obtained by Lanczos smoothing function in this method, as an additional advantage this function smoothen the peaks result in Gibbs phenomenon due to Fourier approximation. The user is allowed to define a walking period without the freedom of assigning the partitions of single and double support phases in it.

In [48] this downside is eliminated by defining a continuous ZMP reference generation which allows user to assign the durations of double and single support phases

within a walking period. This feature is especially useful since the tuning of double and single support phase partitions plays a crucial role in experiments as suggested in [49] and [50]. This method is tested via simulations on the full dynamics three-dimensional model of a 12-DoF biped robot.

In 2009, the CoM reference trajectory generation method in [48] is implemented on SURALP. The experiments verified the applicability of the proposed method for natural ZMP reference generation and CoM reference trajectory generation. In [51] an omni directional pattern generation method is proposed with the ZMP based reference algorithm in the context of gait generation. This method is tested via experimental studies on humanoid robot SURALP too.

3.1.2 Alternative Walking Reference Generation Methods

Although the ZMP criterion is the most widely used method for walking reference generation for bipedal robots there are alternative approaches too. These methods can be investigated under three different categories. Central Pattern Generation (CPG), parametric function based method and heuristic methods.

CPG is a bio-inspired technique often used for legged robots. Designing self-oscillating systems which allows the derivation of synchronized periodic motions of the joints is the main idea behind this method [52]. Although this technique is used for the walking reference generation of multi-legged robots (quadrupeds, hexapods) in general, some of the works [53-56] address biped robots as well. The stand-alone application of CPG for any mechanism is impossible due to the dynamics of the environment. As a result an additional algorithm or model is adopted for the implementations.

In 1990 Zheng proposed an autonomous gait synthesis mechanism for generating the motion trajectories of a biped robot [55]. The mechanism consists of a CPG, an adaptive neural network and a switching unit. CPG is responsible for generating gait patterns for both voluntary and involuntary joint motions. Here, if the motion is voluntary than the synchronized periodic walking trajectory is generated directly by CPG whereas if the motion is involuntary it is sent to adaptive neural network for generating reflexive motions accordingly. The switching unit is used for making real time decisions between voluntary and involuntary motions according to the environment.

In 1991 Taga et al. presented a CPG driven walking reference generation, the stability of the locomotion is maintained by a global limit cycle [54]. The global limit cycle is

achieved by using a nervous system which generates rhythmic joint motions. The nervous system composed of CPG driven neural oscillators and a musculo-skeletal system which includes Newton-Euler driven dynamic interactions with environment. Figure 3.5 presents the overall control architecture of the system. The stability of the method is verified by a simulation of 4 DoF planar biped robot.
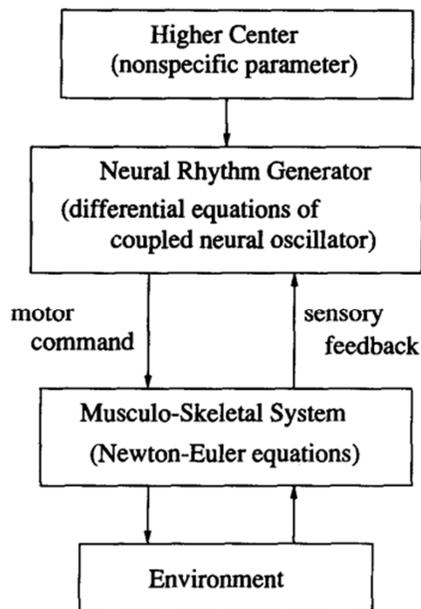
Figure 3.5: Control architecture proposed in [54]

In 2005, Aoi and Tsuchiya proposed a CPG based walking reference generation method which obtains steady walking by achieving a stable limit cycle [53]. In order to maintain the stable limit cycle during the walking of the robot, three preliminary problems are addressed. Designing the motions of the robot limbs, determining the interlimb coordination and connecting the joint motions to stable limit cycles through a relationship. The design of limb motions is managed by creating nominal trajectories of the joints of each limb. The phase of a nonlinear oscillator is used to obtain stable rhythmic motion. The interlimb coordination is achieved via the phase relation between the generated nonlinear oscillations. Finally, regarding the third problem the phases of oscillators are reset and modified nominal joint trajectories are generated according to sensor feedback. The proposed joint trajectory generation system is tested on HOAP-1, a 20 DoF kid-size humanoid robot, and stable walking is achieved.

25

In addition to the bio-inspired CPG techniques, there are also periodic function based walking reference generation techniques. These techniques generate a walking reference trajectory by combining periodic functions (sinusoid, cosine) according to kinematic or dynamic constraint conditions of the robot.

Kawamura et al. proposed a function based parametric trajectory generation method in 2000. The method based on the computation of foot position and orientation references with respect to the trunk coordinate frame [57]. Foot references are generated as sinusoidal functions in *x, y* and *z* directions. In 2004 this method is improved by adding kinematic constraints to the foot references [58]. The improved method states that the foot must land to the floor with zero velocity in order to expose minimum amount of impact from the floor. So the position, velocity and acceleration along *x, y* and *z* directions of each foot must be equal to zero during landing phase which means there are six constraint conditions. In z direction there is an additional constraint condition which states the swing foot reach its peak along z – direction at the half time of swing phase. According to the determined constraints the feet trajectories along *x* and *y* direction are designed as 5th order polynomial function of time whereas the feet trajectories along *z* direction designed as 6th order polynomial function of time. The method used in [58] is tested by experimental studies on a 14 DoF biped robot MARI-1.

Taşkıran et al. proposed a similar method with smooth foot trajectories and introduced a ground push motion in 2009 [59]. The foot references are generated as sinusoidal functions similar to [57] however the additional time phases are added to these functions in order to achieve smooth trajectories. The ground push motion is introduced for the foot reference trajectory along *z*-direction in order to obtain a successful take-off for the foot. The method is verified by stable walking of SURALP in experiments.

Apart from CPG and periodic function based methods, there are also direct applications of heuristic methods for walking reference trajectory generation. The works which uses such methods, proposed cost functions including the fall of the robot to ground. Therefore, the experimental studies are carried out using kid-size humanoid robots which do not severely damage by falling down.

Yamasaki, Endo, Kitano and Asada presented a method for humanoid walking acquisition through minimizing the energy consumption based on a two-stage genetic algorithm in 2002 [60]. In the first phase of the evolution, the total walking distance traveled without falling down is considered. The second phase calculates the sum of energy consumption for each joint during the walking. Each individual is tagged according to the

results obtained from the given phases and processed for cross-over and mutation. The resulting fitness functions by the evolutionary process are used for walking reference trajectory generation. The GA based walking references are compared with the conventional ones in terms of torque consumptions via walking experiments on a 26 DoF kid-size humanoid robot PINO. GA based walking references prove to be more energy efficient compared with the conventional method.

3.2. Reference Generation Tuning of Bipedal Robots

For a biped robot to practice a complex task, the generation of a walking reference generation is vital but not sufficient. Additional improvements of the walking in terms of speed, power consumption and stability are necessary. To design an optimal walking gait for biped robots is theoretically possible by using dynamic analysis. However the dynamic equations involved in a walking process are often too complex, especially for robots with large number of DoF. As a result the works on model-based non-heuristic optimal walking gait trajectory generation often used extremely simple biped models which make the direct applicability impossible.

In 1998, Roussel and Cannudas-de-Wit proposed a method to generate an energy optimal walking gait cycle [61]. However the presented method uses a simplified robot dynamics which ignores the effects of centripetal forces. Moreover the real-life phenomenons such as friction are not considered in dynamic equations of the biped model. The generated gait cycle is applied on simulation which uses a four DoF planar biped mechanism.

Chevallereau and Aoustin presented a method to determine the minimum energy consumption trajectory of a walking and running biped robot in 2001. [62] The proposed method assigns fourth order time polynomial functions to position and velocity of each joint using three different configuration phases for each step, namely; initial, intermediate and final. The results are applied to a four DoF planar biped robot via simulation.

Although [61] and [62] have contributions to field of biped robots in terms of theoretical guidance, the proposed methods are not suitable for experimental humanoid robot platforms. As a result most of the studies in this field employ a heuristic method in order to further improve the walking trajectory. This section presents a survey on the heuristic methods used for walking gait parameter tuning and improvement of walking gait of legged robots.

There are various heuristic methods applied to improve the gait or further tune the walking parameters of a biped robot. Fuzzy systems, genetic algorithm, neural networks, reinforcement learning, nelder-mead optimization and optimal gradient method are the ones used most commonly. These methods are preferred due to their robustness in search and optimization and easy adaptability.

In 2003 Erbatur and Bebek proposed an online fuzzy adaptation scheme for one of the walking trajectory parameters (x-reference offset) [63]. The algorithm runs offline. This parameter is assigned to compensate the uneven weight distribution of the biped robot in the

walking (x) direction. In order to maintain the robot's balance during the tuning simulations, virtual torsional springs are attached to the body origin of the biped robot about the x, y and z axes of the trunk. In addition, the resulting torque from the pitch torsional spring is used as an input to a fuzzy system which computes the x-reference offset. The x-ref asymmetry parameter converges to the same value after fuzzy training approaches using different initial values. The method is verified by a successful walk simulation after removing the virtual torsional springs.

Picado, Gestal, Lau, Reis and Tome proposed an automatic walking reference generation method for robotic soccer using GA in 2009 [64]. The joint trajectory planning is achieved by partial Fourier transforms and a GA is used for tuning the parameters of each partial Fourier transform. The fitness function is stated as the sum of the distance to the ball and average oscillation of the torso. The resulting Fourier transform parameters for walking reference generation are tested by simulations of 25 DoF kid-size humanoid robot NAO and stable walking is achieved.

Kim et al. proposed a method which determines optimal via-points data using a GA which minimizes the sum of deviation of velocities and accelerations [65]. This method further improves the reference trajectory of the joint velocities and accelerations of a ZMP based reference. The fitness function of the genetic algorithm is assigned as sum of square of differences of velocities and accelerations between the sampling times for each joint. Resulting trajectories are tested on an 8 DoF biped robot IWR-III and stable walking is achieved.

Chapter 4

4. SURALP: A FULL BODY HUMANOID ROBOT

SURALP is a full-body humanoid robot platform designed for bipedal walking experiments. The project was funded by TUBITAK in the construction period and completed in 2009. This chapter introduces SURALP in terms of hardware, implemented walking reference generation and control architecture. The overall view of SURALP is shown in Figure 4.1.
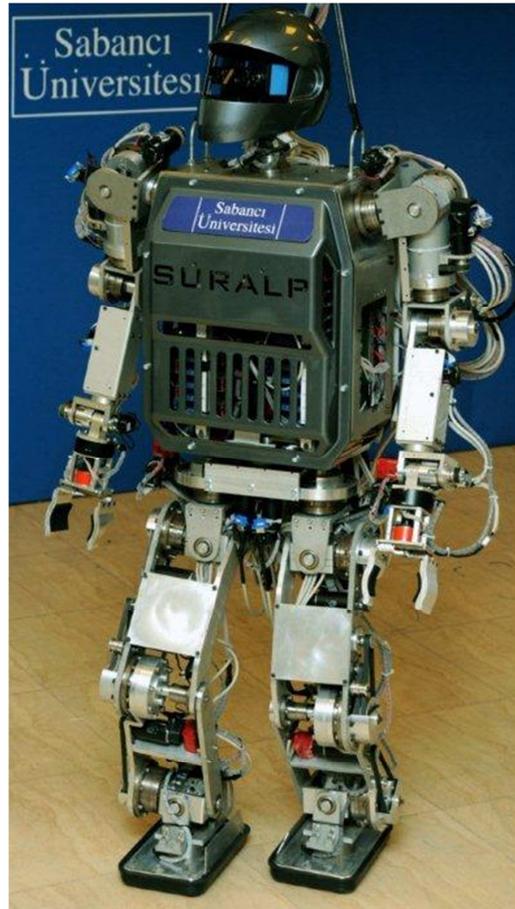
Figure 4.1: Humanoid robot SURALP

4.1. Hardware

This section briefly explains the hardware properties of SURALP in terms of mechanical design, actuation mechanism, controller hardware and sensor system. SURALP has 29-DoF, including 6-DoF legs, 6-DoF arms, 1 DoF hands, a 2-DoF neck and a 1-DoF

waist. It has a centralized controller hardware attached to its trunk. SURALP has a height of 1.66 m and a weight of 114 kg. The dimensions of the robot are given in Figure 4.2.
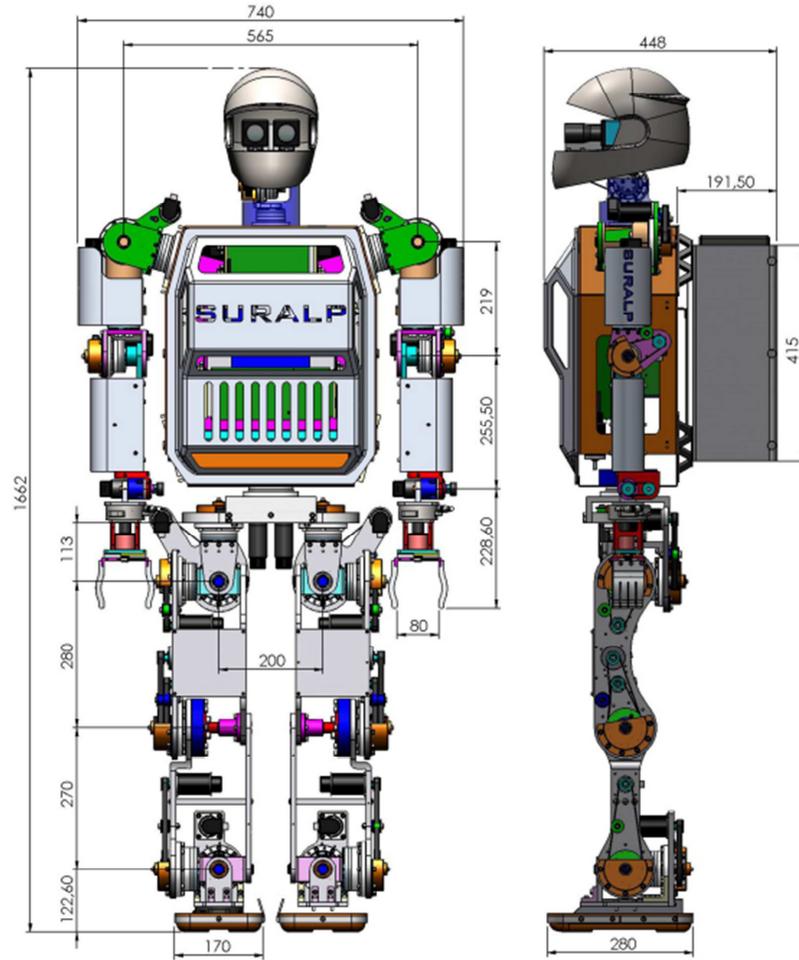
Figure 4.2: Dimensions of SURALP

The arrangement of the joints is designed as follows. At the legs, hips are composed of three orthogonal joint axes intersecting at a fixed point. The knee axis follows the pitch axis of the hip and the ankle is attuned to knee pitch axis. There are two ortogonal joint axes located at the ankle to move around ankle pitch and roll axes. The arms are connected to the trunk by shoulder joints which consists of three orthogonal axes like hip joints. The joint axis of elbow is configured to follow the the yaw axis of the shoulder. The elbow is followed by a roll axis in the forearm and a pitch axis in the wrist. At the endpoints of the arms there are 1 DoF grippers generating a linear motion to provide hand-like behaviour. Figure 4.3 shows the overall kinematic arrangment of the SURALP.
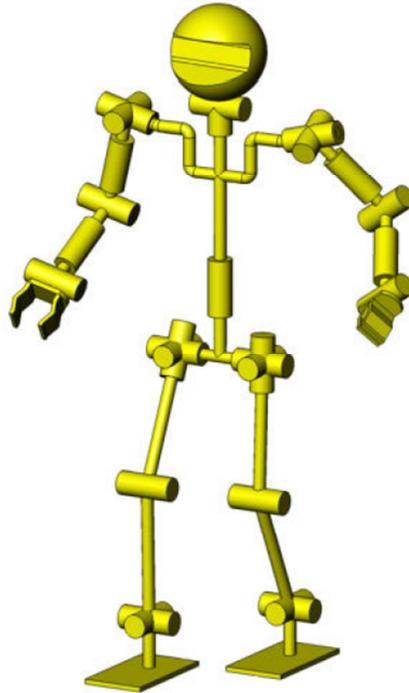
Figure 4.3: Kinematic arrangement of SURALP

The Denavit-Hartenberg axis assignment for the 6-DoF leg is shown in Figure 4.4. The Denavit-Hartenberg table is presented in Table 4.1.
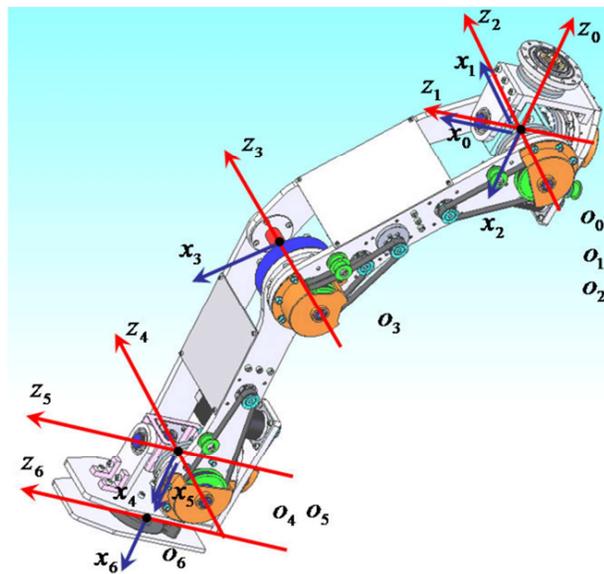
Figure 4.4: Denavit-Hartenberg axis assignment for 6-DoF leg

Table 4.1: Denavit Hartenberg table with respect to Figure 4.4

	a	α	d	θ
Link 1	0	$-90°$	0	θ_1^*
Link 2	0	$90°$	0	θ_2^*
Link 3	L_3	$0°$	0	θ_3^*
Link 4	L_4	$0°$	0	θ_4^*
Link 5	0	$-90°$	0	θ_5^*
Link 6	L_6	$0°$	0	θ_6^*

The length and weight information of each link are given in Table 4.2.

Table 4.2: Length and weight information of links

Upper Leg Length	280mm
Lower Leg Length	270mm
Sole-Ankle Distance	124mm
Foot Dimensions	240mm x 150mm
Upper Arm Length	219mm
Lower Arm Length	255mm
Robot Weight	114 kg

For the actuation of the joints DC motors are used. Every joint has a single motor for actuation except knee joint. In order to satisfy the high torque requirement knee joints are driven by two DC motors. Harmonic drive gears are used to obtain high reduction ratios within a compact space. Belt-pulley systems are used to transfer the generated motion from DC motors to harmonic drive gears. Table 4.3 shows motor powers together with the reduction ratios of harmonic drive gears and belt-pulley systems.

The sensor feedback is procured by joint incremental encoders which measure the motor angular position, force/torque sensors, an inertial measurement system and CCD cameras. The angular positions of the motors are measured by 500 ppr (pulse per revolution) optic incremental encoders. Force and torque measurements are taken by the 6 axis force/torque sensors attached to wrists and ankles. The Inertial measurement system consists

of a gyroscope, an inclinometer and a linear accelerometer positioned inside the trunk. All together these sensors give the information of roll and pitch angles and angular rates in roll, pitch and yaw axes. The CCD cameras are mounted to the head of the robot via USB cables for visual information. Table 4.4 shows the working ranges, mounting locations and allocated control board channels.

Table 4.3: Joint actuator specifications

Joint	Motor Power	Pulley Ratio	HD Ratio	Motor Range
Hip-Yaw	90W	3	120	-50 to 90 deg
Hip-Roll	150W	3	160	-31 to 23 deg
Hip-Pitch	150W	3	120	-128 to 43 deg
Knee 1-2	150W	3	160	-97 to 135 deg
Ankle-Pitch	150W	3	100	-115 to 23 deg
Ankle Roll	150W	3	120	-19 to 31 deg
Shoulder Roll 1	150W	2	160	-180 to 180 deg
Shoulder Pitch	150W	2	160	-23 to 135 deg
Shoulder Roll 2	90W	2	120	-180 to 180 deg
Elbow	150W	2	120	-49 to 110 deg
Wrist Roll	70W	1	74	-180 to 180 deg
Wrist Pitch	90W	1	100	-16 to 90 deg
Gripper	4W	1	689	0 to 80 mm
Neck Pan	90W	1	100	-180 to 180 deg
Neck Tilt	70W	2	100	-24 to 30 deg
Waist	150W	2	160	-40 to 40 deg

The controller electronics of the robot is based on dSPACE modular hardware. The DS1005 of dPACE family is the central controller board used for SURALP's control mechanism. Bipedal locomotion algorithms of the robot run on this board. In addition to the central DS-1005 board there are seven DS3001 incremental encoder input boards used for the connectivity of 35 joint encoders. Currently 31 of these connections are occupied by SURALP's encoders. A DS2002 board is used for A/D conversion of inertial and force/torque sensors and a DS2103 is used for the D/A conversion of reference signals of the actuators respectively.

34

Table 4.4: Sensory system of SURALP

	Sensor	Number of Channels	Range
All joints	Incremental optic encoders	1 channel per joint	500 pulses/rev
Ankle	F/T sensor	6 channels per ankle	± 660 N (x, y-axes) ± 1980 N (z-axis) ± 60 Nm (all axes)
Torso	Accelerometer	3 channels	± 2 G
	Inclinometer	2 channels	± 30 deg
	Rate gyro	3 channels	± 150 deg/s
Wrist	F/T sensor	6 channels per wrist	± 65 N (x, y-axes) ± 200 N (z-axis) ± 5 Nm (all axes)
Head	CCD camera	2 with motorized zoom	640x480 pixels (30 fps)

These boards are located in dSPACE Tandem autobobox. The overall hardware structure is presented in Figure 4.5.
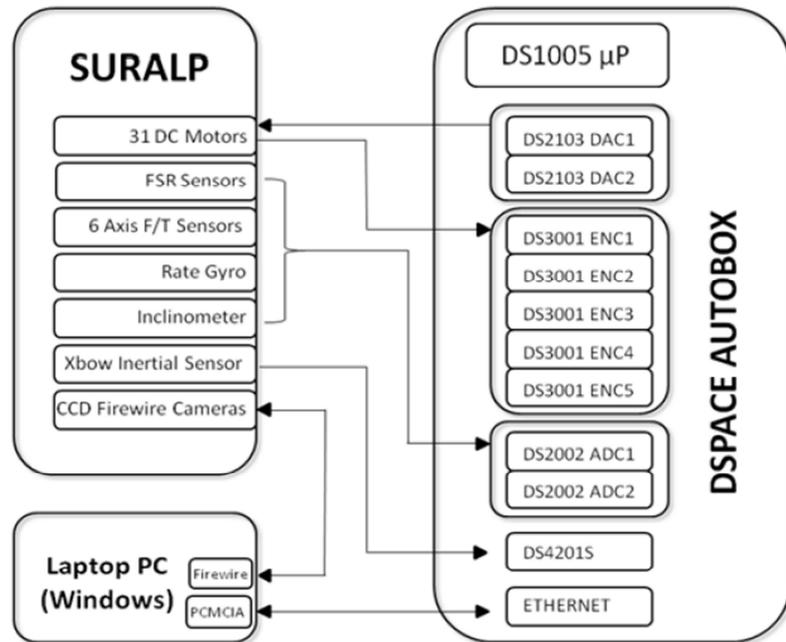
Figure 4.5: The complete hardware architecture of SURALP

4.2. ZMP Based Walking Reference Generation

In this section ZMP based walking reference generation of SURALP is explained. The sketch in Figure 4.6 shows the typical biped robot with 6-DoF legs for which the reference generation and control algorithms presented below can be applied.
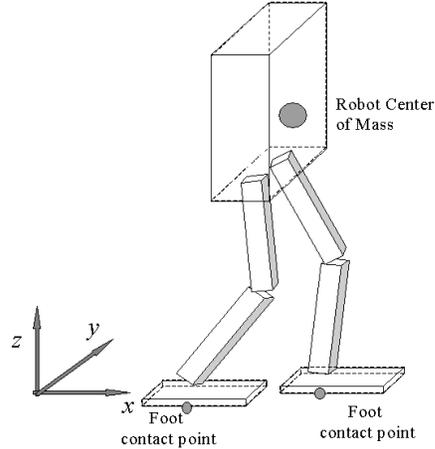
Figure 4.6: Typical biped robot kinematic arrangement. In single support phases, it behaves as an inverted pendulum.
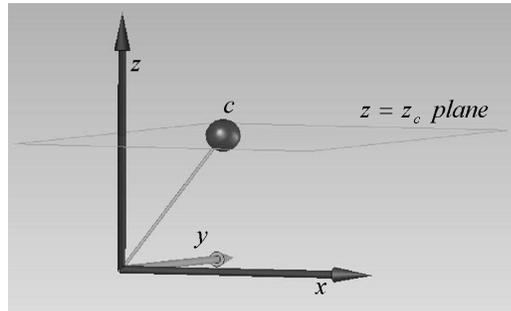
Figure 4.7: The linear inverted pendulum model

Instead of using this complex full dynamics models, the simple linear inverted pendulum model is more suitable for reference generation and controller design purposes. A point mass is assigned to the CoM of the robot and it represents the body (trunk) of the robot. The point mass is linked to a stable contact point on the ground over a massless rod. The rod is an idealized model of a supporting leg. The swing leg is assumed to be massless too. With the assumption of a fixed height for the robot CoM, a linear system which is decoupled in the x and y directions is obtained. The system described above is shown in Figure 4.7 $c = (c_x \quad c_y \quad c_z)^T$ is the coordinates of the point mass in this figure.

The ZMP criterion is the most widely accepted and used stability criterion in biped robotics. The ZMP is defined as the point on the $x-y$ plane where no horizontal torque components exist. For the point mass structure shown in Figure 4.7, the expressions for the ZMP coordinates p_x and p_y are [66]:

$$p_x = c_x - \frac{z_c}{g}\ddot{c}_x \tag{4.1}$$

$$p_y = c_y - \frac{z_c}{g}\ddot{c}_y \tag{4.2}$$

z_c is the height of the plane where the motion of the point mass is constrained and g is the gravity constant.

The ZMP and the CoM can be related to each other with the equations (4.1) and (4.2). A suitable ZMP trajectory can be generated for reference generation purposes. As the stability constraint, the ZMP should always lie in the supporting polygon defined by the foot or feet touching the ground. In the following, a ZMP reference is generated incrementally, by the discussion of three versions. The ZMP location can be chosen as the middle point of the supporting foot sole. In [66], the reference ZMP trajectory shown in Figure 4.8 is created with this idea. A is the distance between the foot centers in the y direction, B is the step size and T is the half of the walking period in this figure. It can be seen from the figure, firstly, step locations are determined. This selection of support foot locations and the half period T defines the staircase-like p_x and the square-wave structured p_y curves.

Investigations in [67-69] show that the natural human ZMP moves forward under the foot sole.

In order to address this issue, the p_x reference curve shown in Figure 4.9 is employed in [46]. In this figure, ZMP moves forward in single support phases too. b defines the range of the ZMP motion under the sole.

Still, there is room for improvement for the reference ZMP trajectory shown in Figure 4.9: The transition from right swing to left swing phases (and vice versa) occurs instantly, as indicated by the discontinuities in Figures 4.9.b and 4.9.c. [48] proposes the ZMP reference trajectory in Figure 4.10 to solve this problem by inserting double support phases between swing periods.
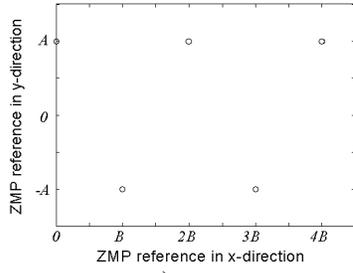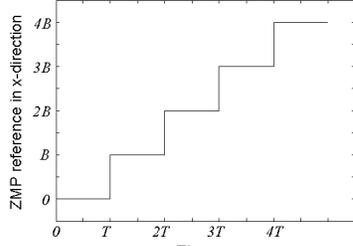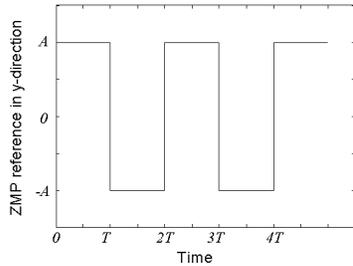
Figure 4.8: Fixed ZMP references.

a) $p_x^{ref} - p_y^{ref}$ Relation on the $x-y$ plane

b) p_x^{ref}, the x-axis ZMP reference

c) p_y^{ref}, the y-axis ZMP reference
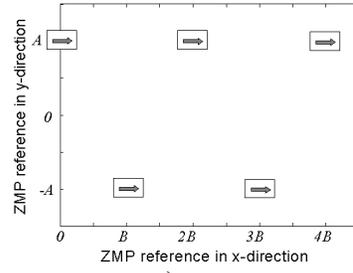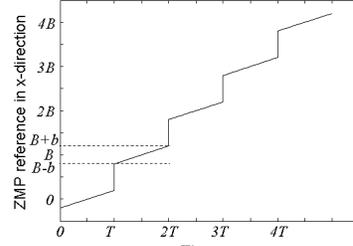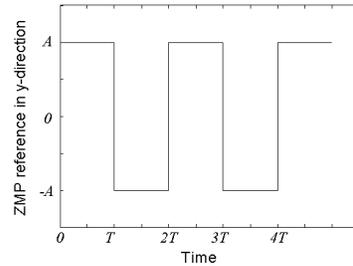
Figure 4.9: Forward moving ZMP reference

a) $p_x^{ref} - p_y^{ref}$ Relation on the $x-y$ plane

b) p_x^{ref}, a natural x-axis ZMP reference. Note the difference of the x-reference with the one shown in Fig. 4.8.

c) p_y^{ref}, the y-axis ZMP reference.
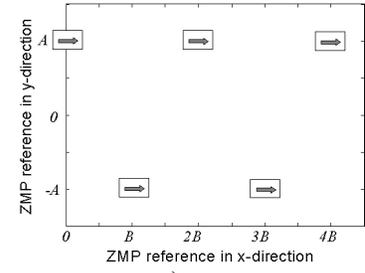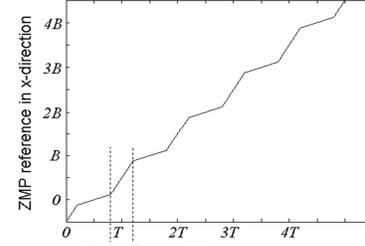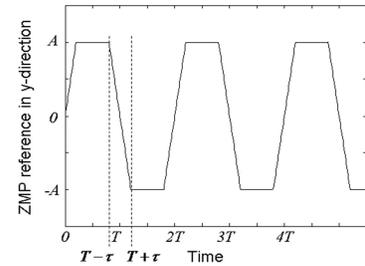
Figure 4.10: Forward moving ZMP references with pre-assigned double support phases.

a) $p_x^{ref} - p_y^{ref}$ Relation on the $x-y$ plane

b) p_x^{ref}, the x-axis ZMP reference

c) p_y^{ref}, the y-axis ZMP reference

38

The introduced ZMP reference trajectory is presented in Figure 4.10. The double support phase is introduced by using the parameter τ in this figure. A linear interpolation interval is inserted around multiples of the half walking period T. The durations of the intervals are equal to 2τ and they correspond to double support periods. Hence the double support period is freely adjustable with the parameter τ.

The mathematical description of the $p_x^{ref}(t)$ in Figure 4.10 is given by

$$p_x^{ref} = \frac{B}{T}(t - \frac{T}{2}) + p_x^{\prime ref} \tag{4.3}$$

where $p_x^{\prime ref}$ is periodic with period T. $p_x^{\prime ref}$ can be expressed as a combination of three line segments on $[0, T]$.

$$p_x^{\prime ref} = \begin{cases} \Omega_1 + \sigma_1 t & \text{if} \quad 0 \le t \le \tau \\ \Omega_2 + \sigma_2 t & \text{if} \quad \tau < t \le T - \tau \\ \Omega_3 + \sigma_3 t & \text{if} \quad T - \tau < t \le T \end{cases} \tag{4.4}$$

Here,

$$\Omega_1 = 0, \quad \sigma_1 = \frac{\delta}{\tau},$$

$$\Omega_2 = \delta - \tau \sigma_2, \quad \sigma_2 = \frac{-2\delta}{T - 2\tau}, \tag{4.5}$$

$$\Omega_3 = -\delta - (T - \tau)\sigma_3, \quad \sigma_3 = \sigma_1.$$

with

$$\delta = \frac{T - 2\tau}{T} (\frac{B}{2} - b). \tag{4.6}$$

Note that δ is the magnitude of peak difference between p_x^{ref} and the non-periodic component $\frac{B}{T}(t - \frac{T}{2})$ of p_x^{ref}. δ can be computed from Figure 4.11 geometrically.

$p_y^{ref}(t)$ in Figure 4.10 is expressed as

$$p_y^{ref} = \sum_{k=1}^{\infty} A(-1)^k \left[\frac{2}{2\tau}(t - kT)[u(t - (kT - \tau)) - u(t - (kT + \tau))] \right.$$

$$\left. + [u(t - (kT + \tau)) - u(t - (kT + T - \tau))] \right] \tag{4.7}$$

where $u(\cdot)$ represents the unit step function.

Having defined the curves, and hence the mathematical functions for $p_x^{ref}(t)$ and $p_y^{ref}(t)$, the next step is obtaining CoM reference trajectories from $p_x^{ref}(t)$ and $p_y^{ref}(t)$. There are various approaches used for the CoM computation from ZMP references [66-69]. From these, the authors in [46] implement a straight walk ZMP reference and perform Fourier series approximation technique to compute the CoM reference trajectory and [48] presents experimental results for this method on the humanoid robot SURALP . [41] uses preview control method to compute the CoM reference trajectory and [42] shows experimental results for this method on the humanoid robot HRP-2.

Position control schemes for the robot joints with joint references obtained by inverse kinematics from the CoM locations can be derived once the CoM trajectory is computed.

Defining $\omega_n \equiv \sqrt{g/z_c}$, we can rewrite (4.1) and (4.2) for the reference variables as follows.

$$\ddot{c}_x^{ref} = \omega_n^2 c_x^{ref} - \omega_n^2 p_x^{ref}$$

(4.8)

$$\ddot{c}_y^{ref} = \omega_n^2 c_y^{ref} - \omega_n^2 p_y^{ref}$$

(4.9)

Note that the y-direction ZMP reference $p_y^{ref}(t)$ is a periodic function with the period $2T$. It is reasonable to assume that $c_y^{ref}(t)$ is a periodic function too and that it has the same period. Hence, it can be approximated by a Fourier series
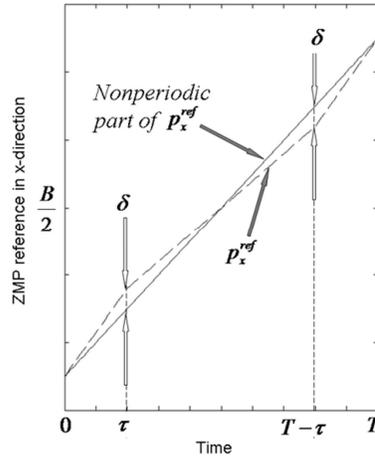
Figure 4.11: The parameter δ

40

$$c_y^{ref}(t) = \frac{a_0}{2} + \sum_{k=1}^{\infty} a_k \cos(\frac{2\pi kt}{2T}) + b_k \sin(\frac{2\pi kt}{2T}) \qquad (4.10)$$

By (9) and (10), p_y^{ref} can be expressed as

$$p_y^{ref}(t) = c_y^{ref} - \frac{1}{\omega_n^2} \ddot{c}_y^{ref} = \frac{a_0}{2} + \sum_{k=1}^{\infty} a_k (1 + \frac{\pi^2 k^2}{\omega_n^2 T^2}) \cos(\frac{2\pi kt}{2T}) + b_k (1 + \frac{\pi^2 k^2}{\omega_n^2 T^2}) \sin(\frac{2\pi kt}{2T}) \qquad (4.11)$$

Noting that this expression in the form of a Fourier series for $p_y^{ref}(t)$, and since $p_y^{ref}(t)$ is an odd function, we can conclude that the coefficients $a_0/2$ and $a_k (1 + (\pi^2 k^2)/(\omega_n^2 T^2))$ for $k = 1,2,3,\cdots$ are zero. In order to compute the coefficients $b_k (1 + (\pi^2 k^2)/(\omega_n^2 T^2))$ we can employ the Fourier integral:

$$b_k (1 + \frac{\pi^2 k^2}{\omega_n^2 T^2}) = \frac{2}{2T} \int_0^{2T} p_y^{ref} \sin(\frac{2\pi kt}{2T}) dt \qquad (4.12)$$

As a result, after some arithmetical steps (omitted here due to space considerations), the Fourier coefficients b_k of $c_y^{ref}(t)$ in (4.10) can be obtained as

$$b_k = \begin{cases} \frac{\omega_n^2 T^2}{\omega_n^2 T^2 + \pi^2 k^2} \frac{2A}{\pi k} \left\{ \left[\frac{2}{\tau} \left\langle \frac{T}{\pi k} \sin(\frac{\pi k \tau}{T}) - \tau \cos(\frac{\pi k \tau}{T}) \right\rangle \right] + \left[\cos(\frac{\pi k \tau}{T}) - \cos(\frac{\pi k (T - \tau)}{T}) \right] \right\} & \text{if } k \text{ is odd} \\ \\ 0 & \text{if } k \text{ even} \end{cases} \qquad (4.13)$$

for $k = 1,2,3,\cdots$.

The second step is finding the Fourier series coefficients for c_x^{ref}. In Figure 4.10 $p_x^{ref}(t)$ is not a periodic function. It cannot be expressed as a Fourier series. However, as expressed above, this function is composed of the periodic function $p_x'^{ref}$ and the non-periodic function $(\frac{B}{T}(t - \frac{T}{2}))$. The periodic part of $p_x^{ref}(t)$ is shown in Figure 4.12. It is again a reasonable assumption that c_x^{ref} has a periodic part and a non-periodic part too. Further, if we suppose that the two non-periodic parts (of $p_x^{ref}(t)$ and c_x^{ref}) are non-equal, then the difference $p_x^{ref}(t) - c_x^{ref}$ will be non-periodic. This is not expected in a continuous walk as the one described in Figure 4.10.

41

Therefore we conclude that the non-periodic parts of the two functions are equal. Note that, as shown in Figure 4.12, the period of the periodic part of $p_x^{ref}(t)$ is T and we can make the same statement for the period of the periodic part of c_x^{ref}. Finally, c_x^{ref} can be expressed as

$$c_x^{ref} = \frac{B}{T}(t - \frac{T}{2}) + \frac{\alpha_0}{2} + \sum_{n=1}^{\infty} \alpha_k \cos(\frac{2\pi nt}{T}) + \beta_k \sin(\frac{2\pi nt}{T}) \tag{4.14}$$
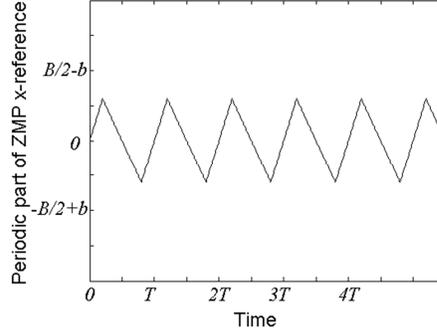
Figure 4.12: $p_x'^{ref}(t)$, the periodic part of the x-direction ZMP reference $p_x^{ref}(t)$

Recalling (4.8), with (4.14) the expression for $p_x^{ref}(t)$ with a Fourier series is

$$
\begin{aligned}
p_x^{ref}(t) &= c_x^{ref} - \frac{1}{\omega_n^2} \ddot{c}_x^{ref} \\
&= \frac{B}{T}(t - \frac{T}{2}) + \frac{\alpha_0}{2} + \sum_{n=1}^{\infty} \alpha_k(1 + \frac{\pi^2 k^2}{\omega_n^2 T^2})\cos(\frac{2\pi kt}{T}) + \beta_k(1 + \frac{\pi^2 k^2}{\omega_n^2 T^2})\sin(\frac{2\pi kt}{T})
\end{aligned} \tag{4.15}
$$

Therefore the Fourier coefficients of $p_x'^{ref}(t)$, the periodic part of $p_x^{ref}(t)$, are $\alpha_0/2$, $\alpha_k(1 + \pi^2 k^2/\omega_n^2 T^2)$ and $\beta_k(1 + \pi^2 k^2/\omega_n^2 T^2)$ for $k = 1, 2, 3, \cdots$. The Fourier coefficients $\alpha_0/2$, $\alpha_k(1 + \pi^2 k^2/\omega_n^2 T^2$ of $p_x'^{ref}(t)$ shown in Figure 4.12 are zero because this is an odd function. The coefficients for $\beta_k(1 + (\pi^2 k^2)/(\omega_n^2 T^2))$ can be found by

$$\beta_k(1 + \pi^2 k^2/\omega_n^2 T^2) = \frac{2}{T}\int_0^T p_x'^{ref}(t)\sin(\frac{2\pi kt}{T})dt \tag{4.16}$$

This yields the result

$$
\beta_k = \frac{\omega_n^2 T^2}{\pi^2 k^2 + \omega_n^2 T^2} \frac{2}{\pi k} \left\{ \sigma_1 \left[-\tau \cos\left(\frac{2\pi k \tau}{T}\right) + \frac{T}{2\pi k} \sin\left(\frac{2\pi k \tau}{T}\right) \right] \right.
$$
$$
+ \sigma_2 \left[\tau \cos\left(\frac{2\pi k \tau}{T}\right) - \frac{T}{2}\left(\cos\left(\frac{2\pi k \tau}{T}\right) \right) \right.
$$
$$
\left. \left. - \frac{T}{2\pi k} \sin\left(\frac{2\pi k \tau}{T}\right) \right] \right\}
\tag{4.17}
$$

for $k = 1, 2, 3, \cdots$.

The curves obtained for c_x^{ref} and c_y^{ref} are shown in Figure 4.13 together with the corresponding original ZMP references (as defined in Figure 4.10). The infinite sums in (4.10) and (4.14) are approximated by finite sums of N terms ($N = 24$).In Figure 4.13, the following parameter values are used: $A = 0.1$ m, $B = 0.1$ m, $b = 0.04$, $T = 1$ s and $\tau = 0.2$ s.

In addition to the CoM references, foot position reference trajectories have to be designed too: Inverse kinematics then can be employed to find the reference positions of the leg joints which bridge the CoM and the feet. The x and z direction components of the foot trajectories are shown in Figure 4.14.a and Figure 4.14.b respectively. These curves are smooth combinations of sinusoidal and constant segments. h_s is the step height parameter. T_{ds} and T_{ss} represent the double and single support periods, respectively. B is the step size from Figure 4.10. The y direction trajectories are constant at $-A$ and A for the right and left feet, respectively, where A is half of the foot to foot y direction distance also shown in Figure 4.10. The foot orientation references used in inverse kinematics are fixed and they are computed for feet parallel to the robot body.
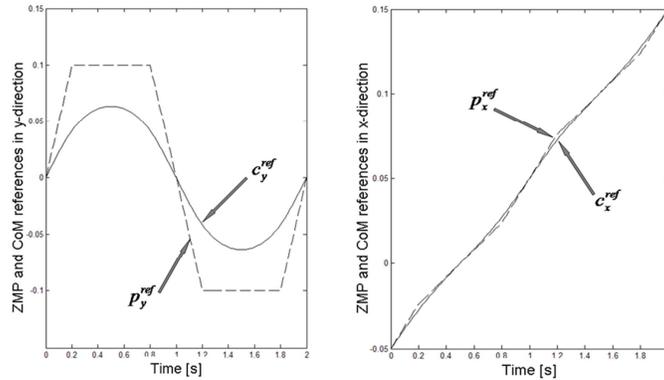
Figure 4.13: x and y-direction CoM references together with the corresponding original ZMP references

43
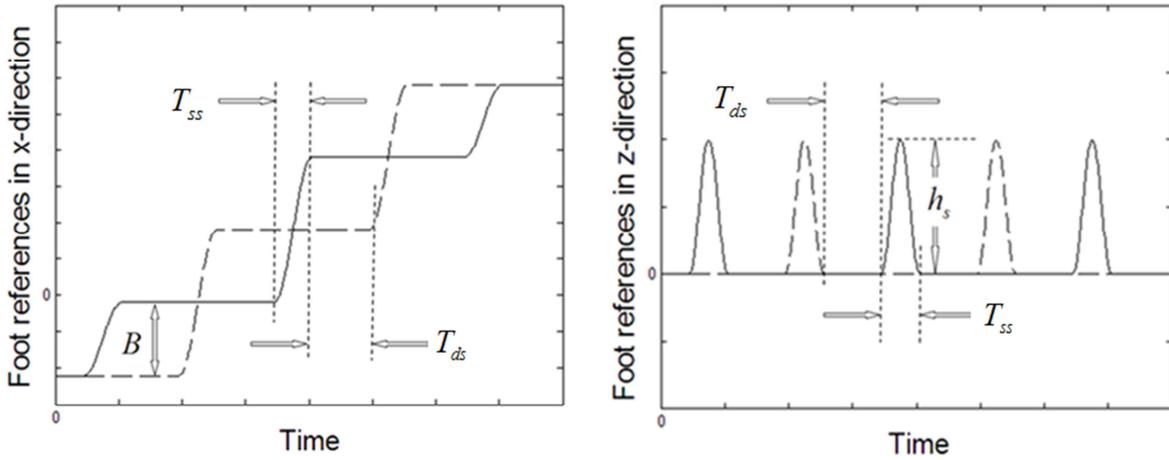
a)

b)
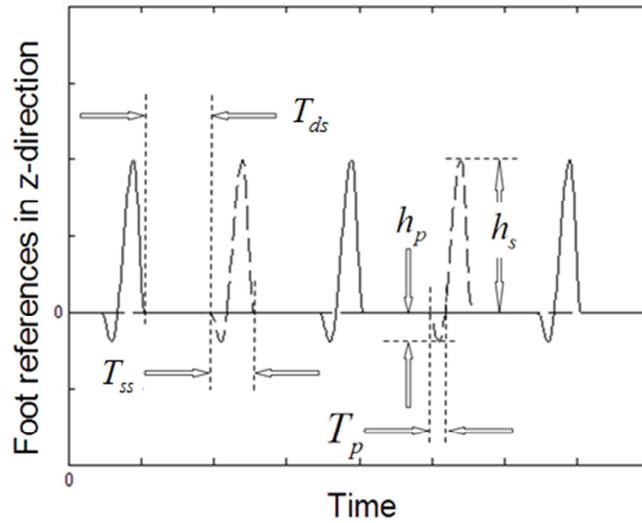
c)

Figure 4.14: x and z-direction foot references expressed in the world frame. Solid curves belong to the right foot, dashed curves indicate left foot trajectories.

For the implementation on SURALP, a further modification is employed. A "kick" period is introduced at the beginning of the swing phases to ease take-off of the swing foot. This version of foot z-directional references is shown in Figure 4.14.c.

4.3. Control Algorithm

The walking control approach of SURALP is as follows. Firstly, the joint position references are generated through inverse kinematics from CoM and swing foot references defined in world frame coordinates are obtained as shown in previous section. Independent PID controllers are used for joint position control. A set of compensators are then employed during the walk for the balance and foot-ground interaction enhancements. A block diagram of the controllers used is shown in Figure 4.15.
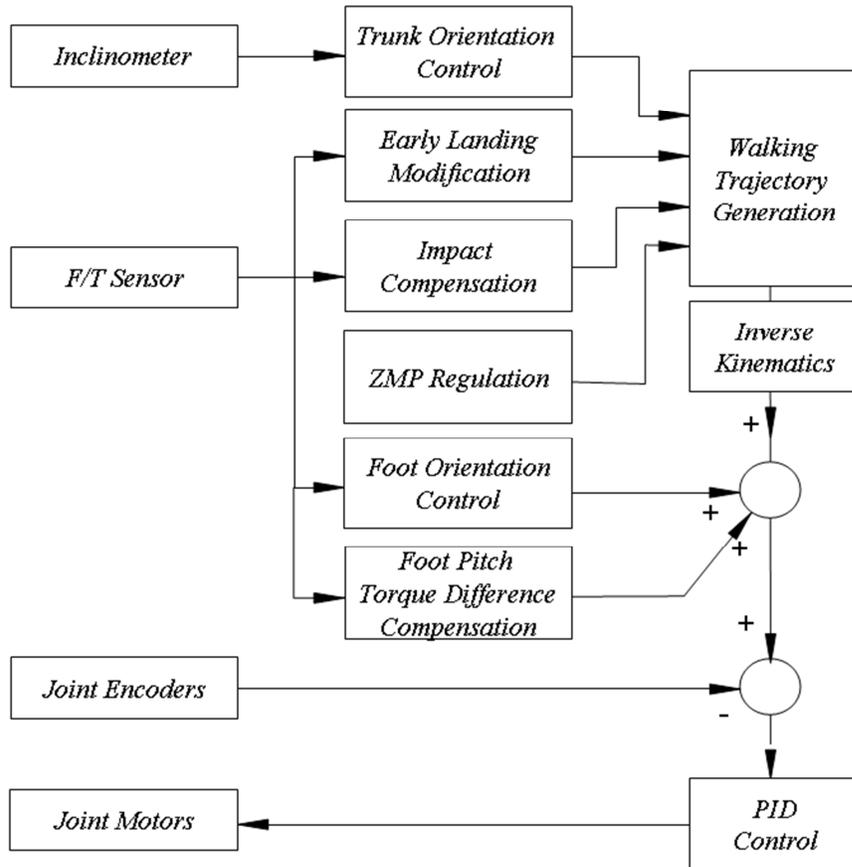
Figure 4.15: The control block diagram of SURALP

Trunk orientation control, ZMP regulation and the foot pitch torque difference compensation are employed only during the automatic robot homing procedure. Early landing modification, foot orientation control and impact compensation constitute the basic walking control algorithm together with reference generation and PID control. [74] Examines the tasks of the blocks in this control scheme in detail.

Chapter 5

5. GAIT TUNING VIA GENETIC ALGORITHM WITH UNCONSTRAINED JOINT VELOCITIES

Evolutionary algorithms can be defined as a generic-population based meta-heuristic optimization algorithms which use the principles of biological evolution process such as selection, reproduction, recombination and mutation. Genetic algorithms can be seen as one of the implementation of evolutionary algorithms. They are applied as a search heuristic which mimics the process of natural evolution. They are proven to be robust for search and optimization problems [70]. In addition genetic algorithm uses randomized operators instead of deterministic rules which make it suitable for the proposed non-deterministic problem.

5.1. Problem Definition

There are many parameters involved in the generation of walking reference of a humanoid robot. Proper tuning of these parameters is necessary to improve the walking performance of the robot. The walking speed is one of the key features. It is a function of several walking reference generation parameters. The average velocity is considered in this thesis as a command variable and related walk parameters are tuned to generate a reference with this locomotion velocity. The average velocity is defined as follows:

$$v_{average} = \frac{B}{T_{ds} + T_{ss}}$$

(5.1)

where B is the step size, T_{ds} is the double support period and T_{ss} is the single support period defined in section 4.2. The genetic algorithm is implemented for tuning T_{ds} and T_{ss} for a given $v_{average}$ value. B is then determined automatically according to (5.1).

5.2. The Setting of Chromosome

After the input parameters (often named as individuals) are defined, the genetic algorithm operates through chromosomes, formed string values of joined parameter values, to mimic the natural evolution. A chromosome can be formed by the use of the binary alphabet for the string [71]. For this problem each of the genes (T_{ds} and T_{ss}) are represented by a 8-bit binary number

such that one unit change within the strings will change the parameters by 0.01 sec. A sample chromosome and corresponding parameter values are given in Figure 5.1 below.

$$\boxed{01100110} \; \boxed{00101100}$$

$$T_{ds} = 1.02s \qquad T_{ss} = 0.44s$$
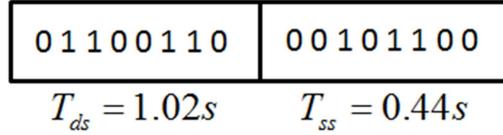
Figure 5.1: Sample chromosome and corresponding parameter values

Since the GA parameters will have physical values the first set of genes are generated within a physically reasonable interval. The intervals of T_{ds} and T_{ss} are set as follows for the first generation.

$$
\begin{aligned}
&T_{ds_{min}} \leq T_{ds} \leq T_{ds_{max}} \\
&T_{ds_{min}} = 0.2s, T_{ds_{max}} = 2.2s \\
&T_{ss_{min}} \leq T_{ds} \leq T_{ss_{max}} \\
&T_{ss_{m'n}} = 0.02s, T_{ss_{max}} = 2.5s
\end{aligned}
\tag{5.2}
$$

5.3. Dependent Walking Reference Generation Parameters

Some of the parameters in the walking reference generation are related with each other. The step size (B) of the robot has a direct relation with the step height (h_s). As B increases, h_s also has to be increased to maintain a reasonable foot reference trajectory in z-direction. As a result, a simple linear correlation is applied between B and h_s values. Figure 5.2 shows this relation.

In addition to the h_s, the height of the legs (h_{leg}) are also related with step size. The specified B value has to be in the work space of the given robot orientation. This relation can be obtained from trigonometric equations. Figure 5.3 shows the robot orientation in the case of the maximum B value for a given h_{leg}.

47
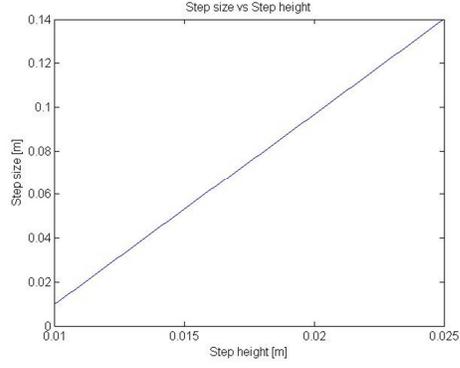
Figure 5.2: Linear relation between B and h_s
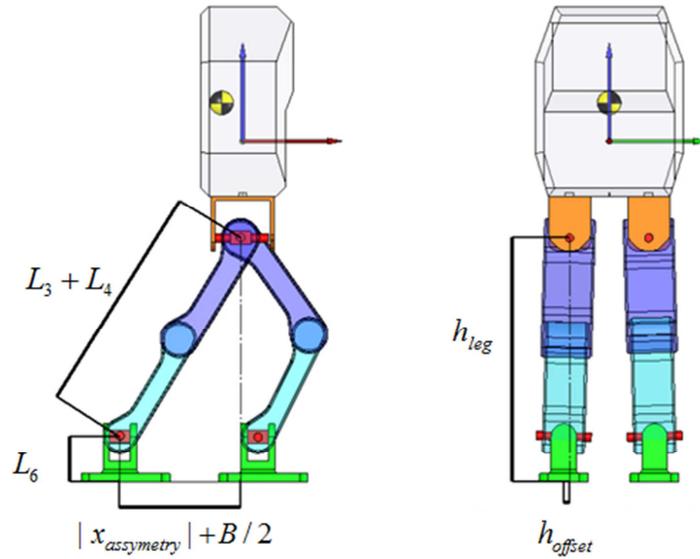
Figure 5.3: The trigonometric relation between h_{leg} and B

Here h_{offset} is the lateral distance between foot sole center and the hip frame of the robot. Using the trigonometric relations in Figure 5.3 the relation between h_{leg} and B is obtained as the inequality below;

$$h_{leg} \leq \sqrt{(L_3 + L_4)^2 - (B/2 + |x_{assymetry}|)^2 - h_{offset}^2} + L_6 \tag{5.3}$$

h_{leg} is limited due to the physical constraints of SURALP. As a result the generated B value also has an upper bound.

48

5.4. Simulation Scenario

A Newton-Euler method based full-dynamics 3D simulation and animation environment as described in [72] is used for simulation studies to observe the results of the GA implementation. In Figure 5.4, a view of the mentioned animation is presented. In this system, an adaptive penalty based method is employed to model the ground contact. The details of the simulation algorithm and the contact model can be found in [72].
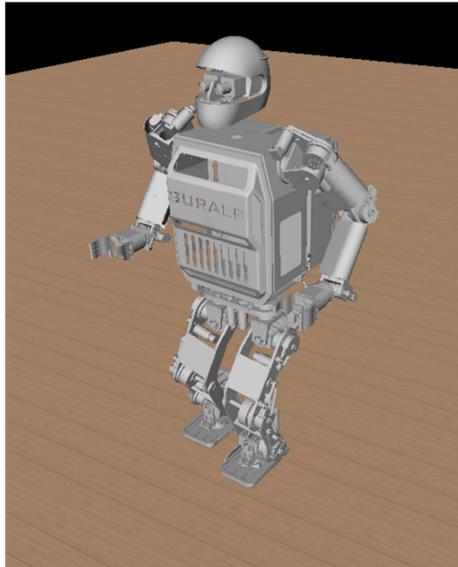
Figure 5.4: The animation window

5.5. Virtual Walking Aid and The Fitness Function

5.5.1. Virtual Walking Aid

In the case of an inadequate parameter selection, the robot will lose its balance and fall in an unrecoverable manner. It is observed that with the ranges of the parameters used in GA, many individuals cannot maintain the stability of the robot. After the start of the simulation if the value of the parameter is unfeasible the robot falls before completing first step. However, in order to assess the feasibility of all individuals (naturally falling ones and naturally not falling ones) in the same standard way, a sufficient number of steps have to be completed by the biped robot without falling down. Therefore, a mechanism is required to keep the robot walking even when the generated parameters are not suitable for steady walking.

The body orientation with respect to a fixed coordinate frame is one of the measures of bipedal robots balance. This orientation can be represented by a set of roll, pitch and yaw angles. In Figure 5.5 these angles are denoted by α, β and γ respectively. In this work virtual torsional spring-damper systems are employed to resist the deviations of these angles from zero and to pull them to the vicinity of zero. By doing so it is aimed to keep robot stable even for parameter sets unsuitable for stable walking. The torsional spring-damper systems are attached to x (red), y (green) and z (blue) axes as shown in Figure 5.5. The value of the spring constant employed is 500 N/m and the damper coefficient is set to be 3000 Ns/m by trial and error. The adjusted coefficients leave a reasonable motion space for the robot trunk.
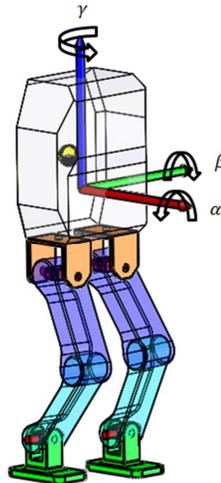
Figure 5.5: Virtual torsional spring-damper systems attached to trunk of the robot

Angular deflections around trunk coordinate frame axes with and without external support for the current walking parameters are tested on simulations. The resulting angles are shown in Figure 5.6.
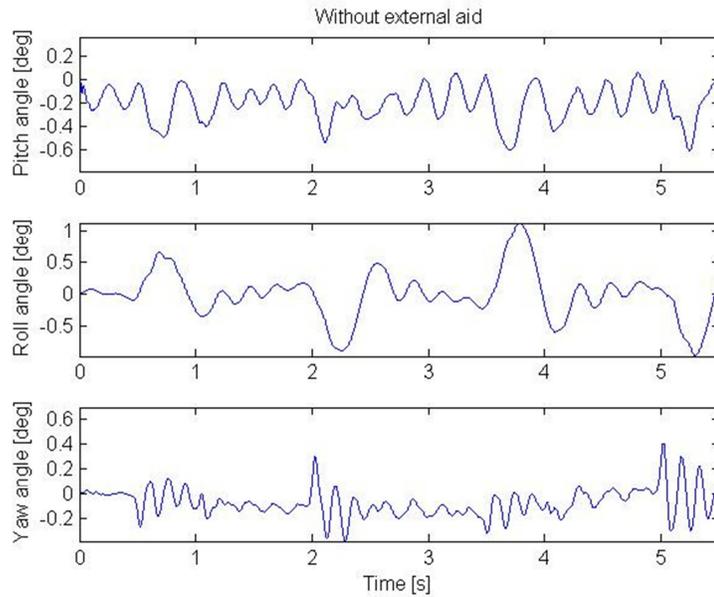
Figure 5.6.a: The deflections around trunk coordinate axes without external aid
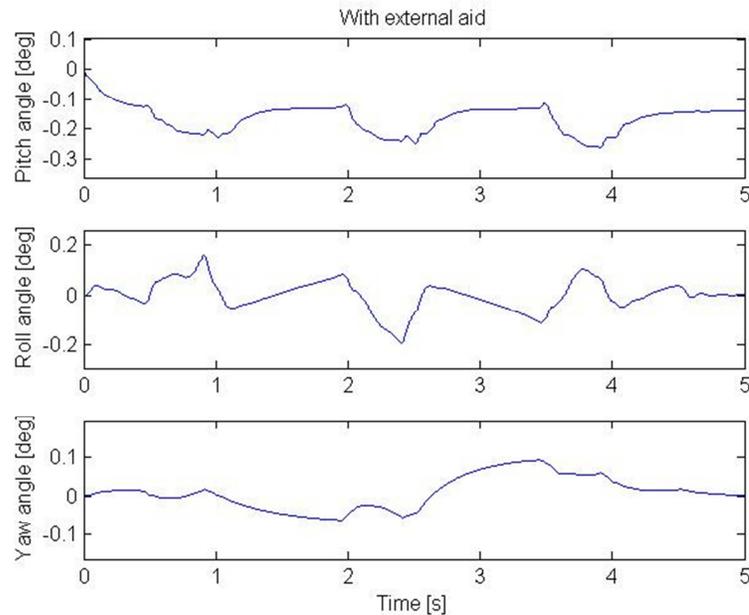
Figure 5.6.b: The deflections around trunk coordinate axes with external aid

As seen from figures the peak-to-peak angular deflections around trunk coordinate frames decreased for each axes with a plausible trunk motion space. Notice also that the decrease in trunk deflections also varies for different axes.

The effect of the proposed spring-damper system can be described by the equations below;

$$
\begin{aligned}
u_{sd\,roll} &= K_{spring}.\alpha + K_{damper}.\dot{\alpha} \\
u_{sd\,pitch} &= K_{spring}.\beta + K_{damper}.\dot{\beta} \\
u_{sd\,yaw} &= K_{spring}.\gamma + K_{damper}.\dot{\gamma}
\end{aligned}
\tag{5.4}
$$

Where $u_{sd\,pitch}$, $u_{sd\,roll}$ and $u_{sd\,yaw}$ denote the supporting torques around the x, y and z axes, respectively.

Maintaining the balance of the simulated robot by virtual torsional springs is also applied in [73].

5.5.2. The Fitness Function

Given a particular chromosome, the fitness function returns a single numerical value which corresponds to a performance measure of the represented individual [71].

The generated torques from torsional spring-damper systems can be considered as a stability measure during the walking of the robot. As the angular deflection around the trunk coordinate frame decreases, the resistance of torsional spring-damper system will decrease as well. A formulation of the torsional spring damper resistance can be applied as a performance measure for GA. For this purpose the following fitness function is defined.

$$
F_{fitness} = u_{ds_{average}} + u_{ss_{average}}
\tag{5.5}
$$

with

$$
u_{ds_{average}} = \sum_{t=0}^{t=T_{ds}} \frac{\left(\left|u_{sd\,pitch}\right| + \left|u_{sd\,roll}\right| + \left|u_{sd\,yaw}\right|\right)}{T_{ds}} + \sum_{t=T_{ss}+T_{ds}}^{t=T_{ss}+2T_{ds}} \frac{\left(\left|u_{sd\,pitch}\right| + \left|u_{sd\,roll}\right| + \left|u_{sd\,yaw}\right|\right)}{T_{ds}}
$$
$$
+ \sum_{t=2T_{ss}+2T_{ds}}^{t=2T_{ss}+3T_{ds}} \frac{\left(\left|u_{sd\,pitch}\right| + \left|u_{sd\,roll}\right| + \left|u_{sd\,yaw}\right|\right)}{T_{ds}}
\tag{5.6}
$$

and

$$u_{ss_{average}} = \sum_{t=T_{ds}}^{t=T_{ds}+T_{ss}} \frac{\left(\left|u_{sd\,pitch}\right| + \left|u_{sd\,roll}\right| + \left|u_{sd\,yaw}\right|\right)}{T_{ss}} + \sum_{t=2T_{ds}+T_{ss}}^{t=2T_{ds}+2T_{ss}} \frac{\left(\left|u_{sd\,pitch}\right| + \left|u_{sd\,roll}\right| + \left|u_{sd\,yaw}\right|\right)}{T_{ss}}$$

$$+ \sum_{t=3T_{ds}+2T_{s}}^{t=3T_{ds}+3T_{ss}} \frac{\left(\left|u_{sd\,pitch}\right| + \left|u_{sd\,roll}\right| + \left|u_{sd\,yaw}\right|\right)}{T_{ss}} \qquad (5.7)$$

The fittest individuals of the population are chosen using the minimum values of $F_{fitness}$ because the resistance (support) of external support torques will decrease as $F_{fitness}$ decreases. The duration of each walking simulation is described by three steps. Since the time consumption of simulation is increased with the number of steps in walking cycle, the minimum required step number is determined as three. The sum of the absolute average values of external torques is more suitable compared with an integral of support forces. These summations are separated into double support period and single support period respectively. Compared to the double support phase, the single support phase is more difficult to stabilize by its nature. Hence the resulting angular deflections are larger in the single support phase. The separation of the averaging periods in the equation above is employed in order to prevent biased computations in favor of the support values during double support periods.

5.6. The Selection of the Next Generation

In a natural environment, the organisms with the highest reproduction rate survive through time. This process, often named as *survivor of the fittest*, composes the core structure of the GA. During the reproductive phase of the GA, certain individuals are selected from the population according to their fitness values. [71] This process, producing offspring individuals, creates the next generation.

The candidates chosen for this process are called parents. Usually the parents are selected randomly using a scheme which favors the more fit individuals. After the selection process, their chromosomes are recombined. In traditional GA, crossover and mutation are the two typical mechanisms.

In this implementation the parent candidates are chosen directly through the fitness value. The crossover and mutation operators are used on randomly selected parents from the candidate pool. Also to reduce the probability of divergence, a number of *elite* (the fittest) members of each population are transferred to the next one.

5.6.1. The Cross-over Mechanism

Crossover takes two individuals, and cuts their chromosome strings at some randomly chosen position. The produced segments are named as *tails* and *heads*. These segments are swapped over to produce two new full length chromosomes. This is known as single point crossover. Figure 5.7 shows a crossover sample for given parents.
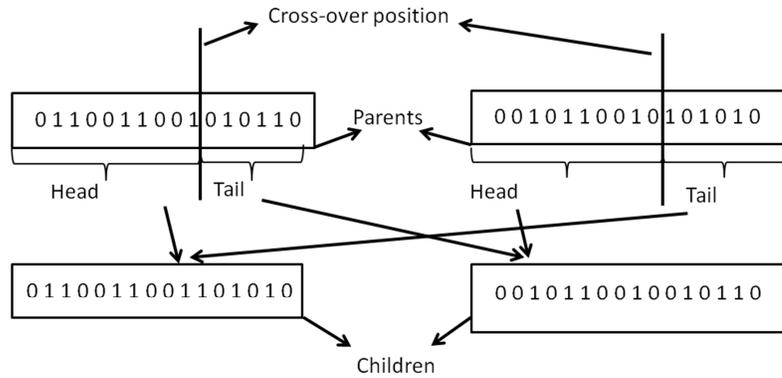
Figure 5.7: A sample cross-over

5.6.2. The Mutation Mechanism

After the crossover process, mutation is applied to randomly chosen individuals. It alters a randomly chosen gene. This mechanism provides a small amount of random search, and helps ensure that no point in the search space has a zero probability of being examined [71]. In Figure 5.8 a mutation scheme of an individual is presented.
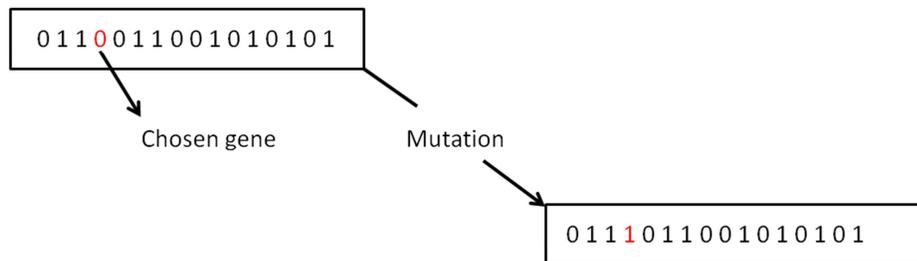
Figure 5.8: Mutation scheme

5.6.3. Overall Reproduction Process

In order to complete the definition of the process, certain parameters has to be determined. The number of individuals within a population and the number of maximum iterations has to be set. Also the amounts of population selected for crossover and mutation are parameterized beforehand together with the amounts of elite members within the population. Table 5.1 shows the parameters of the GA whereas Figure 5.9 presents the overall reproduction scheme.

Table 5.1: The parameters of GA

The amount of population chosen for Cross-over	%45
The amount of individuals exposed to Mutation	%10
Amount of Elite individuals	%10
Population	20
Number of maximum iterations	20
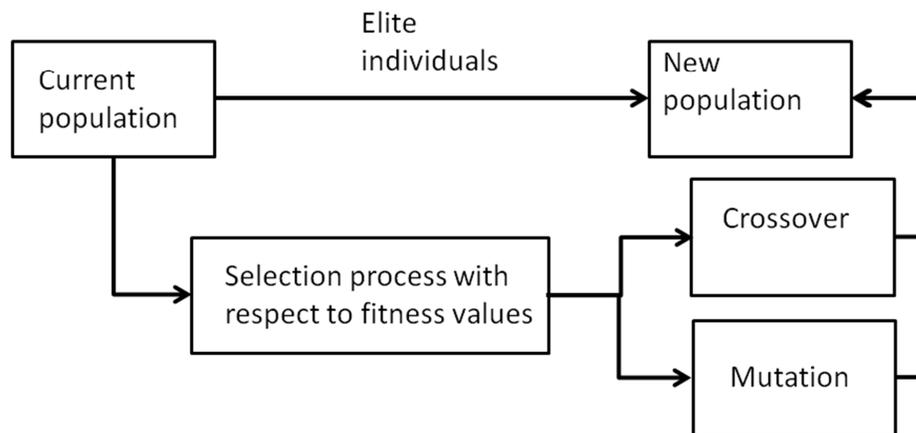
Figure 5.9: Reproduction Scheme

5.7. Outcome of The Tuning Process

The GA is implemented to a 12-DoF biped robot model which is identical with the SURALP in terms of dimensional properties and mass. The GA is applied for the given $v_{average}$ values. These values are generated in a range starting at 0.01 m/s by an increment of 0.01 m/s.

The resulting reference generations obtained for each $v_{average}$ are tested via simulations after removing the virtual torsional spring-damper systems. The maximum $v_{average}$ value obtained from the unsupported simulations was 0.24 m/s. This $v_{average}$ value is almost five times the average walking velocity of a simulation in which the walking reference generation parameters are tuned by trial and error [48].

In order to examine the effectiveness of the tuning and the fitness function, three different successive $v_{average}$ values are selected. The chosen $v_{average}$ values and the resulting reference generation parameters used in tuning process are given in Table 5.2.

Table 5.2: The parameters of GA tuning with respect to chosen velocities

	velocity	T_{ds}	T_{ss}	B
v_{slow}	0.08 m/s	1.34 s	0.62 s	0.0784 m
v_{medium}	0.15 m/s	0.95 s	0.63 s	0.1288 m
v_{fast}	0.24 m/s	0.66 s	0.54 s	0.144 m

The mean and the standard deviation of fitness function values and tuning parameters (T_{ds} and T_{ss}) of each generated population are used to observe the convergence of the GA process. Figure 5.10, Figure 5.11 and Figure 5.12 present this information for average velocity values given in Table 5.2.

The results indicate the proper operation of GA implementation since the average values of the individuals' fitness functions are converging to a minimum value for v_{slow}, v_{medium} and v_{fast}. In addition, the average values of the tuning parameters also converge to a specific point. There are however perturbations on standard deviations. This is originated by the mutation mechanism in GA.
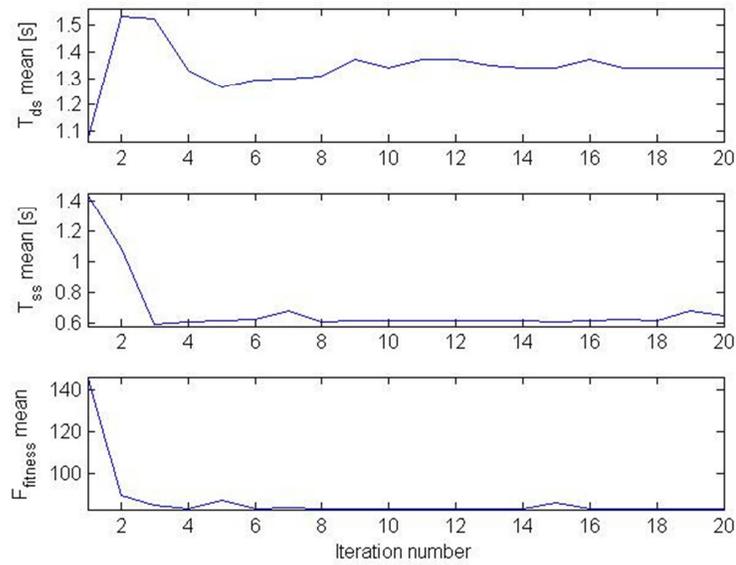
Figure 5.10.a: The mean values of T_{ss}, T_{ds} and $F_{fitness}$ of v_{slow} for each generated
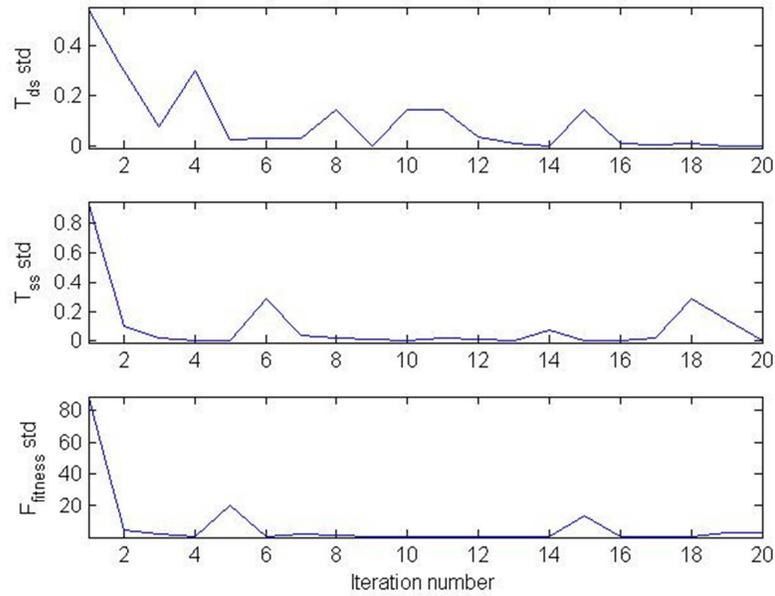
population

Figure 5.10.b: The standard deviation values of T_{ss}, T_{ds} and $F_{fitness}$ of v_{slow} for each

generated population

57
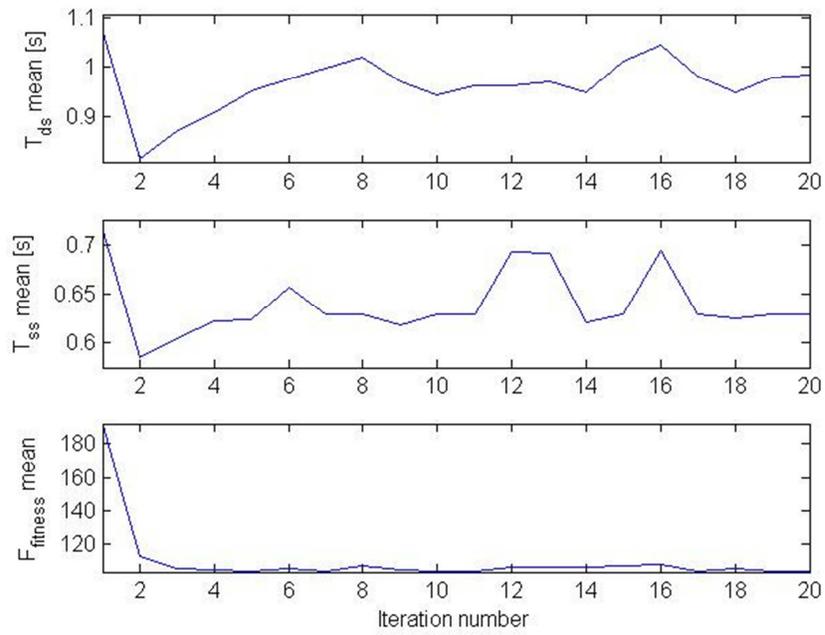
Figure 5.11.a: The mean values of T_{ss}, T_{ds} and $F_{fitness}$ of v_{medium} for each generated
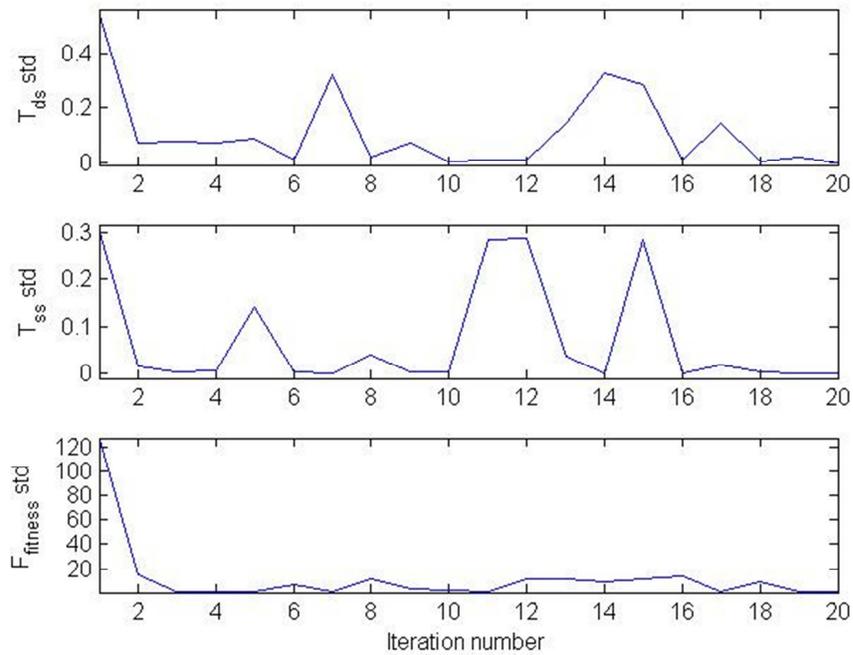
population

Figure 5.11.b: The standard deviation values of T_{ss}, T_{ds} and $F_{fitness}$ of v_{medium} for each

generated population
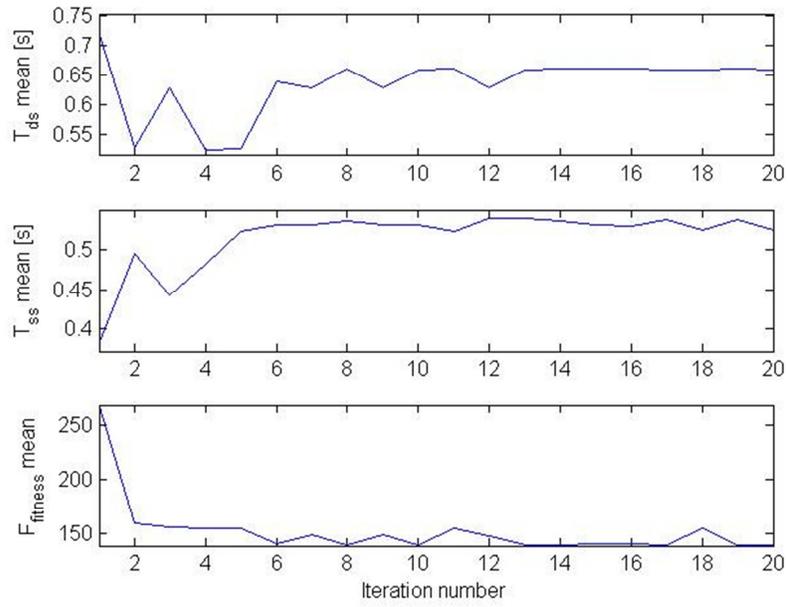
Figure 5.12.a: The mean values of T_{ss}, T_{ds} and $F_{fitness}$ of v_{fast} for each generated population
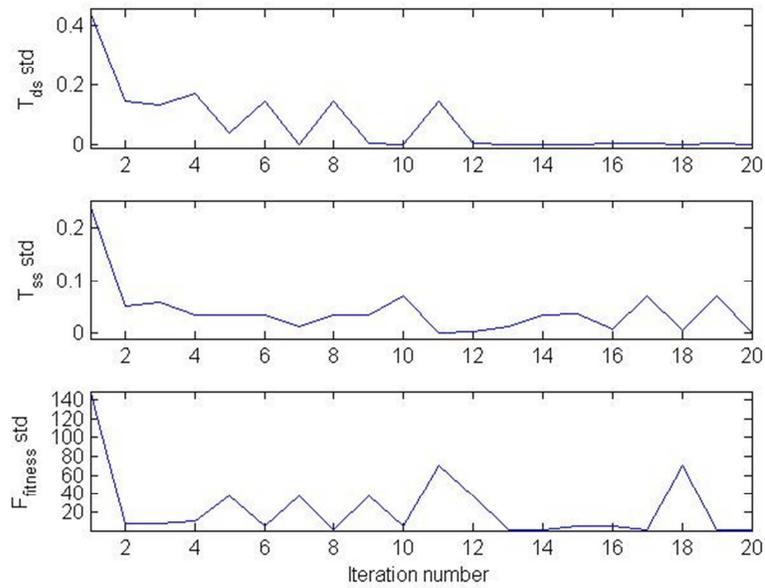
Figure 5.12.b: The standard deviation values of T_{ss}, T_{ds} and $F_{fitness}$ of v_{fast} for each generated population

From the figures it is observed that the mean values of T_{ds} and T_{ss} also have perturbations. This is again due to mutation operator. Since the number of population is low the relatively large T_{ds} and T_{ss} values result from mutation cause these perturbations.

In order to further examine the tuning process, the best and the worst individuals of a randomly chosen generation in terms of fitness values are considered for v_{medium}. Figures 5.13 and 5.14 show the external support values and angular deflections around trunk coordinate axes of the worst and best individuals of the 12th generation. It is observed that the values of support received from the torsional spring-damper system are relatively high for the worst individual when compared with the best one.
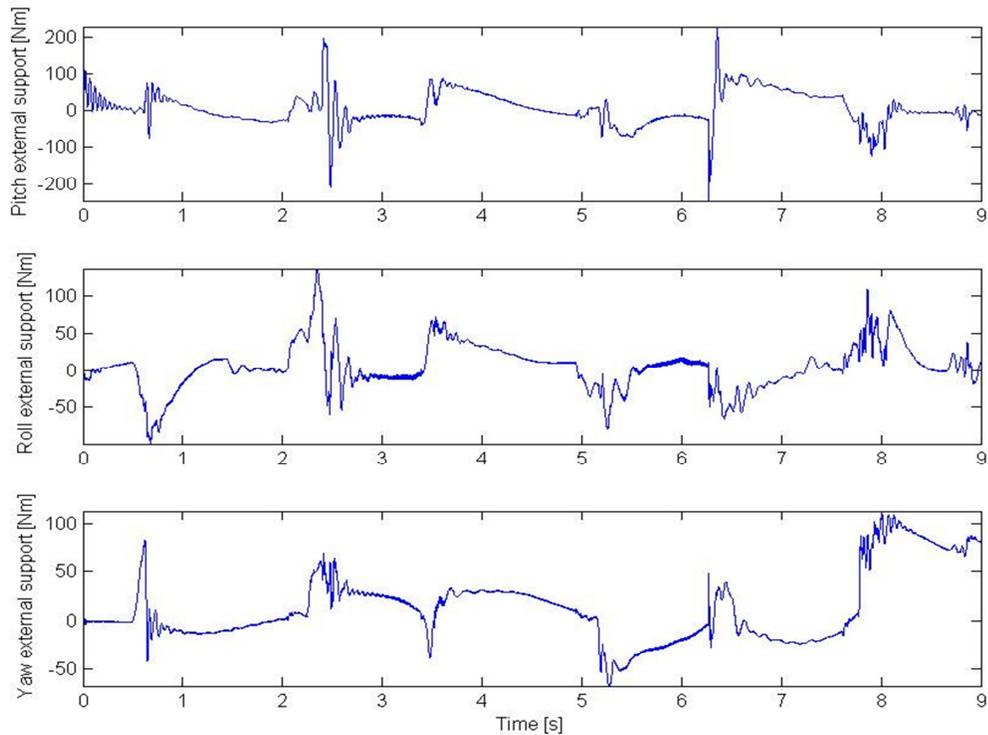
Figure 5.13.a: The resistance of torsional spring-damper systems around pitch, roll and yaw axes for worst individual in the given generation.
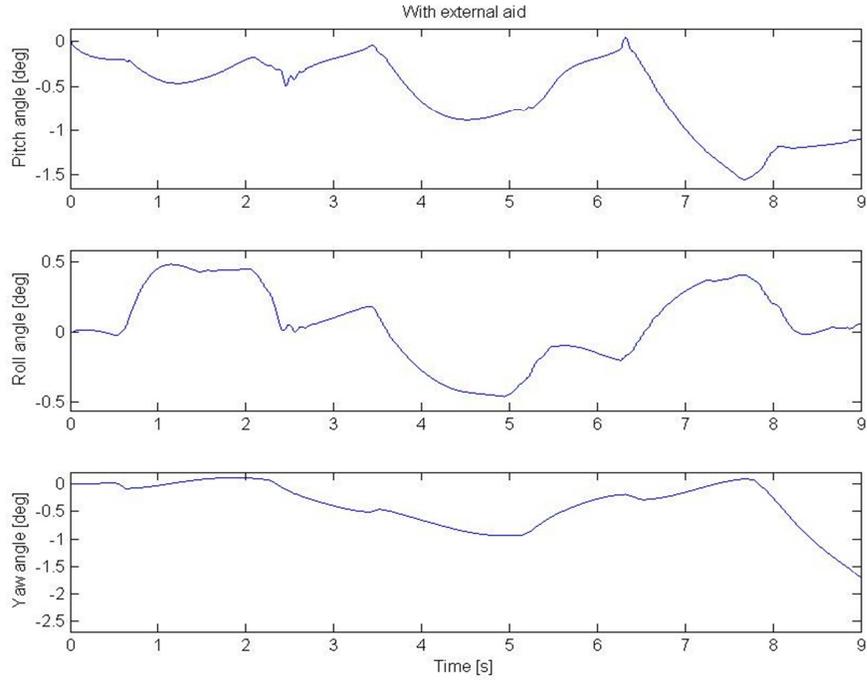
Figure 5.13.b: The angular deflections around robot trunk axes for worst individual in the given generation.
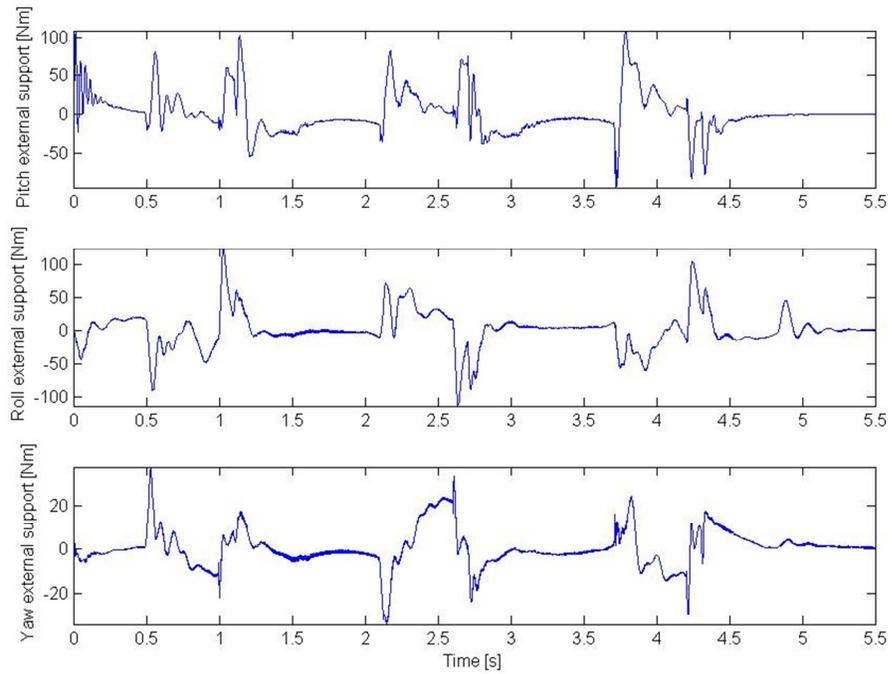
Figure 5.14.a: The resistance of torsional spring-damper systems around pitch, roll and yaw axes for best individual in the given generation.
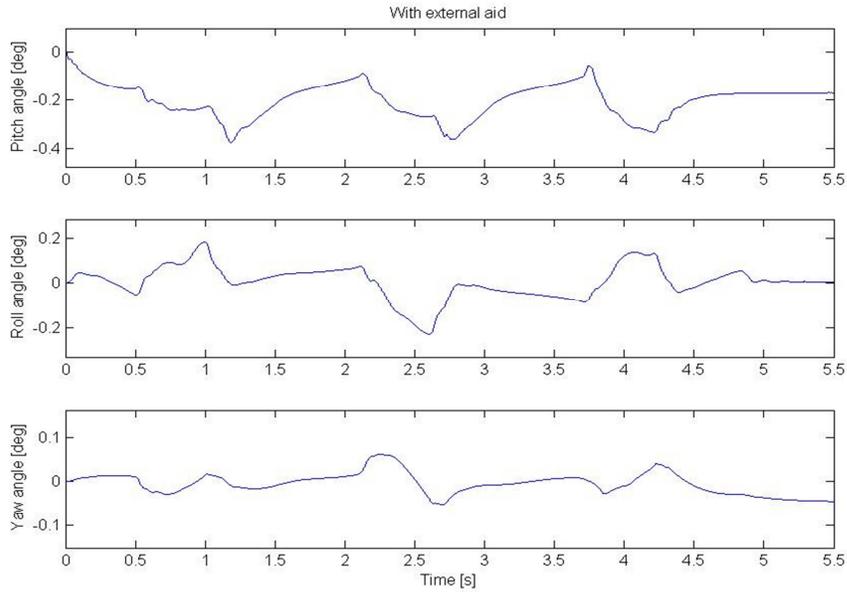
Figure 5.14.b: The angular deflections around robot trunk axes for best individual in the given generation.

Angular deflections around trunk coordinate frame axes with and without external support for the fittest individual of GA process are also driven to show the performance of the algorithm. Figure5.15 shows these deflections with and without the existence of external support respectively.
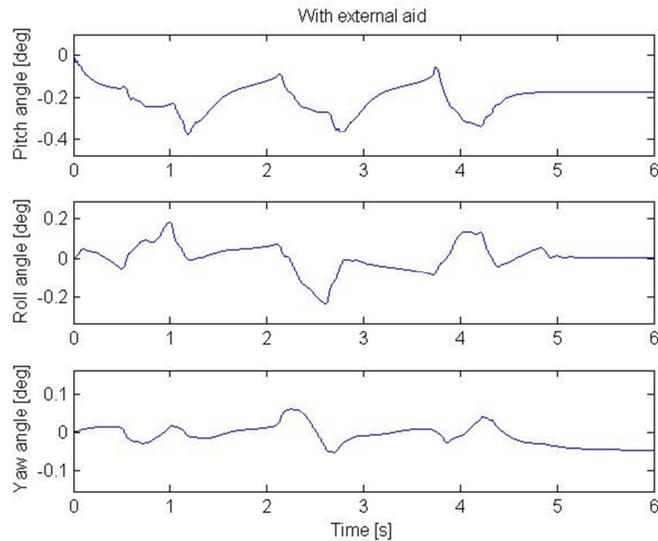
Figure 5.15.a: The angular deflections around robot trunk axes for fittest individual with external aid.
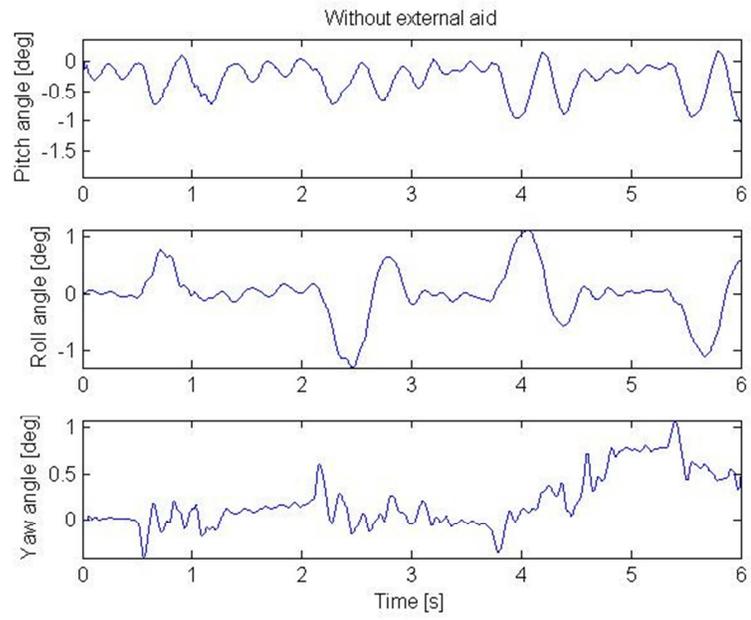
Figure 5.15.b: The angular deflections around robot trunk axes for fittest individual without external aid.

5.8. Discussion

Although the results of the GA tuning process are promising, it is realized that the physical velocity capacities of the DC motors of SURALP do not meet the highest joint velocity reference peaks obtained from the simulations for most of the $v_{average}$ command values. Figure 5.16 indicates the resulting maximum joint velocity reference peaks for a range of $v_{average}$ values.
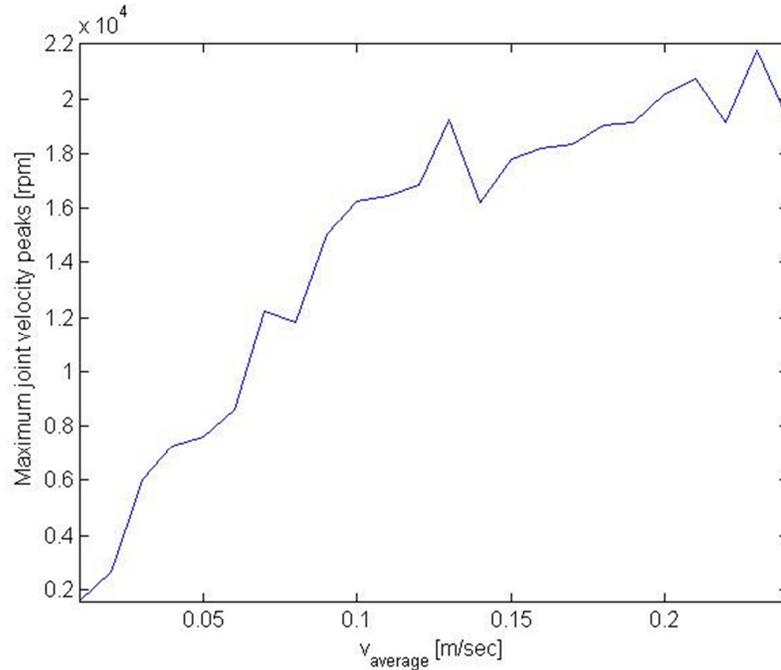
Figure 5.16: Maximum joint velocity peaks with respect to $v_{average}$ values

Notice that the maximum joint velocity peaks tends to increase as $v_{average}$ increases in general. However in two different parts of the figure there are perturbations. These perturbations appear from the ratio between single support period and step size. Since this ratio differs due to the non-linear nature of the problem such perturbations are natural.

The maximum possible velocity obtained from the current DC motors of the SURALP is around 6000 rpm according to operating range specifications of the motors. So the walking reference generation parameters obtained from simulations for $v_{average}$ values above 0.04 m/s are not suitable for the implementation purposes.

In the next chapter, a modified version of the GA implementation is proposed which prevents the individuals of the population from exceeding the maximum joint velocity peak.

Chapter 6

6. GENETIC ALGORITHM TUNING WITH CONSTRAINED JOINT VELOCITIES

In this chapter a solution is proposed for the previously stated problem. A modified fitness function is defined to prevent the maximum joint velocity peaks of the resulting individuals in previous GA tuning process.

6.1. A Modified Fitness Function

The maximum joint velocity reference peaks can be indicated at the end of a simulation by taking the derivative of joint position references obtained from inverse kinematics. According to these results the maximum joint velocity reference can be determined. Hence the exceeding of joint velocity limit can be designated. From this information a new fitness function is derived as follows:

$$K_{penalty} = \begin{cases} 1 & \text{if} \quad \omega_{peak} \leq \omega_{max} \\ \\ 3 & \text{if} \quad \omega_{peak} > \omega_{max} \end{cases} \tag{6.1}$$

$$F_{fitness} = K_{penalty}\left(u_{ds_{average}} + u_{ss_{average}}\right) \tag{6.2}$$

Here $K_{penalty}$ is a penalty coefficient, ω_{peak} is the joint velocity peak obtained from simulation and ω_{max} is the maximum joint velocity for the motor. $u_{ds_{average}}$ and $u_{ss_{average}}$ are the fitness function terms of (5.6) and (5.7). According to the modified function, the fitness values of the individuals which exceed maximum joint velocity limit will be penalized.

This modified function is subjected to the same GA principles as in Chapter 5. The results of the tuning are given in next section.

6.2 Outcome of the Tuning Process

The GA is implemented by the same architecture as described in Section 5.6. Similar to the previous implementation, the resulting reference generations obtained for each $v_{average}$ are tested via simulations after removing the virtual torsional spring-damper systems. The maximum $v_{average}$ value obtained from the unsupported simulations in which the robot did not fall was 0.09 m/sec. Comparing this value with the 0.24 m/s corresponding result of the previous chapter, we can infer that the rotational speed limits of the joint motors are the main factors which limit the highest accessible walking speed. Here, it is also to be noted that this condition is partially due to the high reduction ratios used for joints.

The obtained admissible maximum $v_{average}$ value is almost one and a half times the average walking velocity of the simulation in [48]. This still shows an improvement achieved by the tuning method. As in Section 5.7 three different $v_{average}$ values are selected in order to investigate the effectiveness of the tuning. The chosen $v_{average}$ values and the resulting reference generation parameters obtained via GA tuning process are given in Table 6.1.

Table 6.1: The parameters of GA tuning for chosen velocities with the modified fitness function

	velocity	T_{ds}	T_{ss}	B
v_{slow}	0.03 m/s	1.59 s	0.87 s	0.0369 m
v_{medium}	0.06 m/s	1.98 s	2.37 s	0.1302 m
v_{fast}	0.09 m/s	0.68 s	2.04 s	0.1224 m

As in Section 5.7 the mean and the standard deviation of fitness values and tuning parameters (T_{ds} and T_{ss}) of each generated population are used to observe the convergence of the GA process. Figures 6.1, 6.2 and 6.3 show this information for average velocity values given in Table 6.1.

The results indicate a successful GA implementation since the average values of the individuals' fitness functions are converging to a minimum value for v_{slow}, v_{medium} and v_{fast}. In

addition the average values of the tuning parameters also converge to specific values. There are perturbations on standard deviation calculations. They are caused by the mutation mechanism in GA.
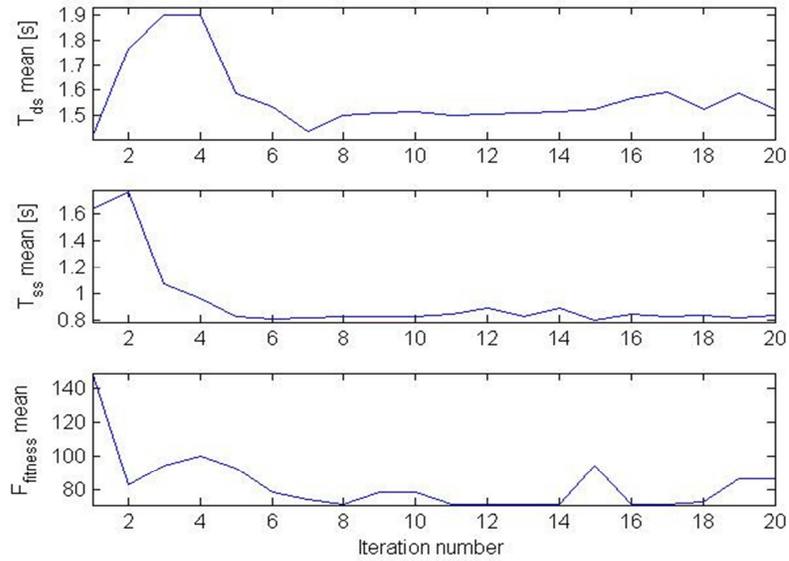
Figure 6.1.a: The mean values of T_{ss}, T_{ds} and $F_{fitness}$ of v_{slow} for each generated population using modified fitness function
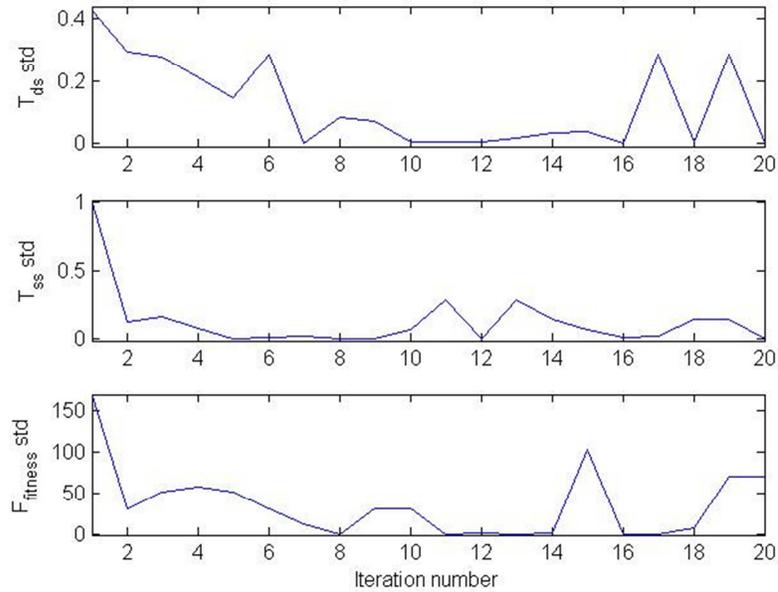
Figure 6.1.b: The standard deviation values of T_{ss}, T_{ds} and $F_{fitness}$ of v_{slow} for each generated population using modified fitness function
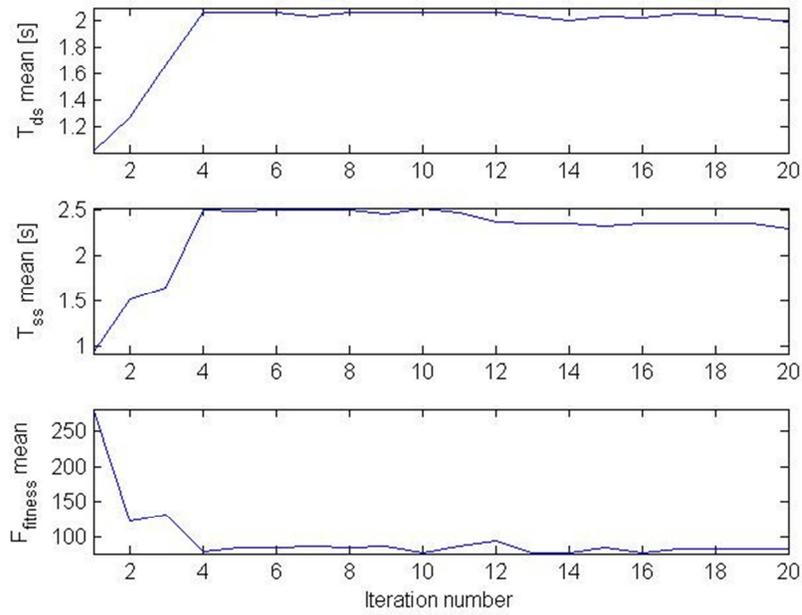
Figure 6.2.a: The mean values of T_{ss}, T_{ds} and $F_{fitness}$ of v_{medium} for each generated

population using modified fitness function
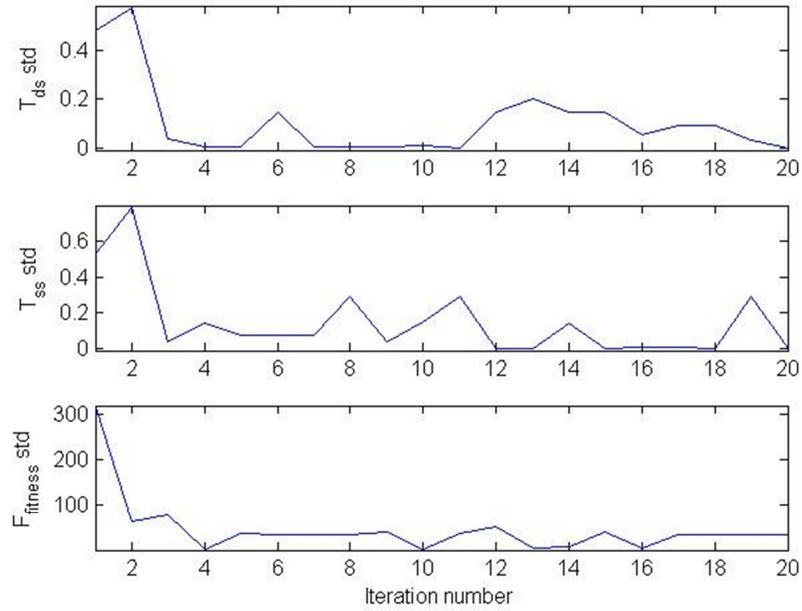
Figure 6.2.b: The standard deviation values of T_{ss}, T_{ds} and $F_{fitness}$ of v_{medium} for each

generated population using modified fitness function

69
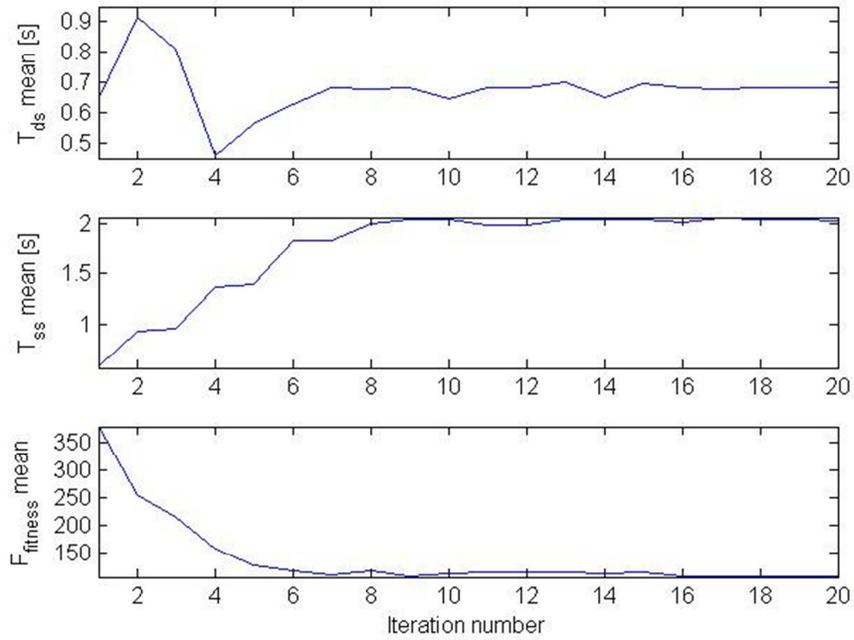
Figure 6.3.a: The mean values of T_{ss}, T_{ds} and $F_{fitness}$ of v_{fast} for each generated

population using modified fitness function
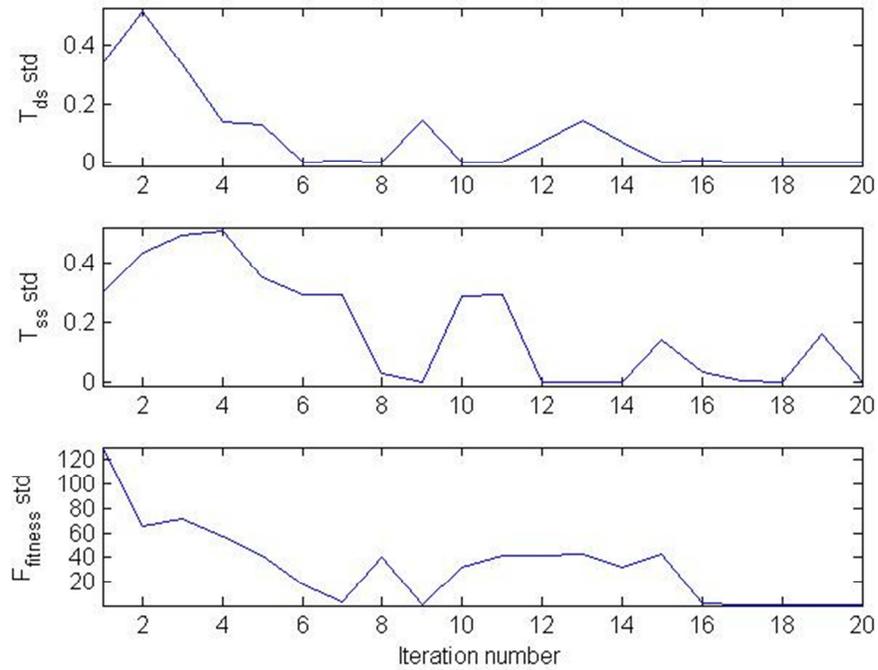
Figure 6.3.b: The standard deviation values of T_{ss}, T_{ds} and $F_{fitness}$ of v_{fast} for each

generated population using modified fitness function

Similar to section 5.7 there are some perturbations in the figures which shows the mean values of T_{ds} and T_{ss}. Compare to the results of genetic algorithm with unconstrained joint velocities the convergence of fitness function values and GA parameters are obtained in later generations in this GA process. This is due to the constrained joint velocity values. Since it alters the searching space of the genetic algorithm such changes are natural.

As in 5.7, in order to further examine the tuning process, the best and the worst individuals of a randomly chosen generation are chosen for v_{medium}. Figures 6.4 and 6.5 show the external support values and angular deflections around trunk coordinate axes for worst and best individual for the 9th generation. The values of average torsional spring support are relatively high for the worst individual when compared to the best one.
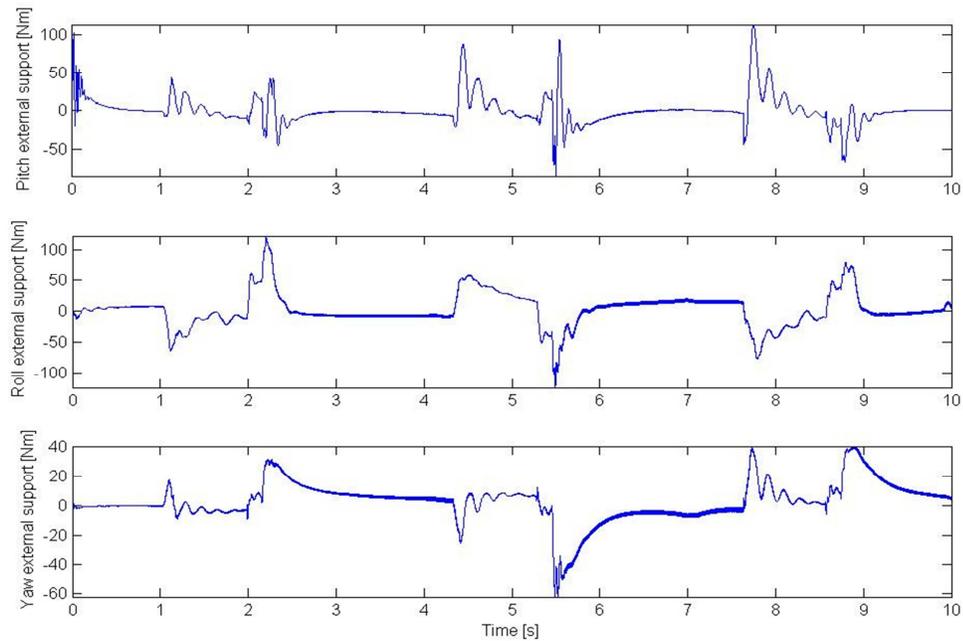
Figure 6.4.a: The resistance of torsional spring-damper systems around pitch, roll and yaw axes for worst individual in the given generation using modified fitness function

71
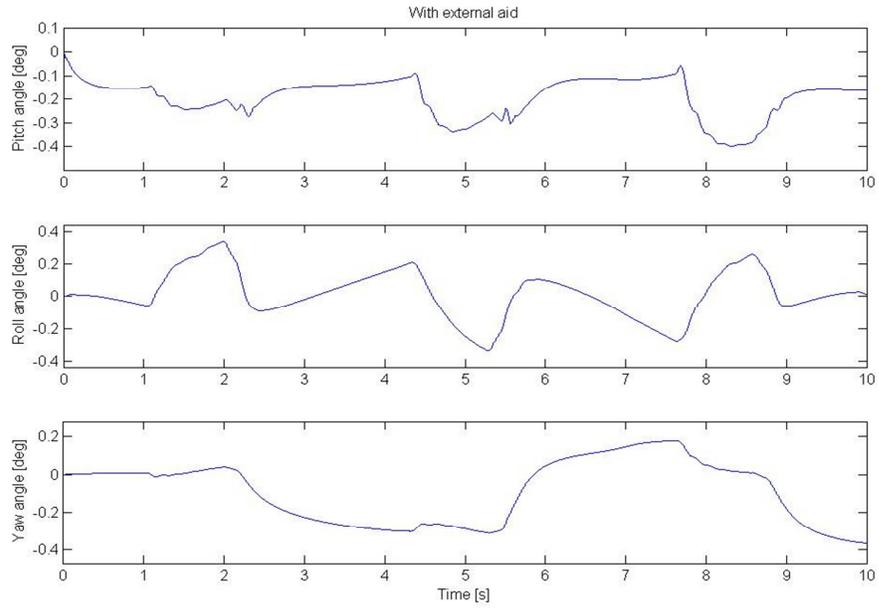
Figure 6.4.b: The angular deflections around robot trunk axes for worst individual in the given generation using modified fitness function
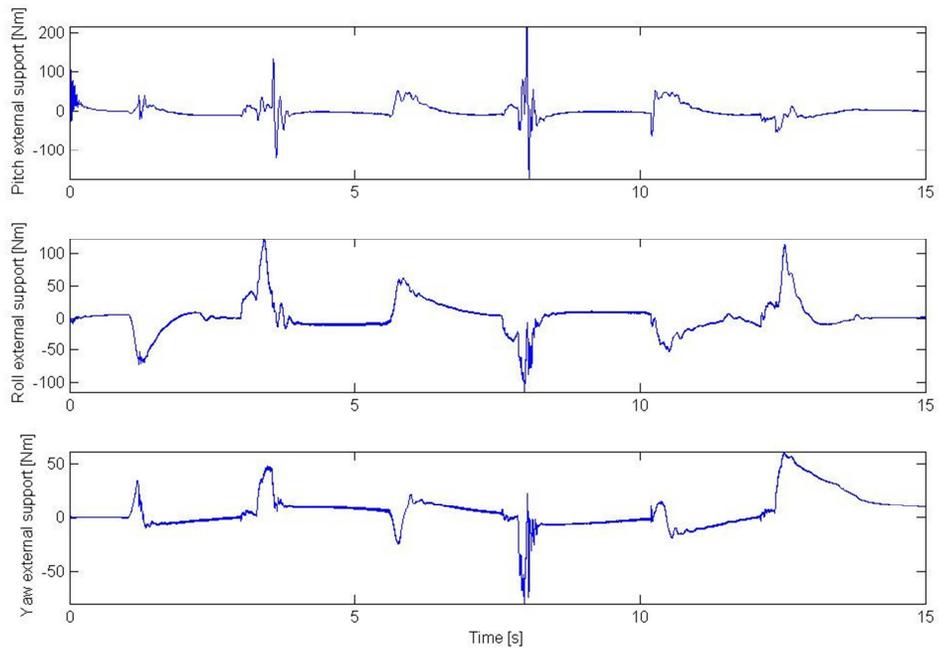
Figure 6.5.a: The resistance of torsional spring-damper systems around pitch, roll and yaw axes for best individual in the given generation using modified fitness function
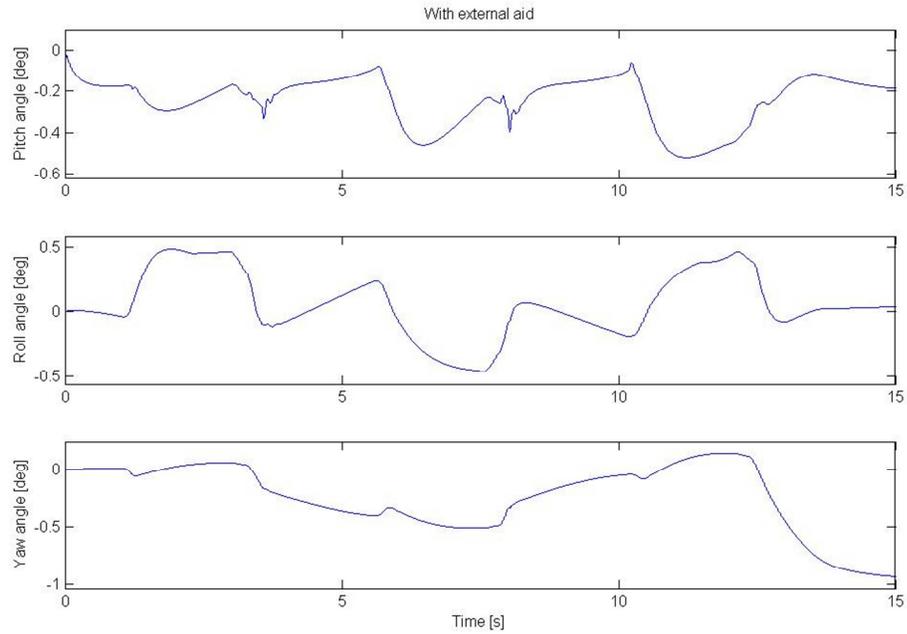
Figure 6.5.b: The angular deflections around robot trunk axes for best individual in the given generation using modified fitness function

Angular deflections around trunk coordinate frame axes with and without external support for the fittest individual of GA process also considered as in 5.7. Figure 6.6 shows these deflections with and without the existence of external support respectively.
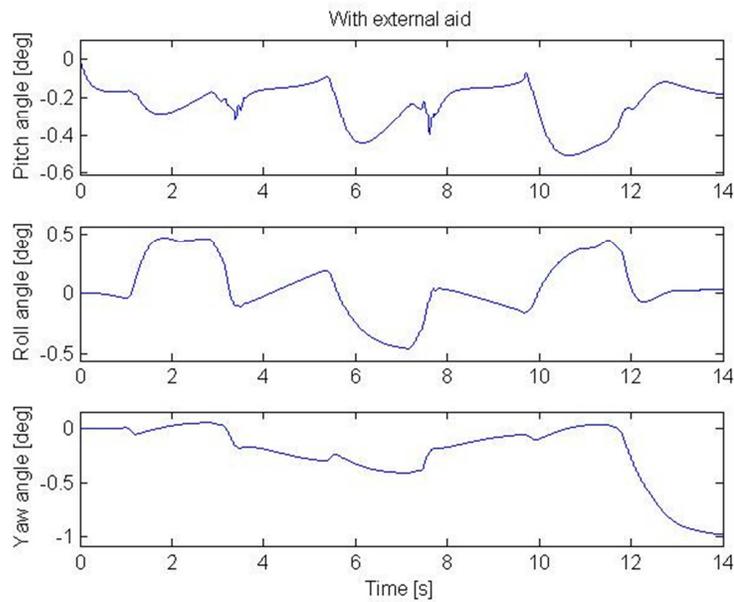
Figure 6.6.a: The angular deflections around robot trunk axes for fittest individual with external aid using modified fitness function.
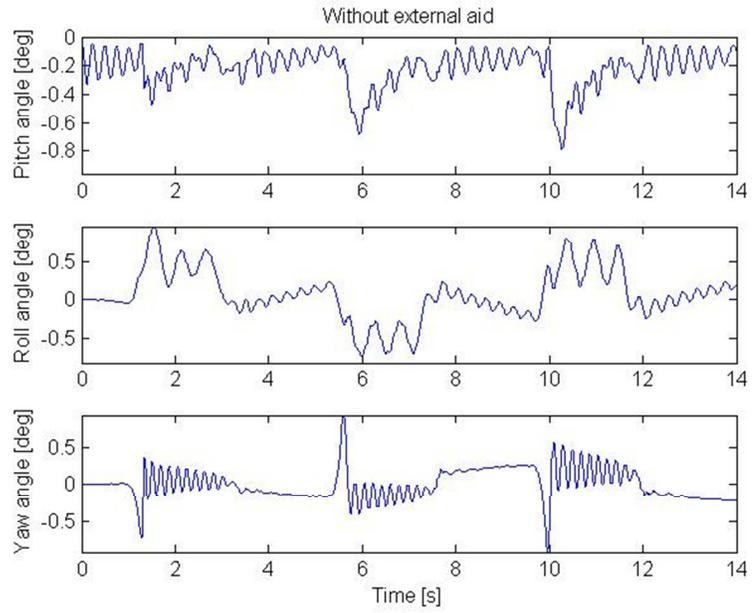
Figure 6.6.b: The angular deflections around robot trunk axes for fittest individual without external aid using modified fitness function.

6.3 Experimental Results

Resulting walking reference generation parameters obtained with GA tuning are tested via experiments using SURALP. In that sense, two different gait reference generation parameter sets are employed according to the $v_{average}$ command values shown in Table 6.2.

Table 6.2: The parameters of GA tuning with respect chosen velocities for modified fitness function

$v_{average}$	T_{ds}	T_{ss}	B	h_s	h_{leg}
0.03 m/s	1.59 s	0.87 s	0.0369 m	0.013 m	0.6296 m
0.07 m/s	1.98 s	2.37 s	0.1302 m	0.015 m	0.6214 m

The body angles around pitch and roll axes are captured with inertial sensors. Figures 6.7 and 6.8 present the body angles for $v_{average}$ values given in the table. Here it is also to be noted that the 0.07 m/s is the highest experimental average walking velocity reported to date with SURALP.
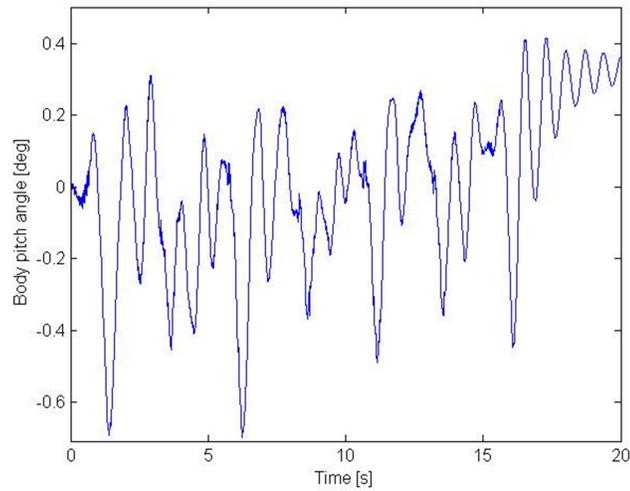
Figure 6.7.a: Body pitch angle of the robot during walking with $v_{average} = 0.03 m/s$
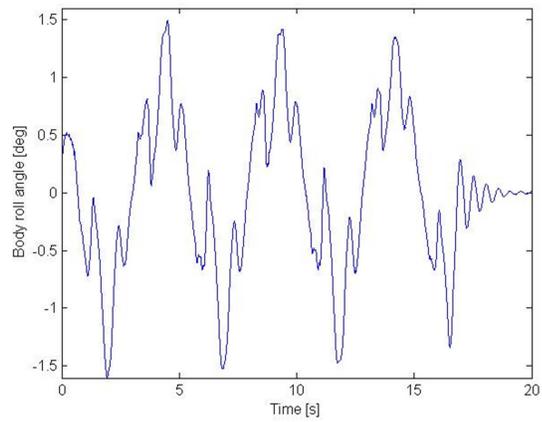
Figure 6.7.b: Body roll angle of the robot during walking with $v_{average} = 0.03m/s$
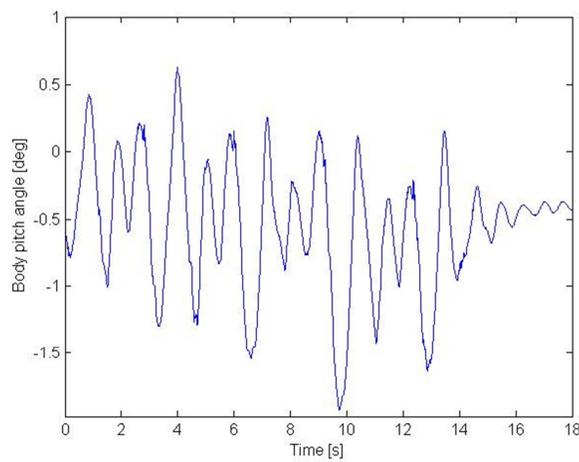
Figure 6.8.a: Body pitch angle of the robot during walking with $v_{average} = 0.07m/s$
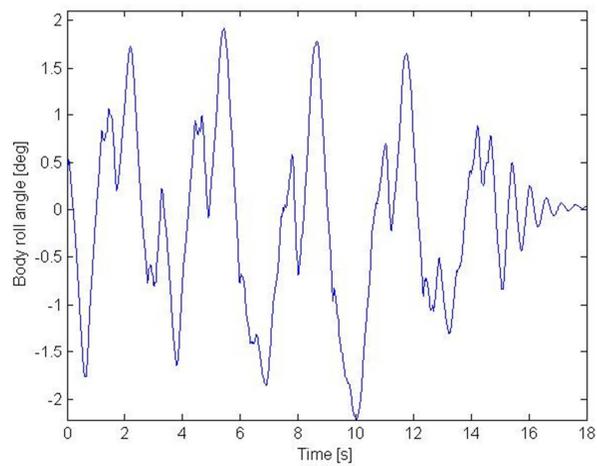
Figure 6.8.b: Body roll angle of the robot during walking with $v_{average} = 0.07m/s$

The snapshots in Figure 6.9 are taken during the walk of SURALP with $v_{average} = 0.07m/s$.

Figure 6.9: Snapshots of SURALP walking with $v_{average} = 0.07m/s$

6.4 Discussion

The results of the experiments were successful for the given average walking velocities. In the experiments illustrated in previous works [49,74] the average walking velocity was set to 0.03 m/s and it was also observed that the pitch and roll angles of the body deviated between ± 3 degrees. In the 0.03 m/s experiments with the GA tuned walking parameters, the pitch and roll angles of the body deviate between ± 0.5 and ± 1.5 degrees, respectively. Furthermore the body pitch and roll angles recorded in the experiments with 0.07 m/s average walking velocity oscillate between ± 2 degrees. Therefore, it can be stated that a more stable walking is achieved by the tuning method proposed in this Chapter. The balance of walking is improved by the GA tuning method.

On account of the improved balance of the walking, a suitable parameter set for higher velocities is obtained and "ground kick" method for swing foot take-off phase is quitted. As a result of decreased body pitch and roll angles and the absence of "ground kick" the naturalness of SURALP's walking is increased.

In the experiments it is observed that the lateral motion of the body highly affects the stability of the walking. Manual adjustment is applied to these parameters in order to obtain successful experimental results. This suggests that for a more automated tuning process, these parameters can also be included in the tuning process. In next chapter an extended chromosome is proposed in order to improve the results and efficiency of tuning method further.

Chapter 7

7. GENETIC ALGORITHM TUNING WITH ADDITIONAL PARAMETERS FOR LATERAL MOTION

In the walking reference generation process the swing offset (as described in section 2.1) and the parameter A (the amplitude of the ZMP lateral motion described in section 4.2) are independent parameters which define the lateral motion of the robot. This chapter proposes an extended chromosome setting by using swing offset and A alongside with the walking reference generation parameters proposed in Chapter 5.

7.1. An Extended Chromosome

The chromosome in Section 5.2 is extended by using the swing offset and A parameters. Since these parameters define the lateral features of the reference gait in a combined way, a relation between them is defined as follows;

$$A = l_{swing\_offset} \pm 0.02 \tag{7.1}$$

Here l_{swing_offset} denotes the swing offset. Due to the kinematic limitations of SURALP, for the typical height of the trunk, the swing offset has to be within the following range.

$$0.1\,\mathrm{m} < l_{swing\_offset} < 0.14\,\mathrm{m} \tag{7.2}$$

The chromosome is extended by 8-bits for the new parameters such that one unit change within the strings will change the parameters by 0.0025 m. A sample chromosome and corresponding parameter values are given in Figure 7.1.

01100110	00101100	0010	1100
$T_{ds} = 1.02s$	$T_{ss} = 0.44s$	$l_{swing\_offset} = 0.105m$	$A = 0.1125m$

Figure 7.1: The extended chromosome setting and corresponding parameter values

7.2 Outcome of the Tuning Process

The GA is implemented by the same architecture as described in Section 6.2. Similar to the previous implementation the resulting reference parameters obtained for each $v_{average}$ is tested via simulations after removing the virtual torsional spring-damper systems. The maximum $v_{average}$ value obtained from the unsupported simulations was 0.11 m/sec.

The obtained $v_{average}$ value is more than two times of the average walking velocity obtained by simulations in [48]. This shows that a further improvement is obtained with the extended chromosomes. Three different successful $v_{average}$ values are selected again as in the previous chapters. The chosen $v_{average}$ values and the resulting reference generation parameters used in tuning process are given in Table 7.1.

Table 7.1: The parameters of GA tuning with respect to chosen velocities with the extended chromosome

	velocity	T_{ds}	T_{ss}	B	A	l_{swing_offset}
v_{slow}	0.03 m/s	2.52 s	2.54 s	0.0759 m	0.1175 m	0.1 m
v_{medium}	0.07 m/s	1.25 s	1.49 s	0.0959 m	0.1175 m	0.1 m
v_{fast}	0.11 m/s	0.39 s	0.63 s	0.0561 m	0.1175 m	0.1 m

As in section 6.3 the mean and the standard deviation of fitness and tuning parameters (T_{ds}, T_{ss}, A and l_{swing_offset}) of each generated population are plotted. Figures 7.2, 7.3 and 7.4 show the curves for average velocity values given in Table 7.1.

The results indicate the GA setup is again proper. The average values of the fitness functions are converging to a minimum value for v_{slow}, v_{medium} and v_{fast}. The average values of the tuned parameters also converge. The mutation based perturbations are again observable.
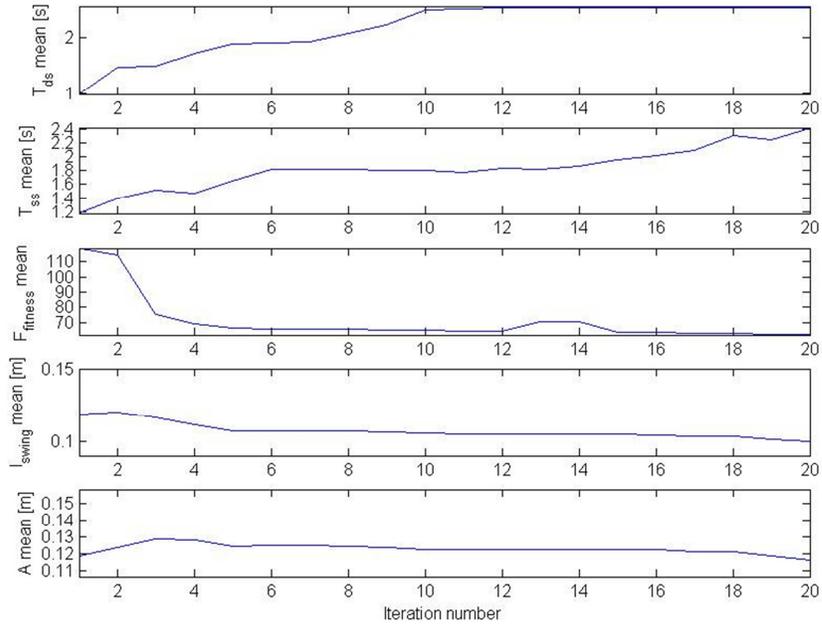
Figure 7.2.a: The mean values of T_{ss}, T_{ds}, A, l_{swing_offset} and $F_{fitness}$ of v_{slow} for each

generated population using extended chromosome
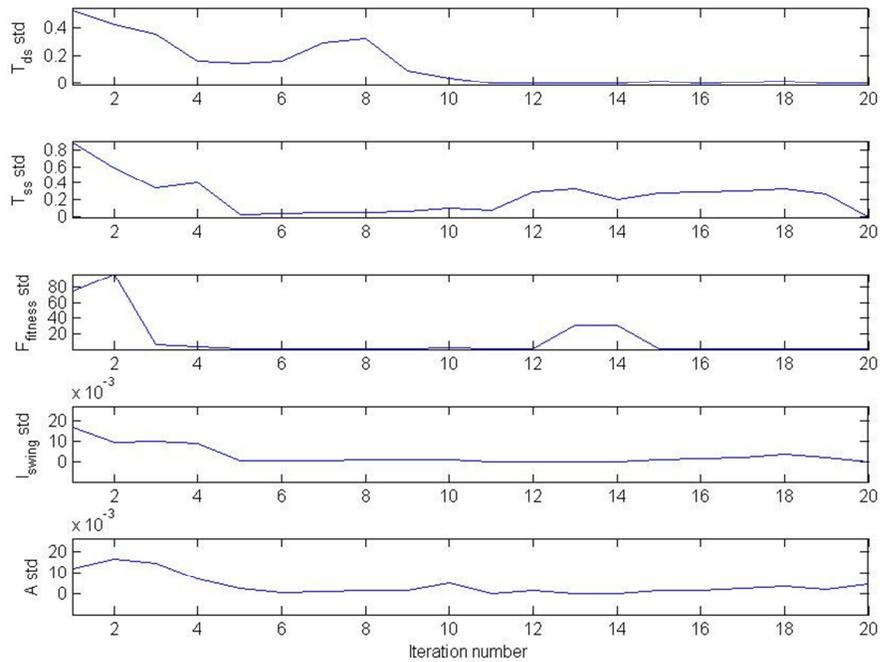
Figure 7.2.b: The standard deviation values of T_{ss}, T_{ds}, A, l_{swing_offset} and $F_{fitness}$ of v_{slow}

for each generated population using extended chromosome
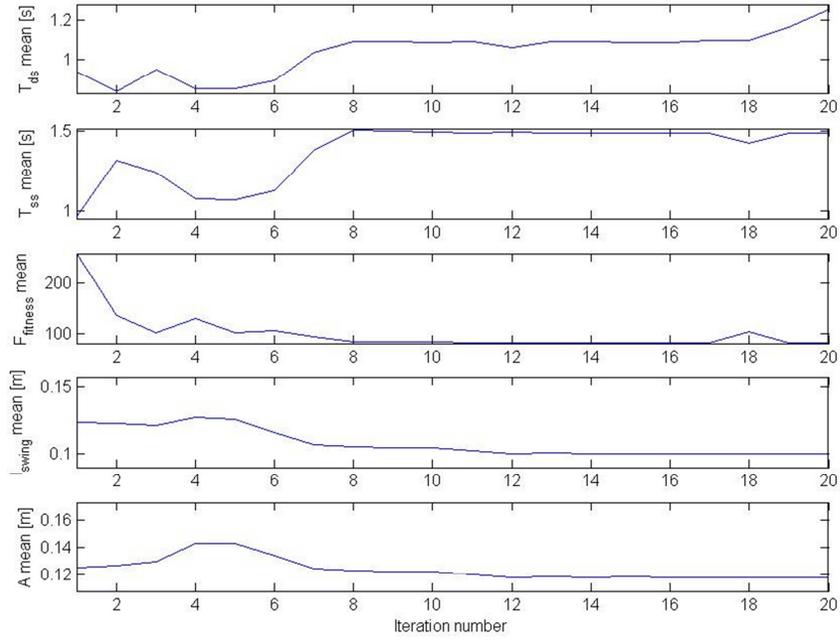
Figure 7.3.a: The mean values of T_{ss}, T_{ds}, A, l_{swing_offset} and $F_{fitness}$ of v_{medium} for each

generated population using extended chromosome
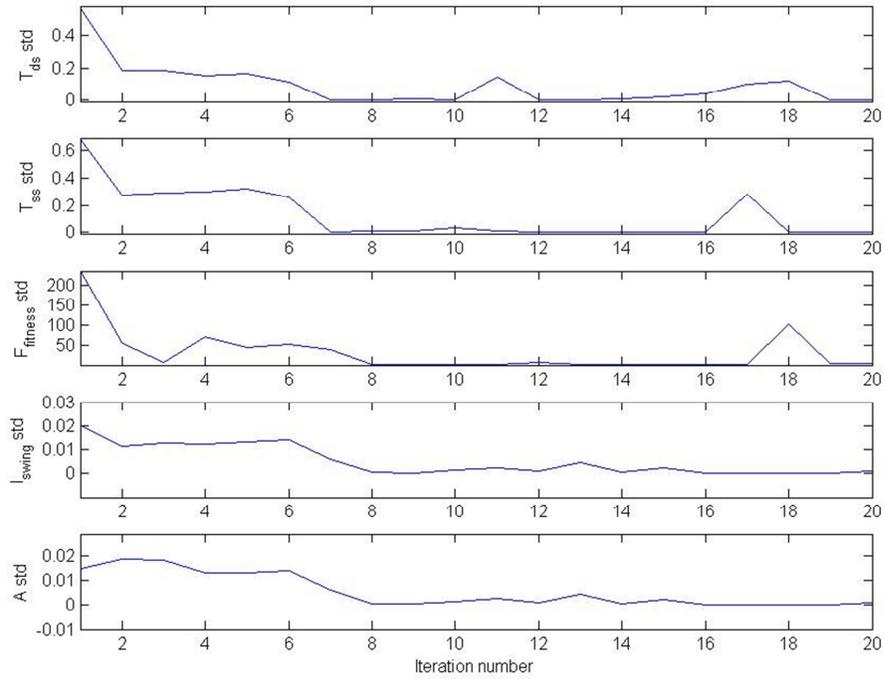
Figure 7.3.b: The standard deviation values of T_{ss}, T_{ds}, A, l_{swing_offset} and $F_{fitness}$ of

v_{medium} for each generated population using extended chromosome
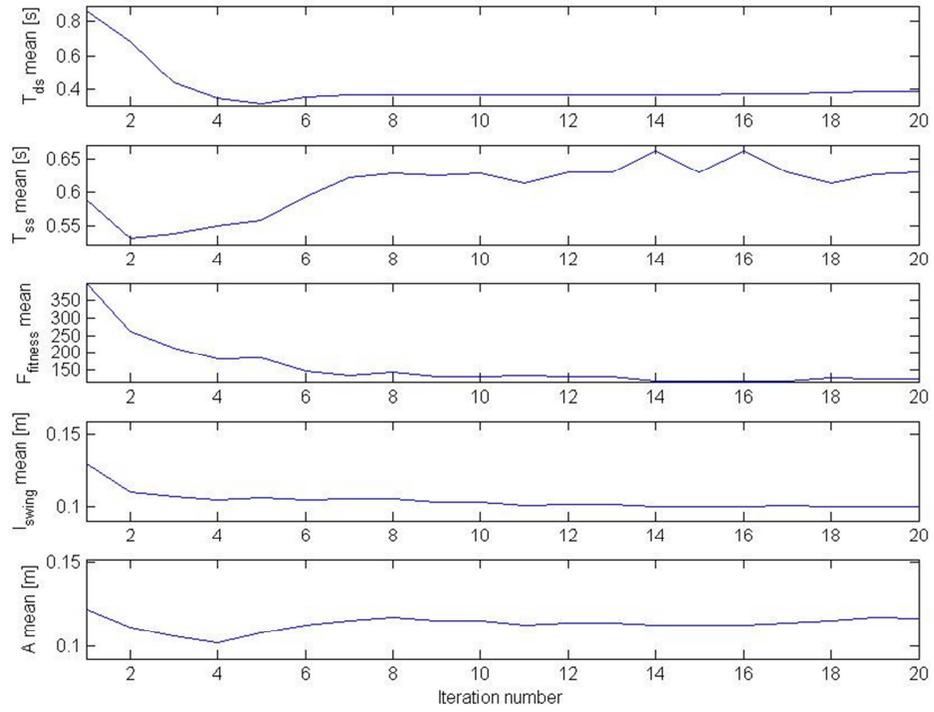
Figure 7.4.a: The mean values of T_{ss}, T_{ds}, A, l_{swing_offset} and $F_{fitness}$ of v_{fast} for each

generated population using extended chromosome
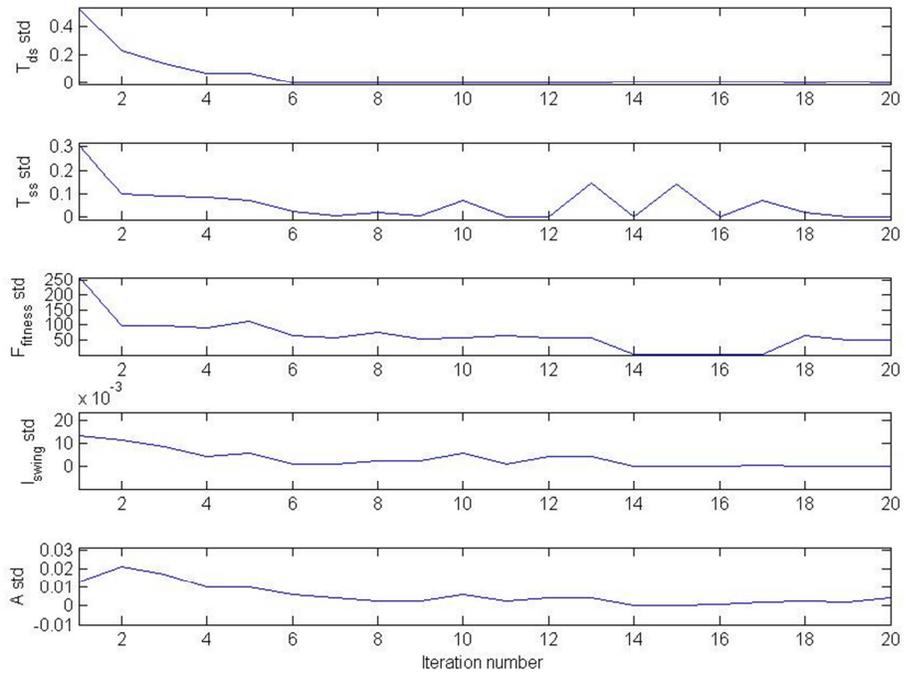
Figure 7.4.b: The standard deviation values of T_{ss}, T_{ds}, A, l_{swing_offset} and $F_{fitness}$ of v_{fast}

for each generated population using extended chromosome

Similar to section 6.3 there are some perturbations in the mean value of genetic algorithm. Compare to the results of previous genetic algorithm processes, the convergence of fitness function and GA parameters are obtained in later generations. This is due to the increase in the searching area of GA process caused by the involvement of additional parameters.

The best and the worst individuals of a randomly chosen population for v_{medium}. Figures 7.5 and 7.6 show the external support torques and angular deflections around trunk coordinate axes for the worst and best individuals in the 9th generation. It is observed that support from the torsional spring-damper systems are relatively high for the worst individual in comparison with the best one.
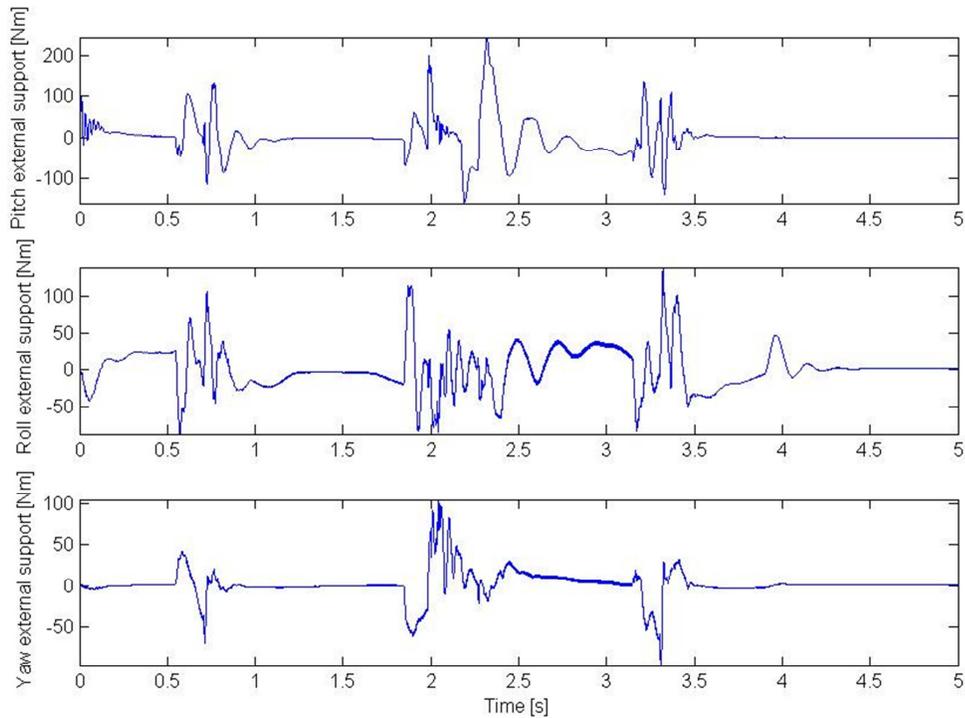
Figure 7.5.a: The resistance of torsional spring-damper systems around pitch, roll and yaw axes for worst individual in the given generation using extended chromosome
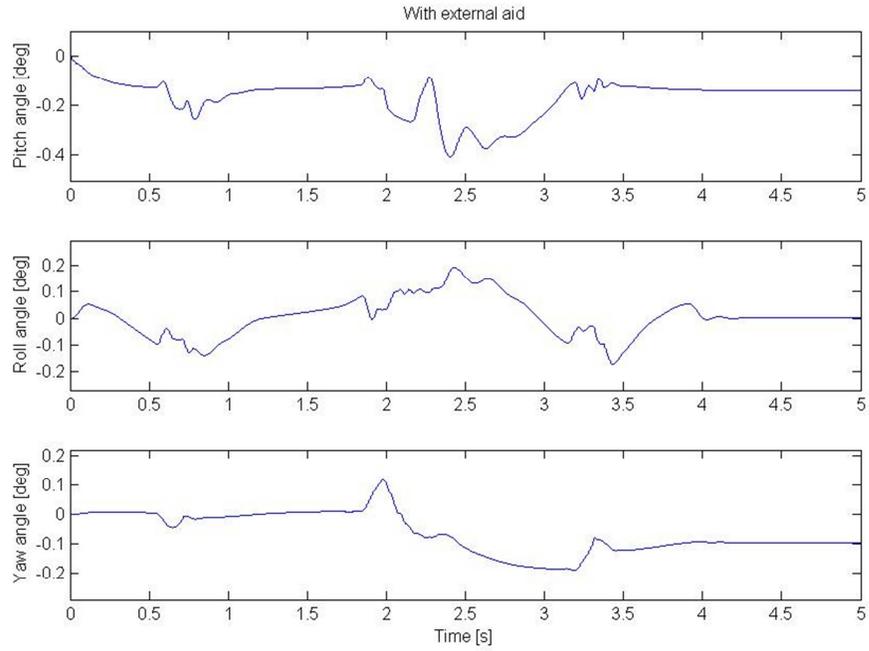
Figure 7.5.b: The angular deflections around robot trunk axes for worst individual in the given generation using extended chromosome
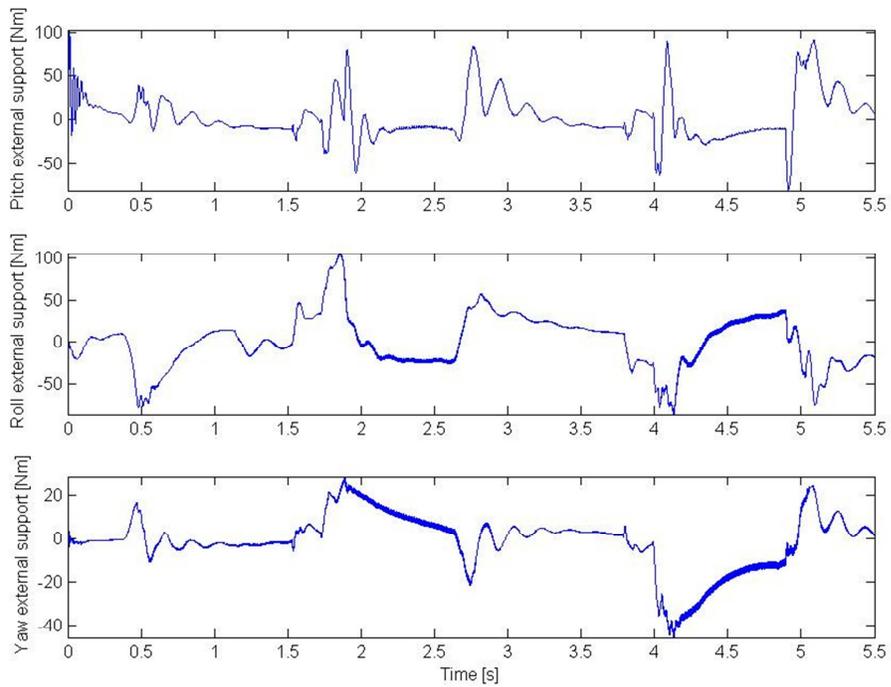
Figure 7.6.a: The resistance of torsional spring-damper systems around pitch, roll and yaw axes for best individual in the given generation using extended chromosome
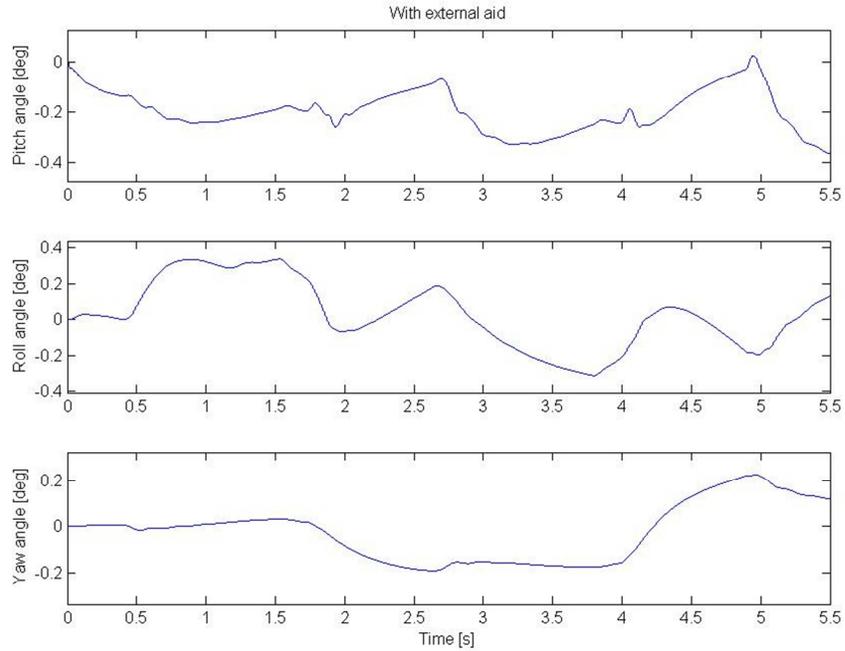
Figure 7.6.b: The angular deflections around robot trunk axes for best individual in the given generation using extended chromosome

Angular deflections around trunk coordinate frame axes with and without external support for the fittest individual of GA process also driven as in 6.6. Figure7.7 shows these deflections with and without the existence of external support respectively.
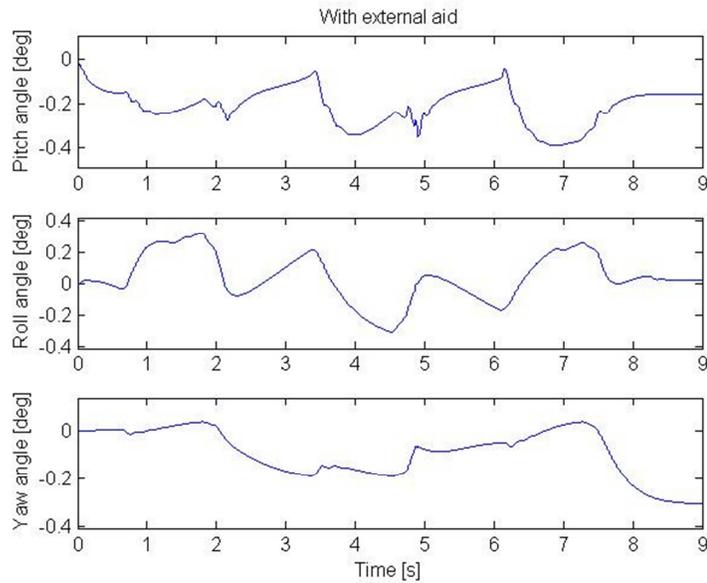
Figure 7.7.a: The angular deflections around robot trunk axes for fittest individual with external aid using extended chromosome.
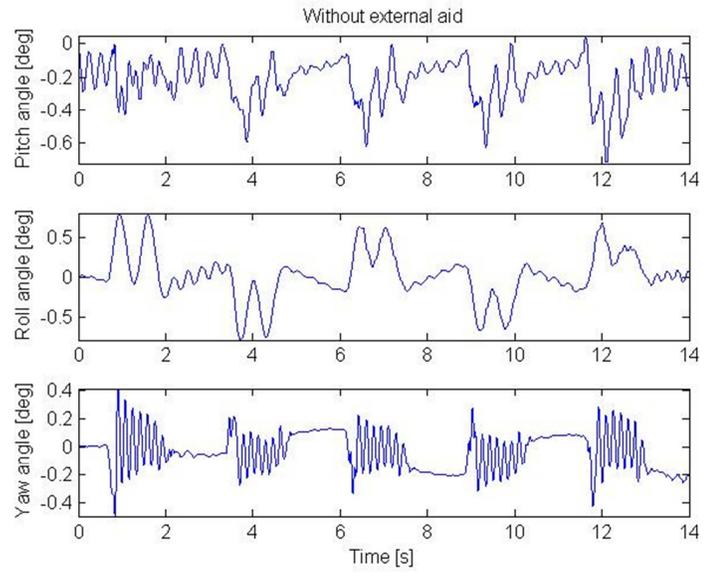
Figure 7.7.b: The angular deflections around robot trunk axes for fittest individual without external aid using extended chromosome.

7.3 Experimental Results

In this case too, walking reference generation parameters obtained from the GA are tested with experiments using SURALP. The reference gait parameter set in Table 7.2 is employed with a command velocity of 0.09 m/s. This speed is three times the walking speed of SURALP exhibited in [49].

Table 7.2: The parameters of GA tuning

$v_{average}$	T_{ds}	T_{ss}	B	h_s	A	l_{swing_offset}	h_{leg}
0.09 m/s	0.67 s	0.87 s	0.0693 m	0.013 m	0.1275	0.11	0.6150 m

The body angles around pitch and roll axes shown in Figure 7.8.
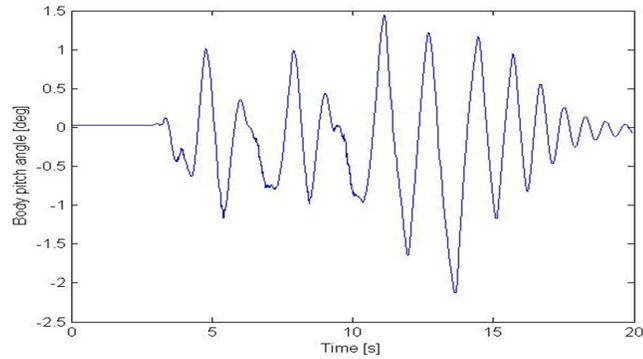
Figure 7.8.a: Body pitch angle of the robot during walking with $v_{average} = 0.09 m/s$
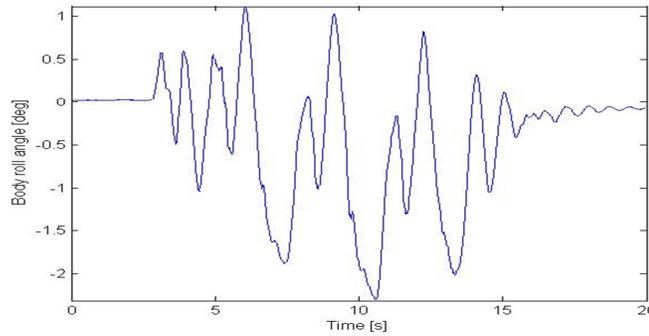
Figure 7.8.b: Body roll angle of the robot during walking with $v_{average} = 0.09 m/s$

88

The snapshots in Figure 7.9 are taken during the walk of SURALP with $v_{average} = 0.09m/s$.
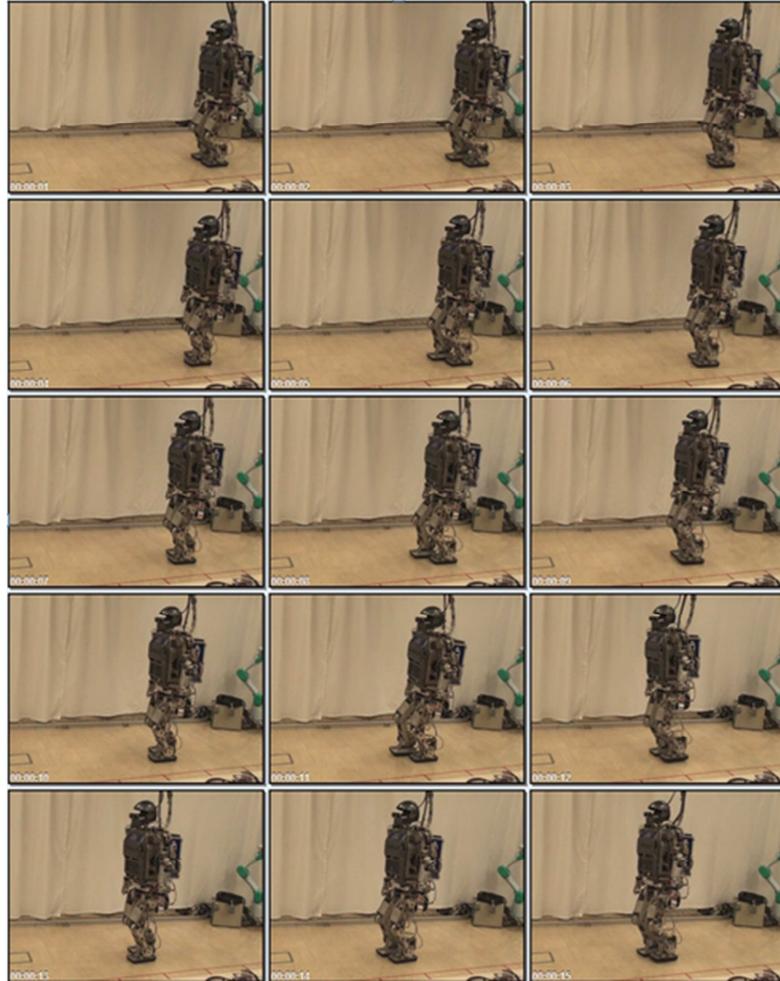
Figure 7.9: Snapshots of SURALP's walk with $v_{average} = 0.09m/s$

7.4 Discussion

The experiments are successful for the given average walking velocity. The proposed extended chromosome further improves the gait of the robot. In 0.09 m/s average walking velocity experiments the pitch and roll angles of the body deviate between ± 2.2 degrees. Compare to previous works [49,74] with 0.03 m/s average walking velocity where the body pitch and roll angles deviate between ± 3 degrees, this result is promising.

Figure 7.10 shows the best fitness function values with and without the use of extended chromosome for a range of average walking velocities. In the figure, the dashed curve indicates the GA tuning process by the use of extended chromosome whereas the solid line indicates GA tuning with the chromosome setting as employed in Chapter 6. It is clear from figure that the use of the extended chromosome results in better fitness function values.
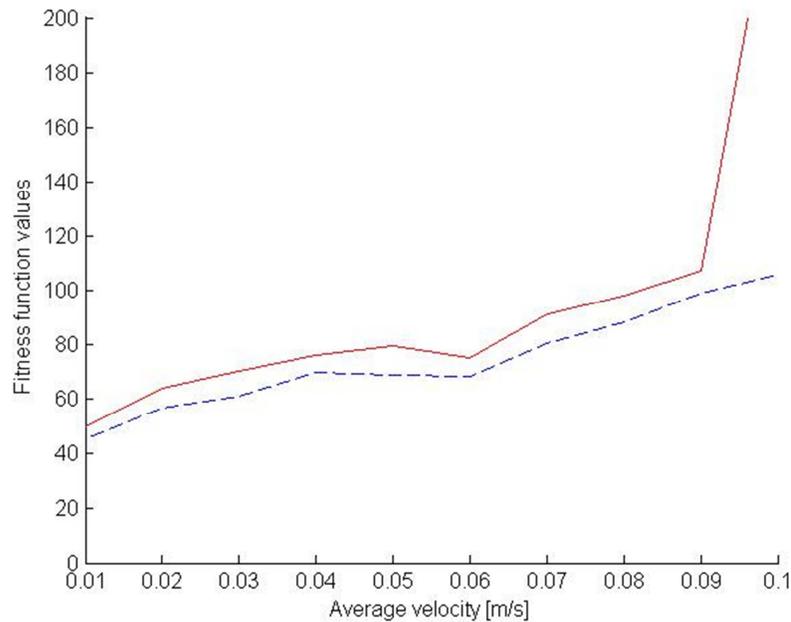
Figure 7.10: Fitness function values with respect to given average walking velocity. Solid curve: Fitness without the lateral motion parameters. Dashed curve: Fitness with the extended chromosomes.

It has to be mentioned that the A parameter is further tuned in experiments to achieve stable walking. It is observed that smaller A parameters compared with the ones obtained from GA tuning create a more stable gait in the experiments. The inevitable mismatches between the modeled and actual robot can be the reason of this observation.

Chapter 8

8. CONCLUSION

This thesis presents a bipedal robot reference gait tuning system which uses evolutionary algorithms as the computational mechanism. A ZMP based reference generation method which makes use of the LIPM is used as the gait synthesis framework. The main goal is finding a suitable set of walking parameters for a desired walking speed. Spatial and temporal parameters which achieve the speed demand without deteriorating the stability of the walk are sought. This task is cast into a GA search problem. The fitness of the individuals is tested via walking simulations.

The stability of the walk is associated with "requiring less support" during the walk. Virtual torsional springs and dampers are attached to the simulated robot body as walking aid mechanisms. They oppose body orientation deviations from an upright posture. The fitness measure is designed as a function of the supporting spring-damper torques.

Three types of GA scenarios are applied.

i)   Single support and double support periods are tuned without imposed joint velocity limits

ii)   Single support and double support periods are tuned with limits imposed on joint velocities

iii)   Single support period, double support period, foot-to-foot lateral distance and lateral ZMP amplitude are tuned with imposed joint velocity limits

The selection of the tuning variables and constraints improved from the first scenario to the last one. The resulting parameters are tested on the experimental humanoid platform SURALP. Stable walking is achieved with speeds which are higher than the ones previously reported with this robot.

This result verifies the virtues of GA tuning over manual trial and error based parameter adjustment techniques. As a result of obtaining suitable parameters for higher speed walking the "ground kick" method for swing foot take-off is abandoned. The effect of this choice can directly be observed in the body roll angle oscillations. The peak-to-peak oscillation readings dropped from 7 degrees (observed in [49]) to 3 degrees.

Our observation is that SURALP walks much more realistic with the newly obtained sets of parameters. A contribution of the thesis is the creation of a set of parameters for a range of walking speeds.

The proposed method is promising for the following future studies;

i)   The admissible off-line tuning times in the order of a few hours suggest that more variables can be included in the tuning process.

ii)   A look-up-table can be implemented for generating walking references for varying speed demands which depend on the task at hand.

REFERENCES

[1]   Kambayashi, T., Takimoto, M., Kodama, T.: "Controlling biped walking robots using genetic algorithms in mobile agent environment", *Proceedings of the 2005 IEEE/ICCC, International Conference on Computational Cybernetics,* pp. 29-34, Seaoul, April 2005.

[2]   Capi, G., Y.Nasu, L.Barolli, M. Yamano, K.Mitobe and K. Takeda . "A Neural Network Implementation of Biped Robot Optimal Gait During Walking Generated by Genetic Algorithm", *In:Proceedings of the 9th Mediterranean Conference on Control and Automation*, Dubrovnik, Croatia, 2001.

[3]   S.-H. Choi, Y.-H. Choi, and J.-G. Kim, "Optimal Walking Trajectory Generation for a Biped Robot Using Genetic Algorithm", *In Proc. of the 1999 IEEE/RSJ International Conference on Intelligent Robots and Systems*, pp. 1456-1461, 1999.

[4]   Xu, K., Chen, X., Liu, W., Williams, M.: "Legged Robot Gait Locus Generation Based on Genetic Algorithms". *In. Proc. International Symposium on Practical Cognitive Agents and Robots*, vol. 213, pp. 51–62. ACM, New York, 2006.

[5]   D.E. Goldberg, "Genetic Algorithm in Search Optimization, and Machine Learning.", Addison Wesley, 1989.

[6]   www.healthpages.org/anatomy-function/anatomy-terms/

[7]   Villeda, L. L., Frisoli, A. and Vega, V. P., "A Mechatronic Analysis and Synthesis of Human Walking Gait", *Proceedings of the 2009 IEEE International Conference on Mechatronics*, pp. 1-6, Malaga, Spain, April 2009.

[8]   Feng, S. and Sun, Z., "A Simple Trajectory Generation Method for Biped Walking", *Proceedings of the 2008 10th International Conference on Control, Automation, Robotics and Vision*, pp. 2078-2082, Hanoi, Vietnam, December 2008.

[9]   Wang, J. W., Xiong, W. L., Liu, H. and Ma, H., "Locomotion Planning Research for a Humanoid Robot Based on the ZMP", *Proceedings of the 2003 IEEE International Conference on Robotics, Intelligent Systems and Signal Processing*, pp. 942-947, Changsha, China, October 2003.

[10] Ha, S., Han, Y. and Hahn, H., "Natural Gait Generation of Biped Robot based on Captured Human Motion Image", *Proceedings of the 2008 IEEE International Conference on*

Multisensor Fusion and Integration for Intelligent Systems, pp. 522-525, Seoul, Korea, August 2008.

[11] Vukobratovic, M., Borovac, B., Surla, D., Stokic, "Biped Locomotion: Dynamics, Stability, Control and Application", Springer-Verlag, 1990.

[12] http://atec.utdallas.edu/midori/Handouts/walkingGraphs.htm

[13] Seven, U., "Linear Inverted Pendulum Model and Swing Leg Dynamics in Biped Robot Walking Trajectory Generation", Thesis (MS), Department of Mechatronics Engineering of the Graduate School of Engineering and Natural Sciences of Sabanci University, July 2007.

[14] H. Lim, A. Takanishi, "Biped walking robots created at Waseda University: WLand WABIAN family", *Philosophical Transactions of the Royal Society A: Mathematical, Physical and Engineering Sciences*, vol. 365, no. 1850, pp. 49–64, 2006.

[15] http://www.humanoid.waseda.ac.jp/booklet/kato_2.html

[16] Takanishi, A., Ishida, M., Yamazaki, Y., Kato, I., "The realization of dynamic walking by the biped walking robot WL-10RD", *Proceedings of International Conference on Advanced Robotics*, pp. 459-466, Tokyo, Japan, September 1985.

[17] Raibert, M., "Legged Robots That Balance", MIT Press, Cambridge, MA, 1986.

[18] Takanishi, A., Lim H., "Waseda Biped Humanoid Robots Realizing Human-like Motion", *Proceedings of the International Workshop on Advanced Motion Control*, pp. 525-530, Nagoya, Japan, March 2000.

[19] Y. Ogura, H. Aikawa, K. Shimomura, H. Kondo, A. Morishima,H. ok Lim, and A. Takanishi, "Development of a new humanoid robot wabian-2," *In Proceedings of the 2006 IEEE International Conference on Robotics and Automation*. IEEE-RAS, May 2006, pp. 76–81.

[20] Hirose, M., Ogawa, K., "Honda humanoid robots development", *Philosophical Transactions of the Royal Society*, Series A, 365 (1850), pp. 11-19, 2007.

[21] Nishiwaki, V., Sugihara, T., Kagami, S., Kanehiro, F., Inaba, M., Inoue, H., "Design and Development of Research Platform for Perception-Action Integration in Humanoid Robot: H6", *Proceedings of the 2000 IEEE/RSJ International Conference on Intelligent Robots and Systems*, vol.3, pp. 1559-1564, Takamatsu, Japan, October 2000.

[22] Nishiwaki, V., Kuffner, J., Kagami, S., Kanehiro, F., Inaba, M., Inoue, H., "The experimental humanoid robot H7: a research platform for autonomous behavior", *Philosophical Transactions of the Royal Society*, Series A, 365 (1850), pp. 79-107, 2007.

[23] Hirose, M., Ogawa, K., "Walking biped humanoids that perform manual labour", *Philosophical Transactions of the Royal Society*, Series A, 365 (1850), pp. 65-77, 2007.

[24] Kaneko, K., Harada, K., Kanehiro, F., Miyamori, G., Akachi, K., "Humanoid Robot HRP-3" *Proceedings of 2008 IEEE/RSJ International Conference on Intelligent Robots and Systems*, pp. 2471-2478, Nice, France, September 2008.

[25] httpwww.humanoid.waseda.ac.jpbookletkato_4.html

[26] K.Kaneko, F.Kanehiro, M.Morisawa, K.Miura, S.Nakaoka and S.Kajita "Cybernetic Human HRP-4C," *Proc. IEEE/RSJ Int. Conference on Humanoid Robots*, pp.7-14, 2009.

[27] Oh, J.-Y., Kim, J.-H., "Realization of dynamic walking for the humanoid robot platform KHR-1", *Advanced Robotics*, vol. 18, no. 7, pp. 749-768, 2004.

[28] J. Y. Kim, I. W. Park, J. H. Oh, "Walking Control Algorithm of Biped Humanoid Robot on Uneven and Inclined Floor", *Journal of Intelligent Robotic SystemJournal of Intelligent and Robotic System* 48:457-484, January 2007.

[29] I. W. Park, J. Y. Kim, J. Lee, and J. H. Oh, "Mechanical Design of Humanoid Robot Platform KHR-3 (KAIST Humanoid Robot – 3: HUBO)," *Proc. IEEE-RAS Int. Conference on Humanoid Robots*, pp. 321-326, 2005.

[30] Park, I.-W., Kim, J.-Y., Lee, J., Oh, J.-H., "Online Free Walking Trajectory Generation for Biped Humanoid Robot KHR-3 (KAIST Humanoid Robot-3: HUBO)". *6th IEEE-RAS International Conference on Humanoid Robots*, pp. 398-403, Genova, Italy, December 2006.

[31] http://www.pal-robotics.comrobotsreem-b

[32] http://www.bostondynamics.comrobot_petman.html

[33] Gouaillier, D., Hugel, V., Blazevic, P., Kilner, C., Monceaux, J., Lafourcade, P., Marnier, B., Serre, J., and Maisonnier, B. 2009. Mechatronic design of NAO humanoid. In *Proceedings of the 2009 IEEE international Conference on Robotics and Automation* (Kobe, Japan, May 12 - 17, 2009). IEEE Press, Piscataway, NJ, 2124-2129.

[34] http://en.wikipedia.org/wiki/RoboCup_Standard_Platform_League

[35] https://spectrum.ieee.orgautomatonroboticshumanoidsvirginia-techs-romela-rocks-robocup-2011

[36] Zhang, Y., Wang, Q. and Fu, P., "A New Method of Desired Gait Synthesis in Biped robot", *Proceedings of the 3rd World Congress on Intelligent Control and Automation*, pp. 1300-1304, Hefei, China, June-July 2000.

[37] Kajita, S., Kanehiro, F., Kaneko, K., Fujiwara, K., Yokoi, K. and Hirukawa, H., "A Realtime Pattern Generator for Biped Walking", *Proceedings of the 2002 IEEE International Conference on Robotics & Automation*, pp. 31-37, Washington, USA, May 2002.

[38] Lim, H. O., Kaneshima, Y. and Takanishi, A., "Online Walking Pattern Generation for Biped Humanoid Robot with Trunk", *Proceeding of the 2002 IEEE International Conference on Robotics & Automation*, pp. 3111-3116, Washington, USA, May 2002.

[39] Sugihara, T., Nakamura, Y. and Inoue, H., "Realtime Humanoid Motion Generation through ZMP Manipulation based on Inverted Pendulum Control", *Proceedings of the 2002 IEEE International Conference on Robotics & Automation*, pp. 1404-1409, Washington, USA, May 2002.

[40] Harada, K., Kajita, S., Kaneko, K. and Hirukawa, H., "An Analytical Method on Real-time Gait Planning for a Humanoid Robot", *Proceedings of the 2004 IEEE/RAS International Conference on Humanoid Robots*, pp. 640-655, November 2004.

[41] Kajita, S., Kanehiro, F., Kaneko, K., Fujiwara, K., Harada, K., Yokoi, K. and Hirukawa, H., "Biped Walking Pattern Generation by using Preview Control of Zero-Moment Point", *Proceedings of the 2003 IEEE International Conference on Robotics& Automation*, pp. 1620-1626, Taipei, Taiwan, September 2003.

[42] Tanaka, T., Takubo, T., Inuoe, K. and Arai, T., "Emergent Stop for Humanoid Robots", *Proceedings of the 2006 IEEE/RSJ International Conference on Intelligent Robots and Systems*, pp. 3970-3975, Beijing, China, October 2006.

[43] Verrelst, B., Stasse, O., Yokoi, K. and Vanderborght, B., "Dynamically Stepping Over Obstacles by the Humanoid Robot HRP-2", *Proceedings of the 2006 IEEE/RAS International Conference on Humanoid Robots*, pp. 117-123, December 2006.

[44] Nishiwaki, K. and Kagami, S., "High Frequency Walking Pattern Generation based on Preview Control of ZMP", *Proceedings of the 2006 IEEE International Conference on Robotics&Automation*, pp. 2667-2672, Florida, USA, May 2006.

[45] Huang, W., Chew, C. M., Zheng, Y. and Hong, G. S., "Pattern Generation for Bipedal Walking Slopes and Stairs", *Proceedings of the 2008 IEEE/RAS International Conference on Humanoid Robots*, pp. 205-210, Daejeon, Korea, December 2008.

[46] Erbatur, K. and Kurt, O., "Natural ZMP Trajectories for Biped Robot Reference Generation", *IEEE Transactions on Industrial Electronics*, vol. 56, no. 3, pp. 835-845, March 2009.

[47] A. Takanishi, H. Lim, M. Tsuda and I. Kato. "Realization of dynamic biped walking stabilized by trunk motion on a sagittally uneven surface," *IEEE/RJS Int. Conf. on Intelligent Rob. and Syst.*, 1990.

[48] Erbatur, K., Koca O., Taşkıran E., Yılmaz M. and Seven, U. "ZMP Based Reference Generation for Biped Walking Robots", ICICRA'09, *Int. Conf. Intelligent Control, Rob. and Aut.*, Venice, Italy, Oct. 2009.

[49] Taskiran, E., Yilmaz, M., Koca, O., Seven U. and Erbatur, K. (2010). "Trajectory Generation with Natural ZMP References for the Biped Walking Robot SURALP," *In Proc. 2010 IEEE International Conference on Robotics and Automation*, ICRA, Alaska, USA.

[50] H. Quiang, K. Yokoi, S. Kajita, K. Kaneko, H. Arai, N. Kovachi and K. Tanie, "Planning walking patterns for a biped robot," *IEEE Transaction on Robotics and Automation*, vol. 11, no. 3, pp. 280-289, June 2001.

[51] Yilmaz, M., "Humanoid Robot Omnidirectional Walking Trajectory Generation and Control", Thesis (MS), Department of Mechatronics Engineering of the Graduate School of Engineering and Natural Sciences of Sabanci University, August 2010.

[52] B. Siciliano and O. Khatib, Springer Handbook of Robotics. New York: Springer, 2008.

[53] S. Aoi and K. Tsuchiya, "Locomotion control of a biped robot using nonlinear oscillators," *Autonomous Robots*, vol. 19, pp. 219–232, 2005.

[54] G. Taga, Y. Yamaguchi, and H. Shimizu: "Self-organized control of bipedal locomotion by neural oscillators in unpredictable environment ," *Biological Cybernetics*, Vol. 65, pp. 147-159, 1991.

[55] Y. Zheng, "A neural gait synthesizer for autonomous biped robots," *In Proceedings of the IEEE International Workshop on Intelligent Robots and Systems* (IROS90), 1990, pp. 601-608.

[56] L. Righetti and A. J. Ijspeert, "Programmable central pattern generators: an application to biped locomotion control," *In Proc. 2006 IEEE Int. Conf. on Robotics and Automation*, 2006, pp. 1585–1590.

[57] Nakajima, Y., Yonemura, A., Kawamura, A., "Experimental Approach for the Fast Walking by the Biped Robot", *Proceedings of the IASTED International Conference on Robotics and Applications*, Honolulu, Hawaii, USA, August 2000.

[58] Zhu, C., Okamura, M., Kawamura, A., Tomizawa, Y., "Experimental approach for high speed walking of the biped robot MARI-1", *Proceedings of the 8th IEEE International Workshop on Advanced Motion Control* (AMC2004), pp. 427-432, March 2004.

[59] Taşkıran, E., "Walking Trajectory Generation and Control of a Humanoid Robot: SURALP", Thesis (MS), Department of Mechatronics Engineering of the Graduate School of Engineering and Natural Sciences of Sabanci University, August 2009.

[60] F. Yamasaki, K. Endo, H. Kitano, and M. Asada, "Acquisition of humanoid walking motion using genetic algorithm—Considering characteristics of servo modules," *In IEEE Int. Conf. Robot. Automation.*, 2002,pp. 3123–3128.

[61] L. Roussel, C. Canudas-de Wit, and A. Goswami, "Generation of energy optimal complete gait cycles for biped robots," *In Proc. IEEE International Conference on Robotics Automation*, Leuven, Belgium, May 1998, pp. 2036–2041.

[62] C. Chevallereau and Y. Aoustin, "Optimal reference trajectories for walking and running of biped robot," *Robotica*, vol. 19, no. 5, pp.557–569, Sept. 2001.

[63] Bebek, O., K. Erbatur, "A Fuzzy System for Gait Adaptation of Biped Walking Robots", *Proceedings of the IEEE Conference on Control Applications*, 2003

[64] Picado, H., Gestal, M., Lau, N., Reis, L.P., Tomé, A.M. "Automatic Generation of Biped Walk Behavior Using Genetic Algorithms." *In: Proceedings of the 10th International Work-Conference on Artificial Neural Networks: Part I: Bio-Inspired Systems: Computational and Ambient Intelligence*. Cabestany, J., Sandoval, F., Prieto, A., Corchado, J.M. (eds.) IWANN 2009. LNCS, vol. 5517, pp. 805–812. Springer, Heidelberg, 2009.

[65] S.-H. Choi, Y.-H. Choi, and J.-G. Kim, Optimal Walking Trajectory Generation for a Biped Robot Using Genetic Algorithm. *In: Proc. of the 1999 IEEE/RSJ International Conference on Intelligent Robots and Systems*, pp. 1456-1461, 1999.

[66] Y. Choi, B. J. You, and S. R. Oh, "On the stability of indirect ZMP controller for biped robot systems", *Proceedings of International Conference on Intelligent Robots and Systems*, pp: 1966 - 1971, vol.2, Sendal, Japan, June 2004.

[67] A. Dasgupta, and Y. Nakamura, "Making feasible walking motion of humanoid robots from human motion capture data" *Proceedings of the IEEE International Conference on Robotics and Automation*, Detroit, Michigan, May 1999.

[68] K. Erbatur, A. Okazaki, K. Obiya, T. Takahashi and A. Kawamura, "A study on the zero moment point measurement for biped walking robots", *Proc. 7th International Workshop on Advanced Motion Control*, pp. 431-436, Maribor, Slovenia, 2002

[69] C. Zhu, Y. Tomizawa, X. Luo, and A. Kawamura "Biped walking with variable ZMP, frictional constraint, and inverted pendulum model", *IEEE International Conference on Robotics and Biomimetics*, pp: 425 – 430, Shenyang, China Aug 2004.

[70] D. Beasley, D. R. Bull, and R. R. Martin, "An Overview of Genetic Algorithms: Part 2, Research Topics" *University Computing*, vol. 15, no. 4, pp. 170-181, 1993.

[71] D. Beasly, D. Bull, and R. Martin, "An overview on genetic algorithms: part 1. Fundamentals," *University Computing*, vol. 15, no. 2, pp. 58–69, 1993

[72] Erbatur, K. and Kawamura, A., "A New Penalty based Contact Modeling and Dynamics Simulation Method as Applied to Biped Walking Robots," *Proceedings of the 2003 FIRA World Congress*, Vienna, Austria, October 2003.

[73] O. Bebek, K. Erbatur, "Adaptive fuzzy systems for tuning biped robot gait parameters", *In FIRA Robot World Congress*, October 1–3, Vienna, Austria, 2003.

[74] Erbatur, K., Seven, U., Taskiran, E., Koca, O., Unel, M., Kiziltas, G., Sabanovic, A. and Onat, A., "SURALP: A New Full-Body Humanoid Robot Platform", *In the Proceedings of the 2009 IEEE/RSJ International Conference on Intelligent Robots and Systems*, Missouri, USA, October 2009.